Mechanisms behind the oncogene-induced senescence (OIS) – oncogene-induced apoptosis (OIA) decision in cells expressing p95HER2

Cristina Bernadó Morales

FACULTAT DE FARMÀCIA

TESIS DOCTORAL

Mechanisms behind the oncogene-induced senescence (OIS) – oncogene-induced apoptosis (OIA) decision in cells expressing p95HER2

Cristina Bernadó Morales

Barcelona, 2015

UNIVERSITAT DE BARCELONA

FACULTAT DE FARMÀCIA

PROGRAMA DE DOCTORAT EN BIOTECNOLOGIA

Mechanisms behind the oncogene-induced senescence (OIS) – oncogene-induced apoptosis (OIA) decision in cells expressing p95HER2

Memòria presentada per Cristina Bernadó per optar al títol de doctora per la universitat de Barcelona

Director de tesis:	Doctoranda:	Tutora:
Dr. Joaquín Arribas López	Cristina Bernadó Morales	Dra. Dolors Serra

Cristina Bernadó Morales
Barcelona, 2015

AGRADECIMIENTOS

Me gustaría expresar mi más profundo y sincero agradecimiento a todas aquellas personas que con su apoyo, cariño y amistad han hecho posible la finalización de esta importante etapa personal y profesional que cierro con la elaboración y defensa de esta tesis.

Un especial agradecimiento al Dr. Joaquín Arribas por haberme dado la oportunidad de formarme científicamente en su laboratorio y por la confianza en mí depositada. Agradezco el apoyo, la orientación, aportación y motivación científica durante todos estos años, así como la dedicación a la supervisión del presente trabajo.
Hago extensivo el agradecimiento profesional a los miembros pasados y presentes del laboratorio, así como también a muchos miembros del resto de laboratorios del VHIO. Por la siempre predisposición a colaborar, la ayuda brindada y la aportación de ideas. Y especial agradecimiento a Águeda y Bea por el tiempo dedicado a la revisión y corrección del texto de esta tesis, mil gracias.

Pero esta etapa no hubiera sido posible sin todas aquellas personas que he tenido la oportunidad de conocer y que más allá de ser compañeros de trabajo han pasado a ser parte importante de mi vida, gracias amigos. A la "city of Hope": A Celina por la paciencia y los consejos; A Águeda por su siempre predisposición y su humor inteligente; A Bea por estar siempre ahí y por sus bromas ácidas; A Rocío por aportar consejos siempre con alegría y espontaneidad; A Olga por estar siempre dispuesta a escuchar; A Irene por los abrazos, por compartir, escuchar, comprender y ayudar siempre. A todas por el cariño, la amistad, los momentos, los viajes, las risas y las confidencias, mil gracias chicas. A Mariano por los mates, los asados y la amistad. A Yasir por su entusiasmo y revolución. A Josep Lluís por estar siempre dispuesto a aportar en todos los sentidos. A Nello por su alegría y el cariño. A Pier Davide por la filosofía y las reflexiones. A Martín por compartir penas sobre p21. A Albert por su simpatía. A todos aquellos que aunque estando ya más lejos dejaron su especial recuerdo como Ben. A todos, gracias.

Y por último, mi más sentido agradecimiento a mi familia, a mis padres Ana y Antonio y a mi hermano Víctor. Por la educación, por el amor, por la alegría, por darlo todo por mí, por ser mi apoyo y por creer y confiar siempre en mí. Mil gracias.

A todos ellos, por formar parte de este proceso,

Gracias, gràcies, thank you.

INDEX

INDEX

SUMMARY

SUMMARY

In response to oncogenic stresses cells activate two different tumor suppressor mechanisms: Oncogene-induced senescence (OIS), a terminal cell proliferation arrest, or oncogene-induced apoptosis (OIA), which leads to cell disintegration.

We have shown that the oncogene p95HER2-611 leads cells to OIS and that senescent cells increase the ability of neighbor proliferating breast cancer cells to metastatize. In contrast, available evidence indicates that OIA does not have this undesirable side effect. The mechanisms by which an oncogenic insult results in OIS or OIA remains poorly characterized.

In this work, we addressed the functional characterization and the mechanism of activation of another previously described, but uncharacterized, p95HER2 fragment, the p95HER2-648. We showed that the expression of p95HER2-648 does not lead to senescence but to apoptosis. In vivo data showed that p95HER2611-induced senescent cells favor the metastatic capability of MDA-MB-231 cells while p95HER2-648-induced apoptotic cells do not have this effect.

We observed that cells bearing p95HER2-611 seem to be protected from apoptosis. Consistently, cells expressing p95HER2-611 showed increased levels of p21, a well-known cell cycle regulator and also an apoptotic repressor. Knock-down of p21 in these cells showed increased apoptosis indicating that p21 is protecting senescent cells against apoptosis.

We conclude that the expression of different active p95HER2 fragments can lead to either apoptosis or senescence, indicating that HER2 signaling can induce both cellular responses depending on the activated pathways. Elucidating the complete mechanism by which these pathways are activated could help to find a way to promote apoptosis on senescent cells, in order to avoid their pro-metastatic effect.

ABBREVIATIONS

ABBREVIATIONS

53BP1 p53-binding protein 1
Akt/PKB Akt/Protein kinase B
ARF ADP-ribosilation factor
AREG Amphiregulin
ATF-2,3 Activating transcription factor 2,3
ATM Ataxia-telangiectasia-mutated
ATR Ataxia-telangiectasia-and Rad3-related
Bcl-2 B-cell lymphoma 2
Bcl-2A1 B-cell lymphoma 2A1
Bcl-XL B-cell lymphoma XL
BH1-4 Bcl-2 homology 1-4
BAK Bcl-2 antagonistic/killer
BAX Bcl-2 related X protein
BID BH3-interacting domain death agonist
BIM Bcl-2-interacting mediator of cell death
CDK1-6 cyclin dependent kinase 1-6
CDKN1A cyclin-dependent kinase inhibitor
Chk1,2 Checkpoint kinase 1,2
Cip/Kip CDK inhibitory protein/kinase inhibitory protein
CTF c-terminal fragment
cyt-c cytochrome-c
DAPI 4',6-diamidino-2-phenylindole
DDR DNA-damage response
EGF Epidermal growth factor
EGFR Epidermal growth factor receptor
EMT epithelial-mesenchymal transition
ER estrogen receptor
ERK1,2 extracellular signal-regulated kinase 1,2
H2AX Histone 2AX
HB-EGF Heparin-binding epidermal growth factor
HDM2 Human double minute 2
HDMX Human double minute X
HER/ErbB 1-4 Human epidermal growth factor receptor/avian erythroblastosis oncogene B 1-4
IL-6,8 Interleukin 6,8
JNK/SAPK c-Jun N-terminal kinase/stress-activated protein kinase
MAPK Mitogen-activated protein kinase
MEK1,2 Mitogen/Extracellular signal-regulated Kinase
mTOR mammalian target of rapamycin
Myc avian myelocytomatosis viral oncogene cellular homolog
Noxa Latin for *damage* also named as PMAIP1 Phorbol-12-myristate-13-acetate-induced protein
OIA oncogene-induced apoptosis
OIS Oncogene-induced senescence
PARP Poly ADP-ribose polymerase
PDK1,2 phosphatidyl inositol-dependent protein kinase
PICS PTEN-loss-induced senescence
PI propidium iodide
PI3K Phosphatidylinositol 3-kinase
PKC protein kinase C
PLCγ Phospholipase C gamma
PR progesterone receptor
PTEN phosphatase and tensin homolog
PUMA p53 up-regulated modulator of apoptosis
RAF Rapidly accelerated fibrosarcoma

Ras Rat sarcoma
Rb Retinoblastoma protein
SA-ßGAL Senescence-associated ß-galactosidase
SASP Senescence-associated secretory phenotype
SH2 Src homology
TGF-α Transforming growth factor alpha
TGFβ Transforming growth factor beta
TNF-α Tumor necrosis factor-alpha
TNFR 1 Tumor necrosis factor receptor 1
TRAIL TNF-related apoptosis-inducing ligand
TRAIL-R1-5 TRAIL receptor 1-5
Vav2 the sixth letter of the Hebrew alphabet (for being the sixth discovered oncogene)

INTRODUCTION

INTRODUCTION

1. Stress-induced apoptosis and senescence

Apoptosis and senescence are two tightly regulated mechanisms that serve the same purpose, to suppress growth and expansion of unnecessary or damaged cells from the organism.

These two mechanisms have been usually compared as opposing, although recent studies indicate that they might be complementary (1). In embryogenesis both mechanisms are activated in order to promote tissue remodeling and one can substitute the other. Still, it is not clear why in different areas of the developing embryo these mechanisms are specifically activated. Moreover, it has been recently shown that when senescence cannot be engaged, apoptosis is alternatively activated inducing comparable tissue remodelation and generating a perfectly viable embryo with no major defects (2, 3). On the other hand, in tumorigenesis, although both are considered as tumor suppressor mechanisms in response to stress, they seem to have different consequences for the overall tumorigenic progression not being completely exchangeable processes, mainly due to the non-cell autonomous effects of senescence.

Both senescence and apoptosis are activated in response to many different insults such as γ-irradiation, UVB light, exposure to oxidants, genotoxic chemotherapies or oncogenes. These insults have in common that they induce DNA-damage. Cellular responses to DNA damage are mediated through highly conserved checkpoint mechanisms that activate a signal amplification cascade known as the DNA-damage response (DDR). Transient activation of the DDR stops cells from proliferating to allow the DNA repair. However, when DNA damage is too severe or not reparable, persistent DDR activation activates a major response to restrain the damaged cell either by elimination by apoptosis or by inducing a permanent cell cycle arrest by senescence (4).

The mechanisms by which a cell undergoes one cell fate or the other upon damage are not fully understood. In this work we will characterize the different implications that the presence of apoptotic or senescent cells could have in the overall progression of a tumor and we will study the mechanism of choice in cells expressing different forms of p95HER2, a constitutively active form of the receptor tyrosine kinase HER2.

1.1. Apoptosis

Apoptosis is a type of programmed cell death that occurs in an organized manner following well-defined molecular pathways. This process is characterized by an ordered series of events, including: membrane blebbing, mitochondrial outer membrane permeabilization (MOMP), nuclear condensation and DNA fragmentation.

The critical executors of apoptosis are the intracellular cysteine-proteases known as caspases that are activated in a self-amplifying cascade. Caspases -2, -8, -9 and -10 are considered the initiator caspases, which are activated by pro-apoptotic signals. Initiator caspases in turn activate the effector caspases -3, -6 and -7. Activated effector caspases and catabolic hydrolases degrade most of the macromolecules of the cell including DNA.

Finally, this leads to shrinkage of the cell, fragmentation into membrane-bound apoptotic bodies and rapid phagocytosis by neighboring cells without associated inflammation. All this process will lead to the complete elimination of the apoptotic cells within few hours time (5-9).

Two independent mechanisms can trigger apoptosis: the mitochondrial or intrinsic pathway, activated by DNA-damage and the death receptor or extrinsic pathway, engaged by ligand-activated death receptors. Both pathways can also be interconnected, for example, through caspase-8, which is activated by death receptors but can engage effectors of both pathways.

1.1.1. The intrinsic pathway

The intrinsic apoptotic pathway, also called mitochondrial apoptotic pathway, involves, as a major effector, the mitochondrial cytochrome-c (cyt-c) release to the cytosol. The release of cyt-c is regulated by a variety of pro- and anti-apoptotic modulators that are sequestered in the mitochondrial intermembrane. These apoptotic regulators form the B-cell lymphoma-2 (Bcl-2) family of proteins, which contains three structurally and functionally distinct subgroups:

- Bcl-2-like pro-survival proteins such as Bcl-2 itself, B-cell lymphoma XL (Bcl-XL) or B-cell lymphoma 2A1 (Bcl-2A1), which share up to four Bcl-2 homology domains (BH1-4).
- Pro-apoptotic effector proteins Bcl-2 related X protein (BAX) and Bcl-2 antagonistic/killer (BAK), which contain the BH1, BH2 and BH3 domains.

- Pro-apoptotic BH3-only proteins such as BH3-interacting domain death agonist (BID), Bcl-2-interacting mediator of cell death (BIM), Noxa (Latin for *damage* also named as Phorbol-12-myristate-13-acetate-induced protein (PMAIP1)) or p53 up-regulated modulator of apoptosis (PUMA), which share only the BH3 domain.

The BH3-only proteins initiate apoptosis, whereas BAX/BAK-like proteins act downstream by disrupting the mitochondrial outer membrane. The balance between the pro-apoptotic BAX/BAK proteins, and their anti-apoptotic Bcl-2/Bcl-XL counter partners determine mitochondrial permeability. The activity of these proteins is positively or negatively regulated by the various BH3-only members, each acting as the terminal effector of distinct signalling pathways. When the balance is broken and results in the net dominance of the pro-apoptotic signals, BAX/BAK proteins permeabilize the mitochondria to release pro-apoptotic factors, such as cyt-c. It is the cyt-c together with the adaptor apoptotic protease activating factor-1 (Apaf-1), the one assembling to a multiprotein caspase-activating complex called apoptosome (10). Caspase-9, the initiator caspase of this pathway, is activated in this complex and in turn activates the effector caspases -3, -6 and -7.

1.1.2. The extrinsic pathway

The extrinsic apoptotic pathway is initiated by transmembrane receptors of the tumor necrosis factor (TNF) superfamily, which are activated by their cognate ligands: Fatty acid synthase ligand/Fatty acid synthase receptor (FasL/FasR), Tumor necrosis factor-alpha/Tumor necrosis factor receptor 1 (TNF-α/TNFR 1), Apo3 ligand/Death receptor 3 (Apo3L/DR3) and TNF-related apoptosis-inducing ligand/TRAIL receptor 1-2 (TRAIL/TRAIL-R1-2). Death receptors contain a Death Domain (DD) in the cytosolic tail and, once activated, recruit several intracellular proteins, including adaptor proteins such as Fas associated death domain (FADD) or Receptor interacting protein (RIP) and certain pro-caspases. Association of these proteins with the activated receptor forms the so called Death-inducing signaling complex (DISC) that ultimately activates caspase-8, and in some cases caspase-10 (11). In certain cell types this pathway also engages the intrinsic pathway through activation of the pro-apoptotic protein BID, which assumes cyt-c-releasing activity upon cleavage by caspase-8 (12-14).

This pathway is regulated by antagonistic decoy receptors, such as TRAIL-R3-5, which bind TRAIL but do not transmit a death signal, and by intracellular molecules, such as the FLICE-like inhibitory protein (FLIP), that compete with caspase-8 for binding to the DISC (12, 15).

Finally, effector caspases -3, -6 and -7 are activated either by direct caspase-8 activation, or by recruitment of the mitochondrial pathway (16).

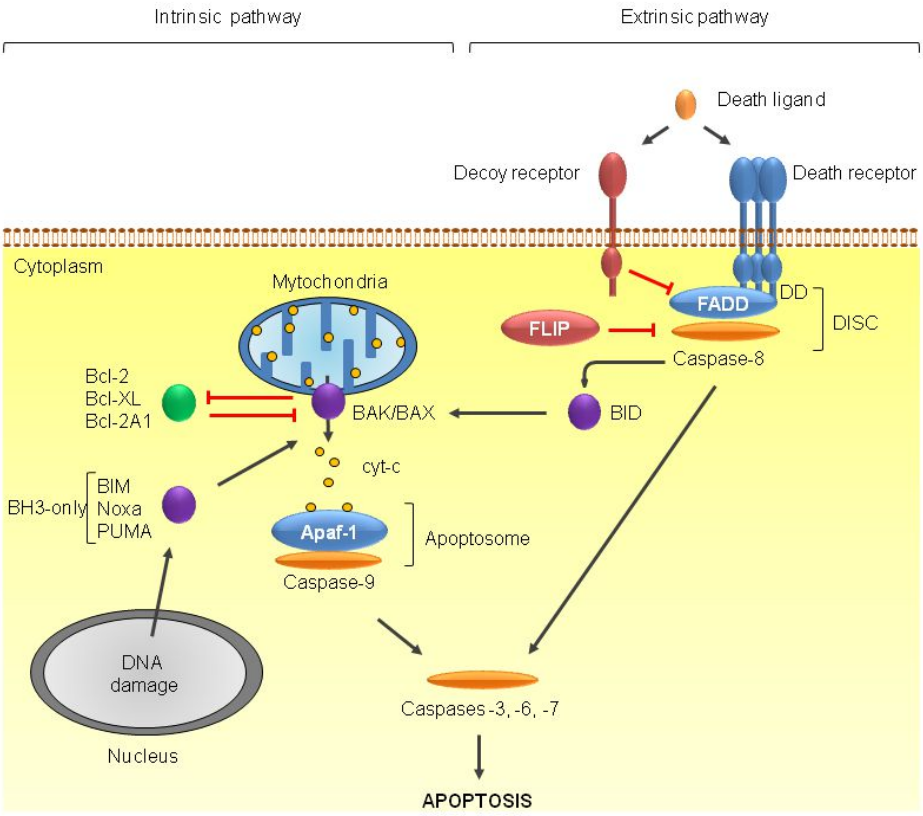

Fig. 1 Intrinsic and extrinsic apoptosis pathways
Key components and regulators of the intrinsic and extrinsic apoptotic pathways. The intrinsic apoptotic pathway is activated after DNA damage. BH3-only proteins initiate the signal activating BAK/BAX proteins, which permeabilize the mitochondrial membrane. Anti-apoptotic Bcl-2 proteins can counteract this effect. Mitochondrial permeabilization enables cyt-c release to the cytoplasm and the apoptosome is assembled to activate the initiator caspase-9, which activates effector caspases -3, -6 and -7. The extinsic apoptotic pathway is initiated by death ligands, which bind death receptors and activate the initiator caspase-8 by formation of the DISC. This process can be inhibited by the binding of the ligands to decoy receptors or by inhibition of the DISC by FLIP. Caspase-8 can directly activate the effector caspases -3, -6 and -7 or engage the intrinsic apoptotic pathway by activation of BID.

1.1.3. Apoptosis markers

Morphological and biochemical features of apoptotic cells are used as markers for apoptosis detection and quantification. The DNA fragments of the internucleosomal DNA fragmentation by endonucleases activity can be detected as a ladder pattern in the electrophoresis of isolated DNA (6). Alternatively, the resulting hypodiploid cells can be detected according to its DNA content, which can be assessed by nucleic acid staining with propidium iodide (PI) and analysis by flow cytometry of the cell cycle

profile. Apoptotic cells accumulate in a SubG1 peak of a histogram of a nucleic acid stain. Cells containing DNA strand breaks can be detected under light microscopic analysis using the terminal transferase mediated DNA nick end labeling (TUNEL) assay (17). In addition, cell surface markers that serve for the early phagocytic recognition of apoptotic cells are also used as apoptosis markers, such as the detection of externalized phosphatidylserine with Annexin V (18). Finally, both caspase activation and caspase substrates cleavage, i.e. Poly ADP-ribose polymerase (PARP), are also easily detectable and commonly used as markers of caspase-mediated proteolysis during apoptosis.

1.2. Senescence

1.2.1. Stress –induced senescence

In principle, senescence is not a form of cell death but, a permanent cell cycle arrest. This phenomenon was first described as an irreversible growth arrest state in fibroblasts after serial cultivation *in vitro* (19). This growth arrest was named *replicative* or *cellular senescence* and is the consequence of the telomeres attrition after an excessive number of cell divisions in the absence of endogenous telomerase activity (20). For that reason, senescence was first linked to cellular ageing. This physiologic senescence process mirrors senescence that is not caused by the limited replications and caused by different stress-inducers, which is known as *premature senescence*. Nowadays, cellular senescence is considered a stress response mechanism with implications in different conditions ranging from cancer to aging.

Two main signaling pathways promote senescence: the p53/p21 and the p16/Retinoblastoma protein (Rb). In response to different stresses the resulting DNA damage, as single-stranded (SS) DNA or double-strand breaks (DSB), is sensed by specialized protein complexes that recruit and activate Ataxia-telangiectasia-mutated (ATM) or Ataxia-telangiectasia- and Rad3-related (ATR) protein kinases at the site of DNA lesion (21-25). The recruitment of either of these so-called apical kinases to the lesion causes the local phosphorylation of the histone 2AX (H2AX) at serine 139, which is a key step in the nucleation of the protein complex that mediates DDR. The phosphorylated form of H2AX (γH2AX) recruits additional ATM kinases in a positive feedback loop, thereby increasing local ATM activity and consequently fuelling the spread of γH2AX along the chromatin. Crucial to the establishment of this positive feedback loop are mediator of DNA-damage checkpoint 1 (MDC1) and p53-binding

protein 1 (53BP1), these so-called DDR mediators, which facilitate the recruitment of ATM complexes to γH2AX (21).

ATM and ATR share sequence homology and have partly redundant functions, the main of which is to activate the tumor suppressor protein p53 by direct phosphorylation or by activating the checkpoint protein kinases 1 and 2 (Chk1 and Chk2), which in turn phosphorylate p53. Although both proteins have overlapping substrate specificity, ATM preferentially activates Chk2, while Chk1 has been shown to be the ATR preferred substrate. p53 phosphorylation will lead to the release of its inhibitors such as the Human double minute 2 and X (HDM2, HDMX).

p53 is a transcription factor that regulates the expression of many genes. Among them, the cyclin-dependent kinase inhibitor (CKI) p21 seems to play a central role in the onset of senescence. The increase of p21 blocks the entrance of cells into the S phase of the cell cycle by inhibiting the cyclin-dependent kinase (CDK) 2-Cyclin E complex and thus, inducing a G1 phase arrest that allows the cell to repair the damaged DNA (26). When the DNA damage is too extensive or severe that cannot be repaired, cells are persistently arrested and another CKI, p16, is upregulated contributing to the maintenance of senescence (27). Expression of p16 inhibits progression through the G1 phase by inhibiting the CDK4/6-Cyclin D-mediated phosphorylation of Rb tumor suppressor protein (28, 29). Hypophosphorylated Rb represses E2F transcription factors resulting in the arrest in the G1 phase. Nonetheless, p53 can also act on the G2/M checkpoint by inducing p21, which also inhibits CDK1-Cyclin B complexes, whose activity is required for the cell to progress into the G2/M transition (30). In fact, expression of p21 has also been shown to induce a G2/M arrest in an Rb-defficient context (31).

To note, DDR-independent senescence has also been reported under some experimental conditions in which p16 is upregulated, p38-MAPK or ATR are constitutively activated or the tumor suppressor PTEN is lost in homozygosi (32-35). In addition, programmed cellular senescence during mammalian embryonic development (developmental senescence) seems to be DDR-independent too (2, 3).

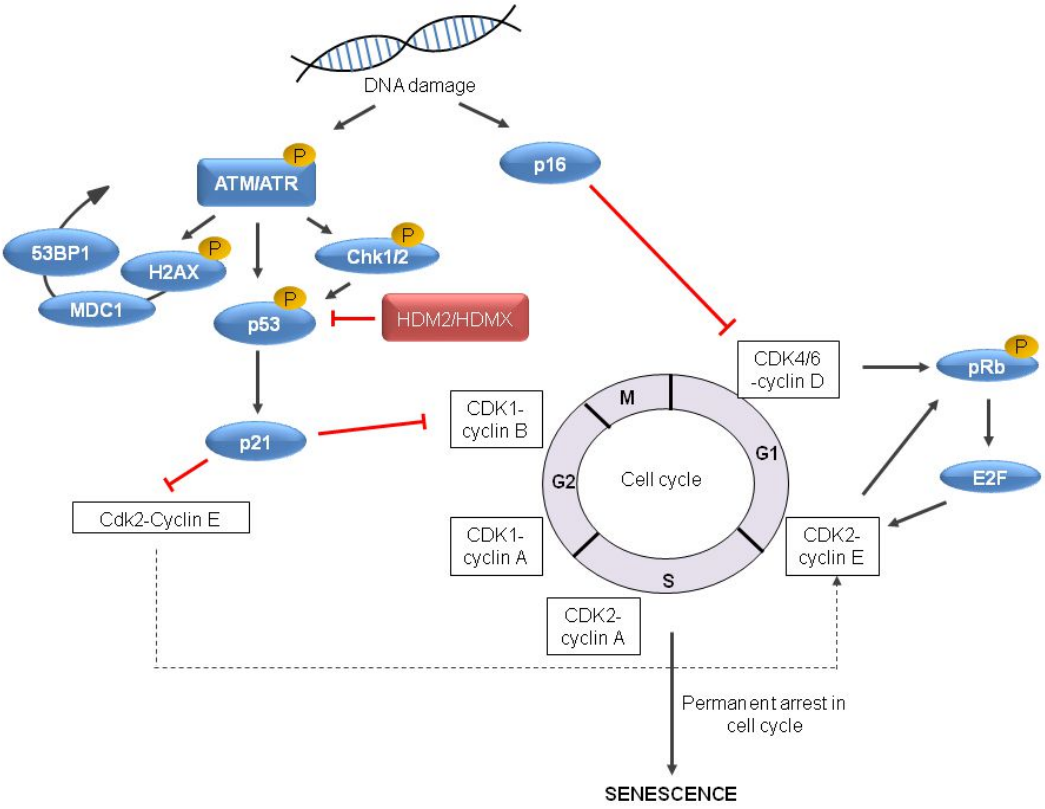

Fig. 2 Senescence regulation by p53/p21 and p16/Rb pathways
Summary of cell cycle control by the DDR pathway. DNA damage is sensed by ATM/ATR kinases which phosphorylate several substrates. Phosphorylation of H2AX recruits DDR-mediators MDC1 and 53BP1 to recruit more ATM and ATR to the DNA damage site. ATM/ATR activate p53, through direct phosphorylation or through Chk1/2 phosphorylation. Activation of p53 induces the CKI p21. p21 prevents cell cycle progression in G1 phase by inhibition of CDK2-cyclin E complexes or in G2/M phase by inhibition of CDK1-cyclin B complexes. Persistent DNA damage also activates p16 which blocks cell cycle progression by inhibiting CDK4/6-cyclin D complexes. Suppression of CDK4/6-cyclin D and CDK2-cyclin E activity blocks cell cycle progression as it prevents Rb phosphorylation and thus, activation of E2F transcription factors.

1.2.2. Senescence markers

Unfortunately, no single marker to unequivocally identify senescent cells has been described to date. In practical terms, senescent cells are identified using multiple markers although not all of them need to be present to define the senescent state. The characteristics of senescent cells include:

- Cell proliferation arrest
- Senescence-associated ß-galactosidase (SA-ß-GAL) activity; i. e. beta-galatosidase activity at pH 6, which is enriched in senescent cells likely because they have enlarged lysosomes.
- Enlarged cell size, flattered morphology and vacuolated cytoplasm.
- Accumulation of DNA damage.

- Expression of cell cycle inhibitors.
- Nuclear heterochromatin foci, also called senescence-associated heterochromatic foci (SAHF) i. e. regions of transcriptionally silenced DNA that can be detected as 4',6-diamidino-2-phenylindole (DAPI)-dense foci (36).
- Focal accumulation of specific SAHFs markers such as heterochromatin protein 1 (HP1) or lysine 9 tri-methylated histone H3 (K9M-H3).
- High metabolic rate
- Senescence associated secretory phenotype (SASP) or Senescence-Messaging Secretome (SMS) (discussed in the next section).

1.2.3. The SASP

The SASP includes a wide variety of factors with different functions, from cytokines and growth factors to metalloproteases and secreted receptors, which can have both cell autonomous and non-cell autonomous effects. Therefore, non-cell autonomous effects, some of which are apparently contradictory, of senescent cells are mediated by these factors.

Cell autonomous effects of the SASP

One of the beneficial effects of the SASP can be attributed to the reinforcement and maintenance of senescence, and therefore the cell growth arrest, in an autocrine manner. In Ras-induced senescence the production of stimulating ligands for chemokine (C-X-C Motif) Receptor 2 (CXCR2), also known as IL-8 receptor type 2, was shown to reinforce and maintain senescence and consequently its tumor-suppressor effect (50).

Non-cell autonomous effects of the SASP

The SASP has been shown to exert both pro-tumorigenic and pro-metastatic effects through the secretion of cytokines such as Interleukin-6 (IL-6), Interleukin-8 (IL-8), growth regulated oncogene-alpha (GRO-α), vascular endothelial growth factor (VEGF) or Amphiregulin (AREG), (33, 37-42). Many of these components can promote pre-malignant cell growth or invasion through their ability to induce angiogenesis, epithelial–to-mesenchymal transition (EMT) and differentiation within the local microenvironment (37, 39, 42-45).

Nevertheless, the non-cell autonomous effects of the SASP can also be beneficial through both the reinforcement and maintenance of senescence in a paracrine manner,

and the recruitment of the innate immune system that can clear senescent cells under certain circumstances (46-49). In the same Ras-induced senescence model as mentioned before, SASP factors of the transforming growth factor beta (TGFβ) pathway were shown to induce senescence through a paracrine effect (50). Furthermore, in oncogene-induced senescence liver models, the SASP is been proposed to promote tumor clearance through what has been termed as tumor surveillance. Some cytokines of the SASP can act as attractants of the immune system. Both the innate and adaptative immune responses have been shown to clear tumor cells by phagocytosis or cytotoxic-mediated killing (46-49, 51). However, this last effect could lead to a local chronic inflammation that ultimately could generate a pro-tumorigenic environment.

Mechanisms that generate the SASP

It has been proposed that persistent DDR is needed to maintain the SASP, as only sustained, but not short DDR is able to induce a SASP (33). Many but not all, SASP components are positively regulated by the DDR proteins ATM, Chk2 and Nijmegen Breakage Syndrome 1 (NBS1) (33). This regulation seems to be independent of the p53 induction, even more, p53 seems to restrain the SASP (52). Inactivation of p53 in senescent cells expressing a SASP showed an increase in the mRNA of several SASP factors (39). Furthermore, p53 inactivation in cells that do not express p16, caused senescence bypass and proliferation, but the SASP remained active (32,(39).

SASP is also positively regulated by the transcription factors nuclear factor kappa-B (NF-κB) and CCAAT/enhancer-binding protein beta (C/EBPβ). NF-κB has been shown to transcriptionaly activate key SASP factors such as IL-6 and IL-8 (35, 53, 54).

Further regulation of the SASP has involved a coupling between autophagy and the mammalian target of rapamycin (mTOR), which seems to enhance protein secretion. In Ras-induced senescence it was described a new cellular compartment at the trans side of the Golgi apparatus, the TOR-autophagy spatial coupling compartment (TASCC). Spatial association of anabolic and catabolic processes by accumulation of lysosomes and mTOR, favored the rapid secretion of SASP components such as IL-8 (55).

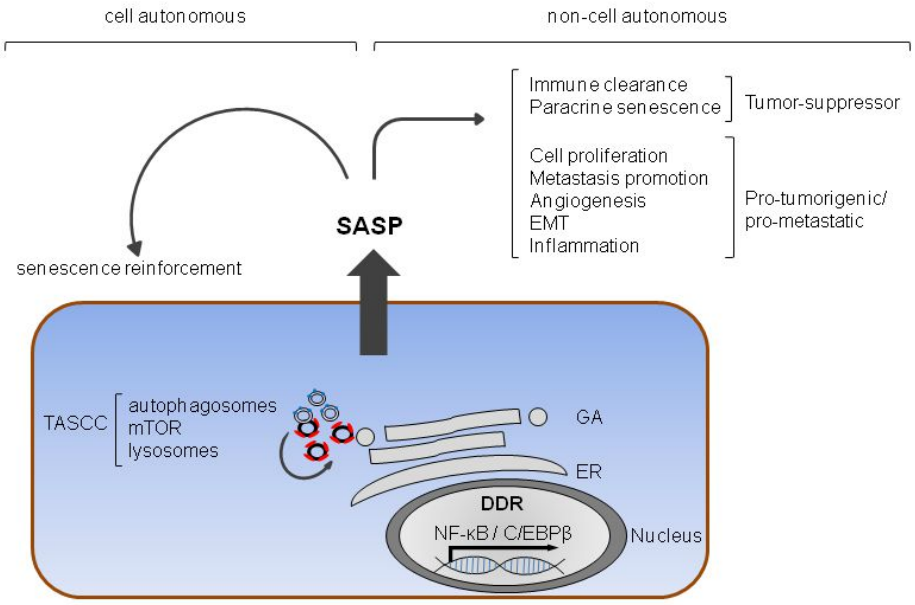

Fig. 3 Effects and mechanisms of generation and regulation of the SASP
Cell autonomous effects of the SASP are anti-tumorigenic as they reinforce senescence. Non-cell autonomous effects of the SASP can be eigher pro-tumorigenic by promoting cell proliferation, metastasis, angiogenesis, EMT and inflammation, or tumor-suppressive by inducing paracrine senescence and immune clearance of both senescent and non-senescent tumoral cells. (GA: Golgi apparatus, ER: endoplasmic reticulum).

1.3. Apoptosis and senescence in cancer treatment

Although it has been assumed that the major response to radio- and chemotherapeutic cancer treatments is apoptosis, a wide variety of commonly used anticancer agents such as doxorubicin, aphidicolin, cisplatin or etoposide, and gamma-irradiation have been shown to induce senescence (56).

Chemotherapy-induced senescence was first described in tumor cell lines (57, 58), as well as in a lymphoma mouse model with impaired apoptosis response, where senescence was shown to act as a tumor suppressor mechanism improving survival of mice (59) A part from *in vitro* studies and mouse models, senescence has also been proven in human tumor samples from breast (23), lung (22) or prostate cancer (39) after anti-cancer therapy.

In human tumors, clinical response to chemotherapy-induced senescence is usually related to a stable disease, rather than tumor regression (22, 23). In breast tumor samples resected after treatment with neoadjuvant chemotherapy, SA-β-GAL activity, together with high p16 and low p53 staining were detected. Those patients were

considered clinically to present a stable disease (23). In lung adenocarcinomas, chemotherapy induced a moderate reduction in tumor volume. This partial response was due to the bypass of therapy-induced senescence by the gain of mutations in CDK1, thus resulting in tumor progression (22).

In several studies, the status of p53 has been proven to determine the response to chemotherapy (23, 58, 60, 61). In ovarian carcinomas with wild-type p53, chemotherapy induced cell cycle arrest, in contrast to p53 loss-of-function (LOF) mutant samples. Although the described cell-cycle arrest was presumably senescence, in this work they did not use senescence markers to assess the cell status. Thus, the described DNA-damage-induced cell cycle arrest could be not senescence and instead a reversible arrest that could resume in proliferation after DNA-damage repair, which would also explain the relapse (61). Interestingly, in a Mouse mammary tumor virus - Wingless-type MMTV integration site family, member 1 (MTV-Wnt1)-inducible mouse model for mammary tumors, treatment with doxorubicin induced an apoptotic response in a p53-mutant background, while wild-type p53 tumors responded with senescence. Paradoxically, wild-type p53 associated with detrimental chemotherapy response. Apoptosis-responding tumors showed a complete response, while senescence-induced tumors were minimally responding and early relapsing. This response was related to the paracrine effects of the SASP inducing proliferation of the non-senescent neighboring cells (60).

The implication of the SASP in the chemotherapy-induced response has also been characterized in human tumor samples. Study of mRNA expression profile in prostate samples prior and after chemotherapy treatment showed increased levels of senescence markers such as p16 and p21, and SASP components such as IL-6 and IL-8. Although a relation between chemotherapy-induced senescence, SASP and clinical outcome was not established, the same SASP components were shown to induce EMT and invasiveness *in vitro* in epithelial breast cancer cell lines (39).

The above presented evidences support the idea that long-lived highly metabolically active senescent cells, can be detrimental in the overall tumoral progression, contrary to apoptotic cells that actually die and disappear from the cellular environment.

2. Signaling pathways regulating apoptosis and senescence

Different signaling pathways may connect the stressors that result in the onset of apoptosis or senescence, such as DNA damage, redox unbalances or oncogene

activation, with the factors required for this fate choice. In this section we will discuss the possible implication of the signaling through Mitogen-activated protein kinases (MAPK) and the phosphatase and tensin homolog (PTEN)-phosphatidylinositol 3-kinase (PI3K)/Akt/mTOR pathways, as well as the activation of the p53-p21 axis.

2.1. MAPK

The MAPKs belong to a family of highly conserved intracellular serine/threonine kinases. Three subfamilies exist in mammals and include extracellular signal-regulated kinases (ERK), c-Jun N-terminal kinases (JNKs, or stress-activated protein kinases; SAPKs) and p38-MAPKs. The MAPK pathways are mainly activated through ligand-binding activation of receptor tyrosine kinases (RTK), although other extracellular stimuli like G-Coupled Receptor (GPCR), UV irradiation, genotoxic agents, oxidative stress or cytokine stimulation can also trigger their activation.

It has been shown that ERKs are important for cell survival after growth stimulation (62, 63). ERK 1 and 2 isoforms are activated by phosphorylation by Mitogen/Extracellular signal-regulated Kinases 1 and 2 (MEK1,2), which convey upstream activation of Ras and Rapidly accelerated fibrosarcoma (RAF). Following activation, ERKs translocate to the nucleus and phosphorylate a variety of substrates which mainly promote cell survival (62). In addition, ERK1,2 have also been shown to be important in Ras-induced senescence by regulating the proteasome degradation of cell cycle progression proteins (64).

On the other hand, JNKs and p38-MAPK are known to regulate stress response modulating proliferation, differentiation, senescence, apoptosis, autophagy or metabolism (62, 63).

JNKs are specifically activated by Mitogen-activated protein kinase kinases 4 and 7 (MKK4 and MKK7). JNKs, which also translocate to the nucleus when activated, have been reported to directly activate transcription factors implicated in both anti-apoptotic and pro-apoptotic signal. These transcription factors include c-Jun, p53 or Myc as well as non-transcription factors such as Bcl-2 and Bcl-XL (62).

p38-MAPKs include the isoforms α, β, γ and δ. However, the majority of the published literature on p38-MAPKs refers to p38α as it is the most ubiquitously expressed (63). Mitogen-activated protein kinase kinases, MKK3 and MKK6 phosphorylate and activate p38-MAPKs. These MAPKs control the function of transcription factors, kinases, or phosphatases (62). Similarly to JNKs, p38-MAPKs are also stress responsive MAPKs

implicated in both pro- and anti- apoptotic signal, as well as in cell cycle regulation and senescence. Early studies related p38 to a mitotic arrest by regulating the spindle assembly checkpoint (65), others have shown that p38 can also modulate the cell cycle by regulating G1/S and G2/M checkpoints by downmodulating cyclin D1 (66) or activating the p53/p21 and/or p16/Rb pathways (67-70). Recently, p38 has been involved in oncogene-induced senescence triggered by oncogenic Ras or its downstream effector BRAF. According to these studies the MKK3/6-p38 pathway acts downstream of the RAF/MEK/ERK cascade to mediate Ras-induced senescence. Active p38 regulates p53 activity through direct phosphorylation and in addition by regulating the downstream Ser/Thr protein kinase PRAK (p38 regulated activated kinase) which in turn phosphorylates p53 (71). Furthermore, it is also known that p38 can suppress the transformation of normal epithelial cells and activate anoikis, which prevents aberrant localization of epithelial cells (72, 73).

2.2. PTEN/PI3K/Akt/mTOR

The PI3K/Akt/mTOR pathway is frequently activated in human cancer. Alterations that lead to constitutive activation of this pathway in cancer include genetic and epigenetic inactivation of PTEN, overexpression or activating mutations of PI3K and overexpression of Akt also known as Protein kinase B (PKB).

Activation of PI3K catalyzes the transformation of the secondary messenger phosphatidylinositol 4,5 diphosphate (PIP2) to phosphatidylinositol 3,4,5 triphosphate (PIP3). The tumor suppressor PTEN antagonizes the PI3K activity by dephosphorylating PIP3 to PIP2. Accumulation of the PIP3 pool in the membrane facilitates the recruitment of pleckstrin-homology (PH) domain-containing proteins including the protein serine/threonine kinases Akt and phosphatidyl inositol-dependent protein kinase 1 and 2 (PDK1 and 2) to the membrane. This localization allows the phosphorylation of Akt by PDK1. Akt is a protein-Ser/Thr kinase that binds to phosphatidylinositol triphosphate with high affinity. PDK1 and mTOR complex 2 (mTORC2) activate Akt by phosphorylating it at Thr308 and Ser473, respectively. Phosphorylation stimulates the catalytic activity of Akt, which in turn phosphorylates and activates the protein-serine/threonine kinase mTOR among other effector proteins involved in the regulation of cell growth and proliferation, cell death and cell survival (74-76).

PTEN deficiency or Akt activation have been described to induce cellular senescence. Loss of PTEN is considered a specific type of oncogene-induced senescence (PTEN-

loss induced cellular senescence, PICS) (34). This type of cellular senescence occurs rapidly without an early phase of hyperproliferation, DDR or ATM activation. Additionally, it occurs through activation of mTOR complex 1 (mTORC1), requires p53 activity and engages p21 (77). Furthermore, PTEN and p53 regulate each other. PTEN protects p53 from the degradation mediated by HDM2, whereas p53 can enhance the transcription of PTEN. Thus, inactivation of either gene results in lower protein levels of the other (78).

Finally, PTEN status can also influence the response to stress. Studies on human glioma cells have shown that in response to irradiation, cells with wild-type PTEN undergo apoptosis, whereas PTEN-null glioma cells undergo Reactive oxygen species (ROS)/p53/p21-dependent senescence (79). Conversely, Akt deficiency confers resistance to replicative- and Ras-induced senescence and promotes apoptosis under conditions of oxidative stress (80).

2.3. p53

p53 is a transcription factor that exerts tumor-suppressive functions by regulating the expression of effector genes implicated in the control of apoptosis (i.e. PUMA, Noxa, BID or BAD) (81), and senescence (i.e. p21, 14-3-3δ). In addition, p53 also regulates the expression of genes involved in energy metabolism and autophagy (82, 83).

Up to 50% of human tumors carry inactivating mutations in the p53 gene (84), making it one of the most frequently mutated genes in cancer. Even in tumors that retain a wild-type p53 gene, its function is generally compromised, largely due to deregulation of its destructor HDM2 (85).

Although much of the regulation of p53 activity is determined by the stability of the p53 protein, a large number of post-translational modifications on p53 also regulate DNA binding and engagement of the transcriptional machinery. These modifications include phosphorylation, ubiquitination, acetylation, methylation, sumoylation and neddylation. Usually, phosphorylation at Ser15 and Ser20 reduces p53 affinity for its negative regulator HDM2 and promotes the recruitment of transcriptional co-activators. HDM2 is an E3-ubiquitin ligase which negatively regulates p53 by mono- or poly-ubiquitinating it. Ubiquitination targets p53 for proteasomal degradation. In addition, HDM2 can also directly bind p53 and consequently repress its transcriptional activity. Additional

regulation of p53 and HDM2 is exerted by a negative feedback loop as HDM2 itself is a transcriptional target of p53 (83).

Some models have been suggested to explain how p53 regulates the onset of apoptosis and senescence (86). Some reports indicate that it could be cell type-dependent as different cell types might keep different p53-regulated genes in regions of active chromatin, and that would determine the group of genes that are transcriptionally upregulated (29, 87). Reactivation of functional p53 in pre-existing p53-deficient tumors resulted in widespread apoptosis or senescence, and lymphomas appeared to be particularly prone to apoptosis, whereas senescence was the primary response in sarcomas and liver carcinomas (46, 88, 89). It has also been proposed that the amount of DNA damage is determinant for the final decision: more profound DNA damage induces higher and prolonged activation of p53, which increases the chances of apoptosis over senescence (90). Finally, it has also been proposed that the availability of transcriptional cofactors is what determines the ability of p53 to activate different subsets of genes (91, 92).

Although p53 is considered the major regulator of apoptosis and senescence upon DNA damage, p53-independent senescence and p53-independent apoptosis have also been described. It has been suggested that p53 independent apoptosis involves caspase-2, the only pro-caspase constitutively present in the nucleus (93, 94). Caspase-2-induced apoptosis also requires caspase-9 activation (95), indicating that caspase-2 acts through the mitochondrial pathway. As for p53-independent senescence, there have been several previous reports showing that genetic loss of p53 does not enable escape from oncogene-induced senescence (96-98).

2.4. p21

The p21 protein, encoded by the cyclin-dependent kinase inhibitor 1A (CDKN1A) gene, is part of the CDK inhibitory protein/kinase inhibitory protein (Cip/Kip) family of CKIs, which also includes p27 and p57.

Although several p21 mutations have been reported in human cancers, and they are present in more than 10% of invasive bladder cancers, the overall conclusion from various large-scale studies is that in general p21 mutations are exceedingly rare (99). Apart from mutational status, p21 expression has also been studied, usually as a marker for functional activity of p53. However, the conclusion from those studies has been that p21 expression either has no prognostic value, or that tumor progression and

bad prognosis can either correlate with lack or with overexpression of p21 depending on the cancer type (100).

p21 can bind and inhibit a broad range of CDK-cyclin complexes, with preference for those containing CDK2. p21 plays an essential role in growth arrest after DNA damage, and its overexpression leads to G1 and G2 arrest (30, 31) or to a delay on the S phase progression (101). Accordingly to the tumor suppressor role of p21, p21 deficient cells are unable to arrest upon DNA damaging agents (102) and p21-null animals develop tumors spontaneously (103) or present increased tumor susceptibility using chemical carcinogenesis (104-108). The tumor suppressor p53 is considered the main transcriptional regulator of p21 (109). However, while p21 is absolutely required for p53-mediated cell cycle arrest (110), p21 can also be regulated in a p53-independent manner (101, 111, 112).

Diverse signals can induce p21 transcription in a p53-independent manner such as TGFβ (111) or the protein kinase C (PKC) among others (101). In addition, p21 transcription can also be negatively regulated by transcriptional repressors such as Myc which acts through the transcription factor Myc-interacting zinc-finger protein 1 (Miz-1) (113). Apart from the transcriptional regulation, p21 is also regulated at the level of mRNA and protein stability (114).

In addition to its role in cell cycle inhibition, and thus, in controlling senescence, p21 has also been shown to act as an anti-apoptotic molecule. The mechanisms by which p21 exerts its anti-apoptotic function are not fully understood, and many have been suggested. Some works indicate that the same CDK inhibitory function is necessary to inhibit apoptosis. Another possible mechanism is the repression of the E2F transcription factor both in a CDK-Rb-dependent and independent manner, as it was found to regulate some secreted anti-apoptotic proteins in a p21-dependent manner. In addition, p21 can also interfere with Myc-induced apoptosis by functional inactivation of the active Myc:Myc-associated factor X (MAX) complexes (Myc:MAX) and by suppressing its expression (115). Finally, p21 can also inhibit cell death via direct binding to apoptosis modulators such as pro-caspase-3 inhibiting its activity (116), cellular inhibitor of apoptosis protein 1 (c-IAP1) causing its stabilization (117) or caspase-2 resulting in its downregulation (118). In addition, other works suggested that p21 exerts its anti-apoptotic function after phosphorylation by Akt in Thr145 and subsequent stabilization in the cytoplasm, although the importance of its subcellular localization seems to be controversial (119) (120).

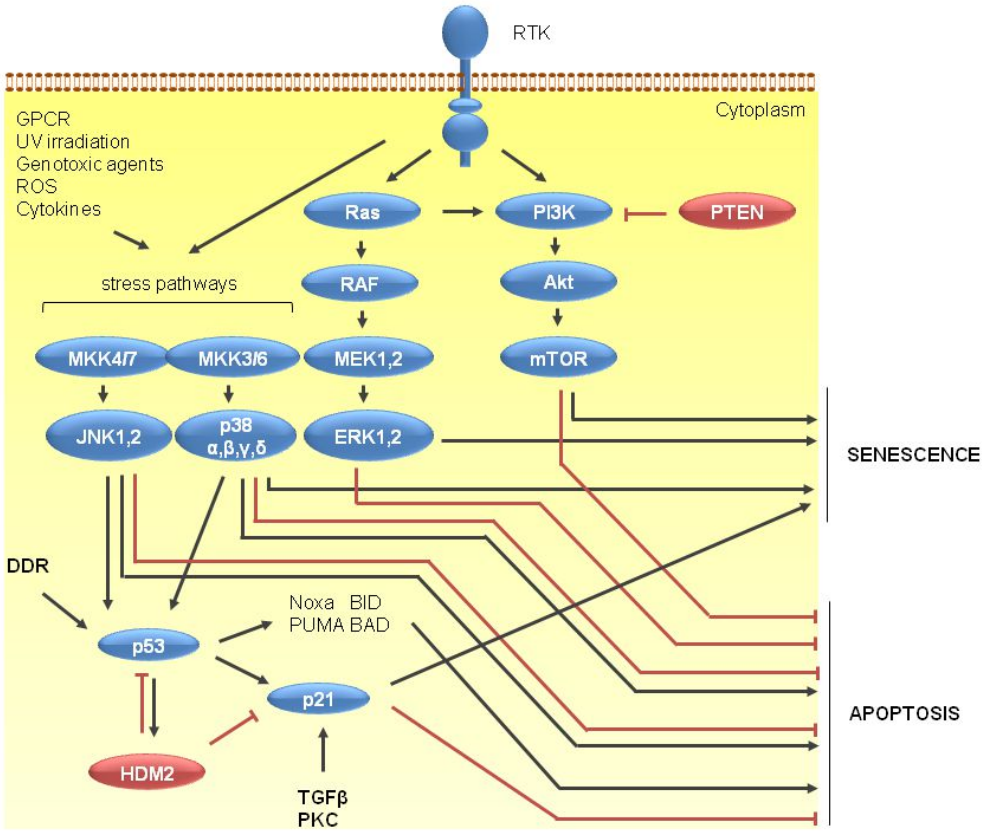

Fig. 4 MAPK, PTEN-PI3K/Akt/mTOR, p53 and p21 pathways in the regulation of both apoptosis and senescence
MAPK and PI3K pathways are activated mainly by RTKs. ERK1,2 MAPK pathway can promote cell survival, by inhibiting apoptosis, or promote senescence downstream of Ras. JNK and p38-MAPKs are stress pathways that can be both pro- and anti- apoptotic. p38-MAPK is also associated to induction of senescence. Both JNK and p38-MAPKs can phosphorylate and activate p53. Transcription factor p53 is also activated by the DDR and regulates transcription of both pro- and anti- apoptotic genes. HDM2 is a p53 negative regulator. p53 induces senescence through induction of p21. p21 induction can be p53-dependent or through TGFβ or PKC. p21 can be both pro-senescent by inhibiting the cell cycle progression or anti-apoptotic.

3. Oncogene-induced senescence and oncogene-induced apoptosis in cancer

Among the many different stimuli that can activate both cellular fates, in this work we will focus on oncogenes. Oncogenesis is a multistep process during which normal cells are reprogrammed to undergo malignant progression. However, cells have intrinsic tumor suppressor mechanisms in response to this aberrant oncogene activation. Oncogenes cause cellular stress that in turn engage the DDR leading to activate two main tumor suppressor mechanisms termed oncogene-induced senescence (OIS) and oncogene-induced apoptosis (OIA).

3.1. Oncogenes inducers of apoptosis

3.1.1. Myc

The c-Myc proto-oncogene encodes for the transcription factor Myc, which is one of the most frequently affected genes in human cancers and even though it has been described to regulate many different processes such as growth, differentiation, apoptosis and senescence, it is the prototypical studied gene for oncogene-induced apoptosis.

Activated Myc usually induces apoptosis in a p53-dependent manner, by initiating the DDR and activating the ADP-ribosilation factor (ARF)/HDM2/p53 pathway. Accordingly, Myc-driven lymphomas are often mutated in this pathway. Transcriptional upregulation of ARF in response to Myc stabilizes p53 and activates p53 controlled pro-apoptotic genes such as PUMA and Noxa as shown in Eμ-Myc lymphoma mouse model (121-124). However, Myc can also induce apoptosis independently of p53 by suppressing anti-apoptotic genes such as Bcl-2 and Bcl-XL (125) or up-regulating the p53-independent expression of pro-apoptotic BIM (126, 127).

Normal expression of the c-Myc gene is tightly regulated at both transcriptional and post-transcriptional levels. The MAPK pathway is responsible to induce c-Myc transcription while both, Ras/RAF and PI3K/Akt signaling cooperate to promote Myc protein stability in response to optimal growth conditions (128).

Myc exerts its effect on cell cycle by activating transcription of D-type cyclins and CDKs to promote cell cycle check point progression (129, 130). At the same time, Myc represses the expression of Cip/Kip family cyclin-CDK inhibitors such as p21 (131). Myc is direcly recruited to the p21 promoter through Miz-1. This interaction, blocks p21 induction by p53 and as a consequence, Myc contributes to the induction of apoptosis by p53.

Moreover, Myc has been shown to inhibit oncogene-induced senscence as co-expression of Ras and Myc showed Myc suppression of Ras-induced senescence dependent on the phosphorylation of Myc by CDK2. However, expected from Myc capacity of inducing DDR activation, Myc is also able to induce premature senescence although only in a CDK2-defficient context (132).

3.2. Oncogenes inducers of senescence

3.2.1. Ras

Activated H-Ras is the prototype oncogene that has been used to study oncogene-induced senescence. It was the first oncogene described to induce senescence in rodent and human fibroblasts (29), but it has also been shown to induce senescence in transformed epithelial cells (133).

The RAS proto-oncogene family consists on H-RAS, N-RAS and K-RAS, which encode for small monomeric GTPases involved in intracellular signal transduction. Activating mutations in RAS genes occur in 30% of all tumors (134). K-Ras-G12V (135, 136) has been shown to trigger senescence during early stages of lung and pancreatic adenocarcinomas (137), and N-Ras-G12D was shown to increase susceptibility to chemotherapy-induced senescence in lymphocytes (138). *In vivo* mouse models have used inducible H-Ras-G12V to trigger senescence in the mammary epithelium (139) or conditional expression of K-Ras-G12V to develop premalignant lesions in the lung and pancreas of mice (135, 136). Inducible H-Ras-G12V in the mammary gland triggered either cellular transformation or senescence depending on the expressed levels, showing that only high levels of the mutant Ras were able to induce senescence (139).

Oncogenic activation of Ras by receptor tyrosine kinases (RTK) is mediated by Grb2/SOS (Growth factor receptor-bound protein 2/ son of sevenless) complex. Activated Ras stimulates several different effector pathways, being the two best characterized the MAPK and the PI3K/Akt pathways (140).

Ras-induced senescence has been shown to happen in a biphasic way as it drives an initial hyperproliferation phase that induces a DDR activation, which in turn ends the hyperproliferative phase and engages and maintains cellular senescence. Thus, the DDR seems to be essential and causative for the establishment and maintenance of not only Ras, but also senescence induced by other oncogenes (21, 24, 141, 142). In contrast to replicative senescence, during OIS DDR is mainly activated by ATR-dependent checkpoint and not ATM (21).

Initial reports showed that H-Ras-G12V-induced senescence required p53 and p16 *in vitro* in fibroblasts (29) and depends on MAPK activation (143, 144). The implication of p53 and p16 in Ras-induced senescence has also been shown *in vivo* in the mammary gland (139) and in a liver sarcoma model (47). H-Ras-G12V expression has also been

shown to induce senescence in human ovarian epithelial cells through induction of p21 in a p53-independent manner (133).

3.2.2. BRAF

BRAF is a member of the RAF family of serine/threonine kinases, which is directly activated by Ras (145). Therefore, a substantial overlap between BRAF- and Ras-regulated genes would be expected. BRAF activates the MAPK pathway by phosphorylating and activating MEK that in turn phosphorylates ERK1,2.

BRAF mutations are common in cancer, particularly in melanoma where they occur at a frequency of 50-70%. BRAF-V600E is the most frequent genetic alteration, accounting for approximately 90% of activating BRAF mutations (146). This mutant form is able to constitutively signal through MEK/ERK independently of Ras activation. BRAF-V600E induces senescence in primary melanocytes *in vitro* and in humans is found expressed in benign nevi together with senescence markers (147). Benign nevi very rarely develop into fully malignant melanomas for which a second genetic alteration is needed.

Studies on BRAF-induced senescence showed that physiological expression levels were enough to induce p16 and cell cycle arrest. However, p16 was not strictly necessary for this arrest (147). In this same direction, a study in human astrocytes showed that human cells might have redundant arrest pathways as in p16/Rb depleted cells, RAF was still able to induce growth arrest through p21 in a p53-independent manner (148). Interestingly, BRAF mediated senescence has also been shown to occur through an autocrine/paracrine pathway that establishes a negative feedback loop through the secreted factor insulin-like growth factor binding protein 7 (IGFBP7) (149).

3.2.3. PTEN

As mentioned before, PTEN is a negative regulator of the PI3K/Akt/mTOR pathway. Thus, PTEN is considered a tumor suppressor and is frequently altered in cancer and, in particular, in prostate cancer in which approximately 70% of primary prostate tumors have lost at least one allele of PTEN. Therefore, senescence induced by PTEN loss cannot strictly be considered as oncogene-induced senescence and has been specifically termed as PTEN-loss-induced cellular senescence (PICS) (34).

Complete loss of PTEN has been shown to induce senescence in both mouse embryonic fibroblasts (78) and in mouse prostate epithelium (34). In the same direction, as PTEN loss induces PI3K/Akt enhanced signaling, PI3K/Akt-induced senescence has also been documented (77). Contrary to Ras-induced senescence, both PTEN-loss and enhanced PI3K/Akt-induced senescence lack the initial hyperproliferative state and occur in the absence of DNA damage, although in a p53-dependent manner (34, 77, 78). The fact that PICS occurs in the absence of DDR and that DDR has been associated to the regulation of the SASP, opens the question whether a specific SASP is induced in PICS, and whereas it is pro-tumorigenic or not needs to be determined (150).

Conditional knock-out mice for concomitant PTEN and p53 deficiency in the prostate, showed increased invasive prostate cancer. In contrast, PTEN deficiency in p53 proficient mice showed that PTEN loss can induce senescence that acts as a tumor barrier (34). In addition, PTEN status has been shown to be determinant for the response of glioma cells to irradiation (IR) exposure. In response to IR, PTEN deficient glioma cells activated senescence in an Akt/ROS/p53/p21-dependent manner, whereas PTEN proficient cells underwent apoptosis (79).

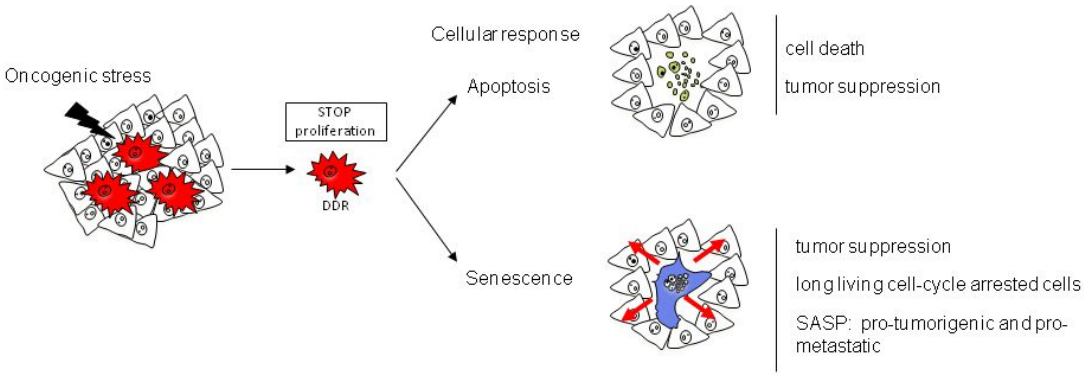

Fig. 5 Oncogene-induced senescence and oncogene-induced apoptosis implications in cancer progression
Upon oncogenic stress DDR is activated leading to either apoptosis or senescence. Cells undergoing apoptosis disappear from the tumor within few hours time, while senescent cells are long living cell cycle arrested cells that can exert pro-tumorigenic and pro-metastatic effects through the SASP.

3.3. Oncogene-induced senescence *in vivo*

3.3.1. Oncogene-induced senescence mouse models

Oncogene-induced senescence effects *in vivo* have been extensively studied with many mouse models.

Conditional K-Ras-G12D expression has been used to study initiation and progression of lung adenocarcinomas allowing the study from precursor lesions to malignant tumors (151). In this model, the presence of oncogen-induced senescent cells was detected along the tumor progression process. Senescent cells were abundant in premalignant lesions while they were almost undetectable in fully blown tumors, pointing to oncogene-induced senescence as an initial tumor suppressor mechanism in the early steps of tumor progression (135). Similarly, a conditional mouse for K-Ras-G12D expression in the pancreas provided a model for development from pre-invasive pancreatic intraepithelial (PanIN) lesions to invasive and metastatic pancreatic cancer. Interestingly, K-Ras-G12D expression induced senescence and development of PanIN lesions that rarely progressed to malignant pancreatic ductal adenocarcinoma (PDAC). Oncogene-induced senescence was considered a tumor barrier also in this model, as the further introduction of a second alteration, such as p53 knockout, was needed to induce tumor formation (136).

Different Ras-induced liver carcinoma mouse models have been used for the study of the induction of immune-surveillance by OIS. Immune surveillance facilitates the clearance of both senescent and tumorigenic cells. Studies on chimaeric liver cancer mouse model expressing H-Ras-G12V (152) combined with conditional p53 shRNA showed rapid formation of invasive hepatocarcinomas. H-Ras-G12V-induced senescence in the presence of functional p53, drove the induction of innate immune responses to clear tumoral cells and limit tumor growth (47). Similarly, premalignant senescent cells were detected in mouse livers transduced with N-Ras-G12V. The SASP produced by these senescent cells was found to mediate immune-surveillance to clear senescent cells (48).

In the same direction, a conditional BRAF-V600E knock-in mouse model was shown to generate benign lung tumors that rarely progressed to adenocarcinomas. Combination with mutation of INK4A/ARF, genomic locus for p16-(INK4A) and p19-(ARF), or p53 was needed to promote cancer progression (153). Finally, PTEN loss-induced senescence has also been studied in mouse models as a tumor suppressive

mechanism. Prostate-specific inactivation of PTEN led to the identification of senescent cells in benign lesions in the prostate of the mice. Combined inactivation of PTEN and p53 induced invasive prostate cancer (78).

3.3.2. Oncogene-induced senescence in human premalignant lesions and tumors

The observation of cell senescence in tumors has not been restricted to mouse models, but has also been reported in human malignancies. Oncogene-induced senescence has been shown to be a physiological mechanism in humans limiting the progression of premalignant lesions (138). Initial reports demonstrating OIS in premalignant lesions showed that nevi, which are largely growth-arrested neoplastic lesions, are in fact BRAF-V600E-induced senescent melanocytes (135, 147). Similarly, senescence is also found in other pre-malignant tumors such as lung adenomas, pancreatic intraductal neoplasias and prostatic intraepithelial neoplasias (PIN) lesions reinforcing the idea of senescence as a barrier for tumor progression (154).

However, some evidences also support the pro-carcinogenic function of normal senescent cells *in vivo* by the findings that SA-β-GAL expression in normal human hepatocytes strongly correlated with the presence of hepatocellular carcinoma in the surrounding liver (155), and that prostate enlargement correlates with SA-β-GAL expression in prostate epithelial cells (156).

4. HER/ErbB oncogenes

4.1. The HER/ErbB family

The Human epidermal growth factor receptor/avian erythroblastosis oncogene (HER/ErbB) receptor tyrosine kinase family includes four transmembrane glycoproteins: Epidermal growth factor receptor (EGFR, ErbB1, HER1), HER2 (ErbB2, neu); HER3 (ErbB3), and HER4 (ErbB4) (157). Deregulated expression or activity of these receptors underlies development of a range of epithelial tumors in numerous tissues such as lung, breast or central nervous system (158). EGFR, HER2 and HER3 are validated therapeutic targets in cancer and inhibitors and monoclonal antibodies have been developed and can be considered among the most successful examples of targeted therapies to date (159, 160).

4.1.1. HER/ErbB family structure and activation

Typically HER/ErbB receptors are activated through ligand-induced homo- or hetero-dimerization driven by their extracellular domains. Ligand binding to the extracellular domain results in conformational changes that promote and stabilize receptor dimerization, resulting in structural changes in the transmembrane and intracellular domains, which lead to the allosterical activation of the kinase domains (161).

HER/ErbB receptors have a large extracellular region of approximately 620 aminoacids that can be subdivided into four domains. Domains I and III are rigid β-helix/solenoid structures related to one another, which serve as the primary ligand binding regions. Domains II and IV are cysteine-rich domains that share similarities with laminin repeats and contain a string of disulfide-bonded modules. A single transmembrane domain links the extracellular region to the intracellular part of the receptor that contains a tyrosine kinase domain as well as a carboxy-terminal tail (159).

EGFR is regulated by at least seven different activating ligands in humans: Epidermal growth factor (EGF), Transforming growth factor alpha (TGFα), Betacellulin (BTC), Heparin-binding epidermal growth factor (HB-EGF), AREG, Epiregulin (EPR) and Epigen (EPGN), all of them synthesized as membrane-bound precursor proteins that can be cleaved by cell surface proteases to yield the active growth factors. HER3 and HER4 are bound by neuregulins (NRGs), also called heregulins (HRGs), produced from four genes (NRG1-4). HER2 is the only member of the family for which no soluble ligand has been described (159, 162).

Dimerization is driven almost exclusively by a dimerization arm that projects from domain II, although inter-receptor domain IV contacts may also contribute weakly. Receptors exist in a “close” or inactive conformation in which domain II dimerization arm is buried by intramolecular interactions with domain IV. Ligand bivalent binding to domains I and III of a single receptor molecule induces a conformational change that exposes the dimerization arm yielding to the “open” or active conformation of the receptor that makes it dimerization-competent. HER2 exists in a constitutively active conformation ready to dimerize mimicking a ligand-bounded form. Finally, both extracellular and transmembrane domains of the receptors contribute to maintain the dimerization (159).

Although HER/ErbB receptors act in a combinatorial fashion, i.e. they can form all ten possible complexes, HER2 is the preferred partner for heterodimerization. Furthermore, complexes containing HER2 are more active (163).

The catalytic domain of HER/ErbB receptors is activated by the formation of an asymmetric dimer in which one kinase domain, the “activator” acts as an allosteric regulator for a second “receiver” kinase domain (164). The juxtamembrane region is thought to regulate this allosteric tyrosine kinase activation (165). This activation mechanism explains how HER2 is activated by HER3, which has a structurally impaired catalytic site and a residual kinase activity. HER3 is regarded as a pseudo-kinase due to the absence of several catalytically important residues, but conserves the activator surface of the asymmetric dimer interface. Thus, it can activate other HER/ErbB kinases by taking the activator position (159).

Following activation, a series of tyrosines in the carboxy-terminal tail become phosphorylated in trans and serve as docking sites for adaptor phosphotyrosine-binding molecules containing Src homology 2 (SH2) and phosphotyrosine-binding (PTB) domains, which initiate the signaling cascades. Ultimately, these cascades regulate the expression of groups of genes that control cell proliferation, differentiation, migration and survival (159, 166, 167).

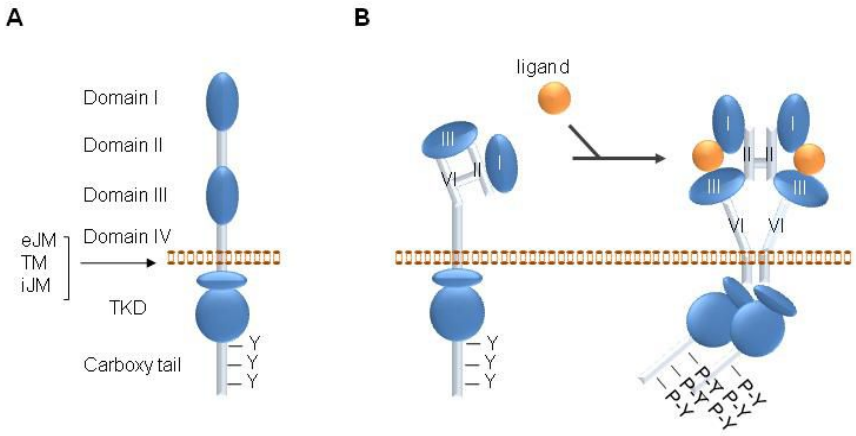

Fig. 6 HER/ErbB receptors structure and activation
Schematic representation of HER/ErbB family receptors and their activation mechanism. **(A)** Domain composition of HER/ErbB family receptors is shown. The extracellular region contains four domains (I-IV), domains I and III are similar in sequence, as well as are domains II and IV. A short extracellular juxtamembrane (eJM) domain separates the extracellular region form the transmembrane (TM) domain. In the intracellular region, a short intracellular juxtramembrane (iJM) separates the tyrosine kinase domain (TKD) from the membrane. The TKD is followed by a carboxy-terminal tail that contains several tyrosine autophosphorylation sites. **(B)** Ligand-induced dimerization and allosterical activation of HER/ErbB receptors, except for HER2 which exists in the activated form and for which no soluble ligand has been described. In the absence of bound ligand, the dimerization arm from domain II forms autoinhibitory interactions with domain IV and the extracellular region adopts the so-called “close” conformation. Upon ligand binding to domains I and III, the dimerization arm from domain II is exposed and extracellular regions dimerize. Proximity between the two TKD induces the formation of an asymmetric dimer that leads to allosterical kinase activation leading to the trans-phosphorylation of tyrosine residues in the carboxy-terminal tail.

4.1.2. HER/ErbB family signaling network

The intracellular signal transduction pathways initiated by dimeric HER/ErbB receptors begin with different signaling molecules able to directly bind to the phosphorylated receptors. Among them, adaptor proteins like Src homology 2 containing (Shc), growth factor receptor-bound protein 2,7 (Grb2, Grb7), CT10 (chicken tumor virus number 10) regulator of kinase (Crk) or non-catalytic region of tyrosine kinase (Nck). In addition, intracellular kinases such as Sarcoma (Src) or PI3K or lipases like Phospholipase C-gamma (PLCγ) also directly bind to the receptors. Finally, the receptors can also bind negative regulators such as members of the ubiquitinilation machinery like the E3 ubiquitin ligase Casitas B-lineage Lymphoma (Cbl) or protein tyrosine phosphatases like Src homology domain 2-containing protein-tyrosine phosphatase 1 and 2 (SHP1 and 2). These bound proteins transmit the activation signal from the receptor to different signaling pathways, regulating a variety of biological functions such as cell proliferation and survival, to angiogenesis or migration and invasion (158, 168).

Activation of the PI3K pathway can occur by direct recruitment of the p85 regulatory subunit to the activated receptors or by indirect binding through adaptor molecules. HER3 and HER4 contain six and one putative p85 binding sites, respectively while EGFR and HER2 bind p85 through adaptors. Signaling through this pathway participates in many cellular processes including cell survival as mentioned in the section 2.2.

The activation of the ERK1/2 MAPK pathway occurs through the adaptor proteins Grb2 or Shc, which bind to several phosphotyrosine residues in all the four members of the family. These adaptor molecules associate with the Ras-guanine nucleotide exchange factor SOS, which mediates the exchange of Guanosine triphosphate (GTP) for Guanosine diphosphate (GDP) initiating the RAS/RAF/MEK/ERK1,2 signaling pathway. Other MAPKs activated in the HER/ErbB signaling are JNK and p38, activated through adaptors like the Rho family of GTPases which activate the upstream kinases for the pathway (MKK4/7 or MKK3/6) via p21-activated kinase 1 (PAK1). Activation of this pathway has already been described in section 2.1. (158, 168).

Additionally, HER/ErbB receptors can bind several adaptor proteins such as Vav2, a guanine nucleotide exchange factor for the Rho family of Ras-related GTPases such as Rho related C3botulinum toxin substrate (Rac), necessary for mediating some protein-protein interactions. Among others, Nck1,2 are SH2 and SH3 containing domains adaptor proteins that interact with and activate many signaling proteins including Ras or CrkI and CrkII, which regulate transcription and cytoskeletal reorganization for cell growth and motility by linking tyrosine kinases to small G proteins (168).

EGFR and HER4 bear binding sites for the non-receptor protein-tyrosine kinase Src, which plays important roles in proliferation and survival. EGFR, HER2 and HER4 have several potential PLCγ phosphotyrosine binding sites. PLCγ binds to the phosphotyrosines of the HER/ErbB family through the SH2 domain and it is activated upon direct phosphorylation by the receptor or by other protein kinases at Tyr783. After activation, PLCγ catalyzes the hydrolysis of PIP2 to form inositol 1,4,5-triphsophate (IP3) and diacylglycerol (DAG). Inositol triphosphate promots the release of Ca2+ from the endoplasmic reticulum and DAG activates the protein Ser/Thr kinase C (PKC), which has a broad substrate specificity with many divergent physiological effects including angiogenesis, cell proliferation, cell death, increased gene transcription and translation, cell migration and cell adhesion (169).

Human Src homology domain 2-containing protein-tyrosine phosphatases 1 and 2 (SHP1 and SHP2) are cytosolic protein-tyrosine phosphatases known to be negative regulators of EGFR by dephosphorylating it (169).

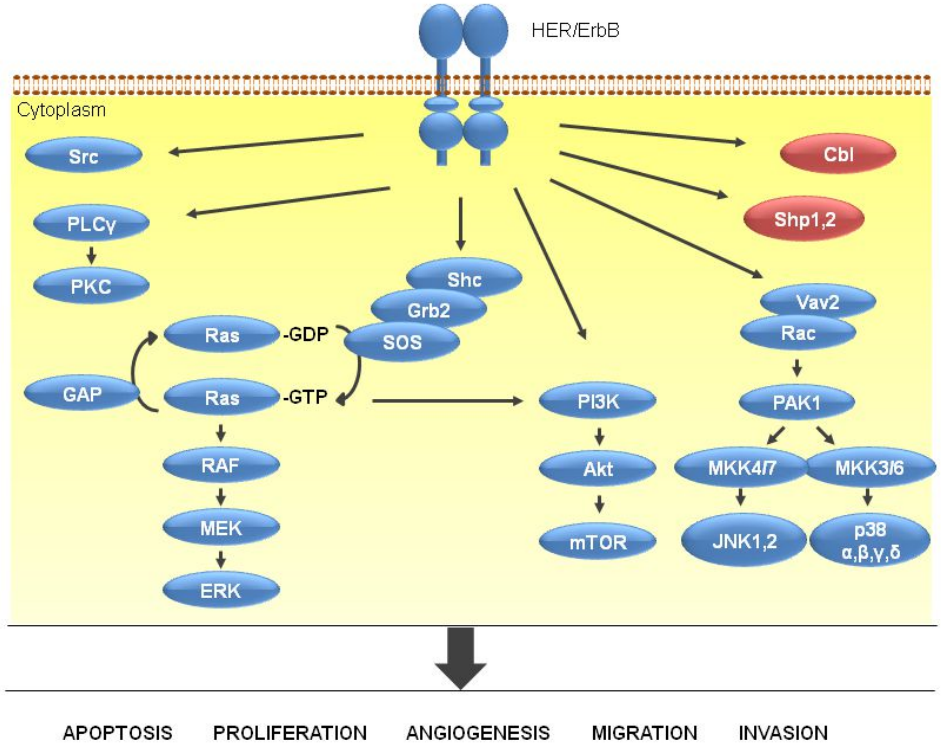

Fig. 7 HER/ErbB signaling network
Representation of the main signaling pathways activated by HER/ErbB receptors depicted in blue. HER/ErbB molecules that bind to the receptors but act as negative regulators depicted in red. Activation of these pathways leads to the regulation of several cellular responses such as apoptosis, proliferation, angiogenesis, cell migration or invasion.

4.2. HER2 and p95HER2 in breast cancer

HER/ErbB family members have a prominent role in the initiation and maintenance of several solid tumors. As a consequence, they have been extensively studied as targets for inhibition of tumor growth and progression. HER2 oncogene and breast cancer will be discussed in detail in the following sections as they are the main focus of this thesis.

4.2.1. Breast cancer classification

Breast cancer is a heterogeneous disease that can be classified in different clinical subtypes with diverse biological features that lead to differences in response to anit-tumor therapies. Traditional classification systems use immunohistochemistry (ICH)

detection of estrogen receptors (ER), progesterone receptor (PR) and HER2 to classify breast cancer into three major groups: hormone receptor positive group, which expresses ER and/or PR; HER2 positive group, which expresses HER2 by IHC or amplification detected by fluorescence in-situ hybridization (FISH); and the triple negative breast cancer (TNBC) group, which is negative for ER, PR and HER2 (170).

More recently, global gene expression profiling studies have provided evidence for classifying breast cancer into distinct molecular subtypes (171). This study identified four groups of samples that might be related to different molecular features of mammary epithelial biology: ER-positive/luminal-like, basal-like, HER2-positive and normal breast. ER-positive tumors, which account for approximately 75% of breast cancers, were found to express, in addition to ER and/or PR, ER-responsive genes and other genes that encode typical proteins of luminal epithelial cells, so they were termed as luminal-like group (sub-classified in luminal-A and luminal-B). The ER-negative group was further divided into distinct biological subtypes of tumors: basal-like, HER2-positive and normal-like subtypes. Basal-like tumors expressed many of the characteristics of breast basal epithelial cells that did not express ER and showed staining with basal keratins (171-173).

4.2.2. HER2 and p95HER2 positive breast cancers

HER2 is overexpressed in 20% to 30% of breast cancer tumors due to gene amplification, and its overexpression correlates with the severity of the malignancy (174-176). In addition, it is also found amplified in esophageal and gastric cancers. Approximately 30% of HER2 positive tumors accounts for a subtype of particularly poor clinical outcome which expresses, in addition to full-length HER2, a heterogeneous series of HER2 carboxi-terminal fragments (CTFs), collectively known as p95HER2 (177). p95HER2 fragments can be generated by at least two independent mechanisms: alternative initiation of translation of the mRNA encoding HER2 from internal initiation codons, or proteolytic shedding, likely by the metalloprotease A desintegrin and metalloproteinase 10 (ADAM10). From these two mechanisms forms of p95HER2, that are located in the cytoplasm, or membrane-bound, arise. Evidence published so far, show that the cytoplasmic fragments are inactive, while membrane-bound isoforms are active (178). From the two active fragments, proteolytic cleavage of the ectodomain of HER2 at a site proximal to the transmembrane domain, likely between A648 and S649, generates a 90-100kDa form, known as p95HER2-90-100kDa or 648-CTF (177, 178), which will be named as p95HER2-648 from now on. This form was previously shown to

act as an active p95HER2 fragment, with an activity comparable to that of full-length HER2, when expressed in MCF7 mammary epithelial cells (178). Alternative initiation of translation, initiated at an internal AUG codon at position 611, generates a form of 100-115 kDa, known as p95HER2-100-115kDa or 611-CTF (177, 178), which will be named as p95HER2-611 from now on. p95HER2-611 conserves 5 cysteines in its extracellular domain and it was shown that this region allows the formation of constitutive homodimers through inter-molecular disulfide bonds (178). p95HER2-611 was also shown to act as a hyperactive form of HER2 able to regulate a specific set of genes, some of them causally involved in metastatic progression (178).

Similar to EGFR, two different approaches for targeted therapies against HER2-positive tumors exist, the use of monoclonal antibodies and TKIs. Trastuzumab is a humanized immunoglobulin G1 (IgG1) antibody that binds to an epitope in the juxtamembrane region IV of the HER2 receptor. It inhibits cleavage of the HER2 ectodomain, uncouples ligand-independent HER2-containing dimers leading to partial inhibition of downstream signaling, and triggers antibody-dependent cell-mediated cytotoxicity (ADCC) (179-183). Pertuzumab is a monoclonal antibody that recognizes an epitope in the heterodimerization domain II of HER2, thus blocking ligand-induced HER2-HER3 dimerization, resulting in partial inhibition of PI3K/Akt signaling (184). Lapatinib is a tyrosine kinase inhibitor for both HER2 and EGFR acting as an ATP-competitive, reversible small-molecule inhibitor (160, 185).

Several studies have correlated p95HER2 with an aggressive subtype of HER2-positive breast cancers (186-188). Moreover, it has been proposed as a mechanism of resistance to anti-HER2 therapies with monoclonal antibodies (189, 190) as it lacks the extracellular domains where trastuzumab or pertuzumab bind, but not to TKI treatments such as lapatinib, as p95HER2 share the same intracellular and kinase domains as HER2. However, recent studies show a much more complex contribution of p95HER2-611 to HER2-positive-treated tumors response. In this study, they showed that, while p95HER2-611 positive tumors are resistant to trastuzumab monotherapy, they are more sensitive to trastuzumab plus chemotherapy. This is probably due to the chemotherapy-induced stabilization of HER2 in p95HER2-611 positive tumors (191).

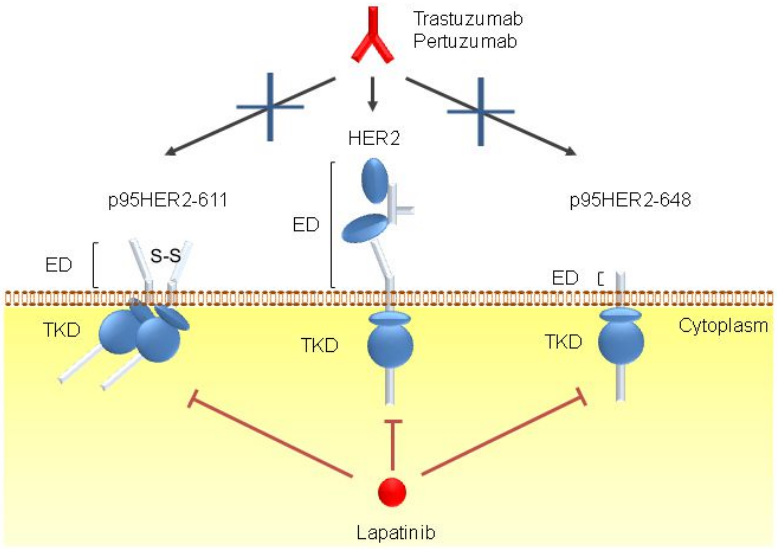

Fig. 8 HER2 and p95HER2 isoforms and their targeted therapies
Representation of HER2 and p95HER2 membrane-bound isoforms: p95HER2-611 (left) generated by alternative initiation of translation from the codon corresponding to M611, HER2 full length (middle) and p95HER2-648 (right) generated by proteolytic cleavage between A648-S649, which conserves five aminoacids in the extracellular domain (ED). Targeted therapies include monoclonal antibodies trastuzumab and pertuzumab, which only bind to the full-length form of HER2 and the TKI lapatinib, which binds to the tyrosine kinase domain (TKD) and inhibits all the isoforms.

4.3. HER2 and p95 in OIS and OIA

Previous reports have associated HER2 oncogene both to the induction of apoptosis and senescence.

HER2-induced apoptosis has been reported to be p53-dependent. The expression of HER2 in ovary carcinoma cells led to the activation of apoptosis or proliferation depending on p53 status. In p53 wild-type cells, HER2-induced apoptosis providing a possible explanation for the observed concomitant p53-mutation/HER2-overexpression status in some breast cancers (192).

On the other hand, HER2-induced senescence has also been observed by overexpression of mutant or hyperactive forms of the receptor. The expression of the oncogenic HER2 variant, NeuT, a rat homologue receptor harboring an activating point mutation in the transmembrane domain, induced senescence in MCF7 breast carcinoma cells. NeuT-induced senescence was p53-independent and p38/p21-dependent, as the suppression of p21 led to the prevention of cell cycle arrest and induction of proliferation. This work pointed to senescence as an initial tumor-barrier mechanism in HER2-driven tumors, which would need a second alteration for the

overcoming of senescence and induction of tumorigenesis (193). Moreover, in a recent work from our group the expression of p95HER2-611 acting as a hyperactive form of HER2 was also able to induce senescence in a panel of different epithelial breast cancer cell lines. In addition, this work described a specific transcriptome and secretome dependent both in the senescence state and HER2 signaling. However, p95HER2-611 SASP was shown to have paracrine pro-metastatic effects *in vivo*, as the presence of p95HER2-611-induced senescent cells enhanced the metastatic ability of proliferating cells (42).

Despite the fact that senescence and apoptosis may primary equally act as tumor suppressor mechanisms, the evidence of the detrimental non-cell autonomous effects of the SASP may argue against the equivalence of those two cell fates. Understanding the mechanisms by which a cell decides to undergo senescence or apoptosis upon an oncogenic insult may provide tools to avoid senescence, and the possible pro-tumorigenic and pro-metastatic effects. Contrary to senescence, the induction of apoptosis that would induce disappearance of the damaged cell, should avoid these adverse effects.

OBJECTIVES

OBJECTIVES

1. Characterization of the mechanism of activation of p95HER2-648

2. Description of the mechanisms leading to oncogene-induced senescence (OIS) or oncogene-induced apoptosis (OIA) in cells expressing p95HER2

3. Determination of the non-cell autonomous effects of OIS and OIA *in vivo*.

MATERIALS AND METHODS

MATERIALS AND METHODS

Antibodies

Primary antibodies for western blot (WB) were from Cell Signaling Technology (Danvers, MA, USA): Cleaved PARP (Asp214) Human Specific (Rabbit polyclonal) #9541, PARP (Rabbit polyclonal) #9542, anti-53BP1 #4937 (Rabbit polyclonal), Phospho-p44/42 MAPK (Erk1/2) (Thr202/Tyr204) (Rabbit polyclonal) #9101, Phospho-Akt (Ser473) (Rabbit polyclonal) #9271, Phospho-Akt (Thr308) (44F9) (Rabbit monoclonal) #4056, EGFR (D38B1) (Rabbit monoclonal) #4267, Phospho-HER2/ErbB2 (Tyr1221/1222) (6B12) (Rabbit monoclonal) #2243, Phospho-p38 MAPK (Thr180/Tyr182) (Rabbit polyclonal) #9211, phosphor-ATF2 (Thr69/71) (Rabbit polyclonal) #9225, Vav2 (C64H2) (Rabbit monoclonal) #2848 and p38 MAPK (Rabbit polyclonal) #9212; from TREVIGEN (Gaithersburg, MD, USA): GAPDH (Rabbit polyclonal) #2275-PC-100; from BioGenex (San Ramon, CA, USA): HER2 (c-erbB-2) (CB11) (Mouse monoclonal) #MU134-UCE; from Santa Cruz Biotechnology (Dallas, Texas, USA): phospho-Vav2 (Tyr172) (Rabbit polyclonal) #sc-16409-R, phospho-p21 (Thr145)-R (Rabbit polyclonal) #sc-20220-R, c-Myc (9E10) (Mouse monoclonal) #sc-40, E2F1 (C-20) (Rabbit polyclonal) #sc-193 and p53 (DO-1) (mouse monoclonal) #sc-126; from Neomarkers (Fremont, CA, USA; part of Thermo Fisher Scientific (Waltham, MA, USA): c-erbB-3/ HER-3 Ab-6 (Clone 2B5) (Mouse monoclonal) #MS-310-P1 and p21 WAF1 (Ab-11) (Mouse monoclonal) #MS-891-P0. The anti-HER4 antibody described in (194), was kindly provided by Dr. Pandiella (Instituto de Bilogía Molecular y Celular del Cáncer, CSIC-Universidad de Salamanca, Salamanca, Spain). All primary antibodies for western blot were used at 1:1000 dilution except for anti-HER2 (CB11) which was used at 1:2000 and anti-GAPDH which was used at 1:5000.

Secondary antibodies for western blot were from Amersham GE Healthcare (Piscataway, NJ, USA): ECL Rabbit IgG, HRP-linked whole Ab (from donkey) #NA934-1ML and ECL Mouse IgG, HRP-linked whole Ab (from sheep) #NA931. All secondary antibodies for western blot were used at 1:2000 dilution.

Primary antibodies for immunofluorescence were from Millipore (Billerica, MA, USA): Anti-phospho-Histone H2A.X (Ser139) (clone JBW301) (Mouse monoclonal) #05-636; and from Santa Cruz Biotechnology: 53BP1 (D-20) (Goat policlonal) #sc-10911. Primary antibody for Fluorescence Activated Cell Sorting (FACS) analysis was from Cell Signaling Technology (Danvers, MA, USA): 53BP1 (Rabbit polyclonal) #4937. All

primary antibodies for both plate-fixed immunofluorescence and FACS analysis were used at dilution 1:100.

Secondary antibodies for both immunofluorescence analysis were from Invitrogen-LifeTechnologies (Paisley, UK): Alexa Fluor 488 Goat Anti-Mouse IgG (H+L) #A-11001, Alexa Fluor 568 Donkey Anti-Goat IgG (H+L) #A-11057, Alexa Fluor 488 Donkey Anti-rabbit IgG (H+L) #A-21206. All secondary antibodies for immunofluorescence analysis were used at dilution 1:500.

Chemical Reagents

Caspase inhibitors were from R&D systems (Minneapolis, MN, USA): General Caspase inhibitor (-1, -3, -8, -9, -10, and -12) Q-VD-OPh #OPH001, and Caspase-8 inhibitor Z-IETD-FMK #FMK007. Necroptosis inhibitor Necrostatin-1 (4311-88-0) #sc-200142 was from Santa Cruz Biotechnology. p38 inhibitor SB203580 #559389 was from Calbiochem (part of Millipore, Billerica, MA, USA). PI3K inhibitor GDC0941 #S1065 was from Selleckchem (Houston, TX, USA). mTOR inhibitor Rapamycin #R8781 was from Sigma-Aldrich (St. Louis, MO, USA). MEK1,2 inhibitors PD0325901 #S1036 and UO126 #U120 were from Selleckchem and Sigma-Aldrich respectively. Bcl-2 inhibitor obatoclax mesylate (GX15-070) #S1057 was from Selleckchem. JNK inhibitor SP600125 #S5567 was from Sigma-Aldrich. Src inhibitor Src I1 #3642 was from Tocris Bioscience (Bristol, UK). TGFβ RI inhibitor #616452 was from Calbiochem. Proteasome inhibitor bortezomib was from Calbiochem. HER2 tyrosine kinase inhibitor lapatinib was kindkly provided by GlaxoSmithKline (Research Triangle Park, NJ, USA).

Plasmids

All HER2 constructs were derived from a cDNA clone identical to the published sequence gi:183986. HER2 deletion constructs were generated (178) as follows, p95HER2-611 cDNA was generated by cloning the HER2 sequence starting at M611, and p95HER2-648 was generated by adding an AUG codon right upstream the proposed HER2 cleavage site between A648 and S649 (195). Using standard PCR, cloning and sequencing techniques the different cDNA fragments were inserted as briefly follows: into XbaI site of pUHD10-3 as described in (178); into BamHI site of pIREShyg (Clontech, Mountain View, CA, USA); Firefly luciferase gene (FLUC) sequence was cloned into pQCXIH vector (Clontech, Mountain View, CA, USA).

Cell lines

MCF7, MDA-MB-468, MDA-MB-231, BT474, SKBR3 and HEK-293 were obtained from ATCC-LGC Standards (Teddington, UK), MCF7 Tet-Off were from BD Biosciences (San José, CA, USA) and TLA-HEK-293T were from Thermo Scientific. All cell lines were maintained at 37ºC and 5% CO_2. MCF7, MDA-MB-468, MDA-MB-231, BT474, SKBR3 and HEK-293 were mainained in Dulbeccos's minimal essential medium:F12 (DMEM:F12) (1:1) #21331-046 (Gibco-LifeTechnologies, Rockville, MD, USA), 10% fetal bovine serum (FBS) #10270-106 (Gibco-LifeTechnologies) and 1% L-Glutamine #M11-004 (PAA Laboratories-GE Healthcare, Pasching, Austria). MCF7 Tet-Off growth medium was further supplemented with 0.2mg/ml G418 #11811-031 (Gibco-LifeTechnologies) and 1µg/ml doxycycline #D9891 (Sigma-Aldrich).

Doxycycline-inducible cell lines

MCF7 Tet-Off transfectants were generated as previously described (178). Briefly, MCF7 Tet-Off cells (BD Biosciences) were transfected with pUHD10-3 plasmids encoding Vector, HER2, p95HER2-648 or p95HER2-611 using FuGENE6 #11988387001 (Roche, Indianapolis, IN, USA). Single stable clones were selected and maintained with MCF7 Tet-Off growth medium supplemented with 0.1mg/ml Hygromycin B #10687010 (Invitrogen-LifeTechnologies).

For induction of the transgenes, cells were detached with trypsin-EDTA and resuspended in MCF7 Tet-Off growth medium without doxycycline (-Dox). Doxycycline was removed from cells by 3 cycles of centrifugation and resuspension in -Dox medium. Twelve hours after seeding, medium was removed and replaced again by -Dox medium.

Viral transduction

MDA-MB-231-Luc cells were obtained by retroviral transduction of FLUC pQCXIH vector. Viral particles were produced by GP2-293 cell line transfected with the envelope encoding plasmid pVSV-G using Lipofectamine 2000 (Invitrogen-LifeTechnologies) as described in (196). Cells were maintained in growth medium supplemented with 0.05mg/ml Hygromycin B #10687010 (Invitrogen-LifeTechnologies).

Transient transfection

For transient expression of HER2, p95HER2-648 or p95HER2-611 in HEK-293 cells, pIREShyg vector constructs were used. Briefly, 6-well plates were coated during

30min with a 20µg/ml collagen type I solution from rat tail #C3867 (Sigma-Aldrich) in DMEM:F12 (Gibco-LifeTechnologies), then coating solution was removed and HEK-293 cells were seeded to reach 50% confluency after 24h and then transfected with the different cDNA constructs in pIREShyg vector using Lipofectamine2000 from Invitrogen-LifeTechnologies (#11668-019) according to manufacturers indications.

siRNA transient knock-down

The levels of HER3, p38, CSNK1D, RIPK2, ATF3 or GADD45A were transiently knocked down by reverse transfection of the corresponding ON-TARGETplus SMARTpool siRNAs from Dharmacon-Thermo Scientific (Epsom, UK). Non-targeting D-001810-10-20, Human ERBB3 (2065) L-003127-00-0010 (J-003127-10, J-0031-27-11, J-003127-12, J-003127-13), Human MAPK14 (p38α) L-003512-00-0010, (Human VAV2 (7410) L-005199-00-0010 (J-005199-05, J005199-06, J005199-07, J-005199-08), Human CSNK1D (1453) L-003478-01-0005 (J-003478-17, J-003478-18, J003478-19, J-003478-20), Human RIPK2 (8767) L-003602-00-0005 (J-003602-09, J-003602-10, J-003602-11, J-003602-12), Human ATF3 L-008663-00-0010 (J-008663-08, J-008663-07, J-008663-06, J-008663-08) and Human GADD45A L-003893-00-0010 (J-003893-07, J003893-08, J-003893-09, J-003893-10).

Briefly, 9x10^5 MCF7 Tet-Off Vector, HER2, p95HER2-648 or p95HER2-611 cells were seeded in 6cm plates in transfection medium with 160pmol of siRNA SMARTpool in 2ml Optimem #31985047 (Invitrogen-LifeTechnologies) with 12µl lipofectamine RNAiMax #13778-150 (Invitrogen-LifeTechnologies) and 1µg/ml doxycycline #D9891 (Sigma-Aldrich). After 8 hours transfection medium was removed and fresh medium with 1µg/ml doxycycline #D9891 (Sigma-Aldrich) was added to the plates. Twelve hours later cells were induced by removing doxycycline as described above, and 1x10^5 cells per well were seeded in 6well/plates. The indicated assays were performed after 3 days of induction.

shRNA stable knock-down

MCF7 Tet-Off Vector, HER2, p95HER2-648 or p95HER2-611 cell lines stably knocked down for HER3 or p21 were generated by lentiviral infection using the corresponding pGIPZ lentiviral shRNA vectors from Open Biosystems-Thermo scientific: GIPZ ERBB3 shRNA (RHS4430-101135536 clone V3LHS-310490) and GIPZ CDKN1A shRNA RHS4430-200281172 clone V3LHS-322234 pGIPZ-Non-Silencing-Control. For p53 knockdown the lentiviral vectors pLKO-p53.1 (REF.

TRCN0000003756) and pLKO-p53.2 (REF. TRCN0000003756) obtained from The RNAi Consortium (TRC) were used.

Briefly, TLA-HEK-293T cell line was transfected with pMD.G2 (Addgene) and pPAX2 (Addgene) packaging vectors, in addition to the corresponding lentiviral shRNA vectors, using standard calcium phosphate transfection protocol. Lentiviral supernatants produced in DMEM:F12 (1:1) (Gibco-LifeTechnologies), 5% FBS (Gibco-LifeTechnologies), 1% L-Glutamine (PAA Laboratories-GE Healthcare) were collected and filtered with 0.45µm PVDF filters (Millipore). Medium from a 15cm plate of packaging cells was used to infect a 15cm plate of target cells at 50% confluence, using 8µg/ml polybrene (REF), infection medium was removed after 6 hours.

Polyclonal populations were selected for HER3 and p53 knock-down cell lines and single stable clones were selected for MCF7 Tet-Off p95HER2-611 knocked down for p21 and p53. All of them selected and maintained with MCF7 Tet-Off growth medium supplemented with 1µg/ml Puromycin #P7255 (Sigma-Aldrich).

Bright field pictures

Bright field pictures were taken using an IX71 Olympus inverted microscope (Olympus Corporation, Tokyo, Japan).

Proliferation assay

Proliferation was analyzed by cell counting. Briefly, $1x10^5$ cells per well were seeded in 6-well plates. At the indicated times: 0 (10h was counted as time 0), 24h, 48h, 72h and 144h cells were detached with trypsin-EDTA and viable cells were determined by trypan blue dye exclusion and counted on a Neubauer-chamber.

For the add-back doxycycline/reversibility assay $1x10^5$ cells were seeded per well in 6-well plates in -Dox conditions (as described above). Doxycycline was added at a final concentration of 1µg/ml at the indicated time points (12h, 24h or 48h) and cells were counted at 12h, 24h, 48h, 72h, 96h and 144h.

Determination of cell cycle and SubG1

The percentage of cells in the different cell cycle phases and in the sub-G1 fraction (i.e., apoptotic cells) was determined based on relative DNA content by means of flow cytometry. Briefly, $1x10^5$ cells were seeded in 6cm plates, in triplicates, for 3 days and kept in culture both in the presence or absence of doxycycline. Then cells were

detached with trypsin-EDTA, washed with 1x phosphate-buffered saline (PBS), fixed for 30 min on ice in 70% ethanol, treated for 10 min at 37ºC with a DNA extraction solution (Na_2PO_4 0,19M, Citric acid 4mM, pH7,8), and stained with propidium iodide (Sigma, #81845) (40µg/ml)/ RNase (Sigma, #R6513) (10µg/ml) solution for 30 min at 37ºC. Stained cells were analyzed on a FACSCalibur flow cytometer (BD Biosciences). The percentage of SubG1 population was determined using BD CellQuest Pro Software program (BD Biosciences) and cell cycle distribution was determined using the FCS Express 3 software program (De Novo Software).

Annexin V/Propidium iodide

Flow cytometric assay of APC-coupled Annexin V (BD Pharmigen, #550475) combined with propidium iodide (PI) staining (Sigma, #81845) was used for early (Annexin V positive, PI negative) and late (Annexin V positive, PI positive) apoptosis determination, all Annexin V positive were considered for representation (PI positive and PI negative). Briefly, $1x10^5$ cells per well were seeded in 6-well plates both in the presence or absence of doxycycline. After 3 days, floating and adherent cells were harvested in tubes by collecting both media and adherent cells detached with trypsin-EDTA. Then, cells were centrifuged and viable cells were determined by trypan blue dye exclusion and counted on a Neubauer-chamber, $2x10^5$ cells per condition were resuspended in 1ml 1xPBS. Cells were washed twice with 1xPBS, resuspended in 500µl of Binding Buffer 1x (10mM Hepes, 14mM NaCl, 0.25mM $CaCl_2$ in dH_2O). 5µl of APC-coupled Annexin V (BD Pharmigen, #550475) were added to each tube and incubated for 15min at room temperature (RT) protected from light, then 5µl of 1mg/ml PI were added to each tube. Analysis was done in a FACSCalibur flow cytometer (BD Biosciences). The percentages of Annexin V and PI positive populations were determined using BD CellQuest Pro Software program (BD Biosciences).

SA-ß-GAL

Senescence-Associated ß-Galactosidase activity was determined using ß-galactosidase staining kit (Cell Signaling Technology) following the manufacturer's indications. Briefly, $1x10^4$ cells per well were seeded on glass coverslips in 24-well plates (previously doxycycline was washed as described above). After 3 days media was removed, wells were washed twice with 1xPBS, fixed for 15min at RT with 1x fixation solution, then washed twice with 1xPBS and stained with X-Gal solution at pH6.0 o/n in a humidified-chamber at 37ºC, following manufacturer's instructions. Images were obtained in bright field as described before.

Western blot

Protein extracts were obtained from cells washed with ice-cold 1xPBS and lysed in 20mM Tris-HCl pH7.4, 137mM NaCl, 2mM EDTA, 10% glycerol, 1% Nonidet P-40 supplemented with 5mM NaF (1M stock, Sigma #56521), 5mM ß-Glycerophosphate (1M stock, Fluka #S6521), 1mM Na_3VO_4 (250mM stock, Sigma #S65508) and 40µl/ml cOmplete EDTA-free Protease Inhibitor Cocktail Tablets (prepared according to manufacturer's instructions, Roche #11873 580 001). Protein extracts were clarified by centrifugation at 16,1x10^3rcf and quantified using DC protein assay reagents (Bio-Rad). Samples were mixed with loading buffer containing DTT (250mM Tris-HCl pH6.8, 10% SDS, 30% Glicerol, 0.5mM 1.4-Dithiothreitol DTT (Roche, #10780984001), 0.2% Bromophenol blue) and incubated at 99ºC for 5min before resolving proteins by SDS-polyacrylamide gel electrophoresis (PAGE) and transferring them to nitrocellulose membranes. Membranes were blocked for 1h with 5% skim milk or 5% Bovine Serum Albumin (BSA) in Tris-buffered saline (TBS) 0.1% Tween-20 and incubated with primary antibodies o/n at 4ºC. Membranes were washed with TBS-Tween 0.1% and incubated with HRP-coupled secondary antibodies for 1h at RT. Proteins were detected by autoradiography upon addition of Immobilon western chemiluminescent HRP substrate (#WBKLS0500, Millipore). Western blots were quantified with ImageJ 1.42q software (NIH, USA).

Immunoprecipitation

For immunoprecipitation, cells were washed twice with ice-cold 1XPBS and proteins were extracted with 50mM Tris-HCl pH7.4, 150mM NaCl, 1% Nonidet P-40 supplemented with 5mM NaF (1M stock, Sigma #56521), 5mM ß-Glycerophosphate (1M stock, Fluka #S6521), 1mM Na_3VO_4 (250mM stock, Sigma #S65508) and 40µl/ml cOmplete EDTA-free Protease Inhibitor Cocktail Tablets (prepared according to manufacturer's instructions, Roche #11873 580 001). Equal amount of protein extracts from MCF7 Tet-Off Vector, HER2, p95HER2-648 and p95HER2-611 were incubated o/n at 4ºC with or without an anti-HER3 antibody. Immunocomplexes were recovered by adding protein A Agarose beads (Millipore) for 2 hours at 4ºC. Immunoprecipitates were washed thoroughly with lysis buffer and released with ß-mercaptoethanol loading buffer (180mM Tris-HCl ph6.8, 4.4% SDS, 0.2% glicerol, 0.06% Bromophenol blue, 2% ß-mercaptoethanol).

Immunofluorescence (Confocal microscopy)

DNA-damage response (DDR) activation was assessed by nuclear immunofluorescence detection of 53BP1 and phospho-H2AX DDR associated proteins foci in fixed and permeabilized cells. Briefly, $1x10^4$ cells per well were seeded on glass coverslips in 24-well plates (both in the presence and absence of doxycycline). After 3 days media was removed, wells were washed with 1xPBS, fixed with 4% formaldehyde solution in 1xPBS for 20min and permeabilized with 0.2% Triton100 solution in 1xPBS for 10min. 1xPBS with 1% Bovine Serum Albumin (BSA), 0.1% Saponin and 0.02% Azide was used for blocking during 40min. Glass coverslips were transferred to a dark humidified chamber up-side-down on 40µl drops of primary antibody (diluted 1:100 in blocking solution) and incubated for 1h. Glass coverslips were transferred to 6-well plates up side up and washed twice with 1xPBS for 5min and then transferred again to a dark humidified chamber up side down on 40µl drops of fluorochrome-conjugated secondary antibody (diluted 1:500 in blocking solution) and incubated for 1h. Glass coverslips were transferred to 6-well plates up side up and washed twice with 1xPBS for 5min. Preparations were mounted on glass slides using Vectashield with 40,60-diamidino-2-phenylindole (DAPI) (#H-1200, Vector Laboratories, Burlingame, CA, USA). All procedures were performed at room temperature.

Images were captured using an Olympus FV1000 confocal microscope (Olympus Corporation, Tokyo, Japan).

Percentage of 53BP1 and phopho-H2AX positive cells was determined by counting foci-positive nuclei relative to total nuclei (DAPI+) in the image field.

Immunofluorescence (Flow Cytometry)

Time course of DNA damage response (DDR) activation was assessed by immunofluorescence detection of 53BP1 DDR-associated protein in fixed and permeabilized cells by flow cytometry. Briefly, $2x10^5$ cells per plate were seeded in 6cm plates (both in the absence and presence of doxycyline). After 48h or 72h, floating and adherent cells were harvested in tubes by collecting both media and trypsin-EDTA -detached adherent cells, then centrifuged, washed with 1xPBS, fixed with a 2.3% formaldehyde solution in 1xPBS for 20min on ice and washed with 1xPBS. Fixed samples were stored at 4ºC in 1xPBS. All samples (48h and 72h) were permeabilized with 0.2% Triton-X100 solution in 1xPBS for 10min on ice and washed once with 1xPBS. At this point all samples were divided in 2 tubes: control staining and primary antibody incubated (diluted 1:100 in 1xPBS with 1% BSA, 0.1% Saponin and 0.02%

Azide) o/n at 4ºC. All samples were incubated with fluorochrome-conjugated secondary antibody (diluted 1:500 in 1xPBS with 1% BSA, 0.1% Saponin and 0.02% Azide) for 1h on ice. Samples were washed once with 1xPBS and finally resuspended in 1xPBS. Analysis was done in a FACSCalibur flow cytometer (BD Biosciences). Obtained data was analysed using the FCS Express 3 software program (De Novo Software). Mean Fluorescence Intensity (Geometric) difference (–Dox)-(+Dox) was calculated (previous substraction of the corresponding control condition with only fluorochrome-conjugated secondary antibody for each sample).

Receptor Tyrosine Kinase (RTK) Array

Receptor Tyrosine Kinase activation was assessed using Proteome Profiler Human Phospho-RTK Array kit from R&D systems #RYD-ARY001B. The assay was performed according to manufacturer's instructions. Heatmap representation was obtained based on the pixel average signal (2 spots for each phospho-antibody) quantified with Adobe Photoshop CS6 version 13.0 x64 (Adobe Systems Inc.)

Inhibitor treatments

Treatment with the different chemical inhibitors (see all references in *Chemical Reagents*) at the indicated concentrations were performed as follows: MCF7 Tet-Off cells were treated with the indicated inhibitors in +dox conditions for 24h. Then treated cells were detached with trypsin-EDTA, and doxycycline was washed for transgenes induction (as described above). Viable cells were determined by trypan blue dye exclusion and counted on a Neubauer-chamber, $1x10^5$ cells per condition were seeded in 6cm plates in the presence of the indicated inhibitor. After 12h, media was removed and fresh media, with or without doxycyline, and with the indicated inhibitor was added to the cell plates. After 3 days the appropriate assays were performed.

Treatment with Lapatinib at the indicated concentrations was carried out from the moment of induction (doxycycline removal) and seeding.

Treatment with the proteasome inhibitor bortezomib at the indicated concentration was done from the moment of induction (doxycycline removal) and seeding ($1x10^5$ cells per condition were seeded in 6cm plates). After 12h, treatment was stopped by removing the media, washing the plates with 1xPBS and adding fresh media (with or without doxycycline) without bortezomib. Samples were collected at 15h for western blot.

In vivo xenograft and metastasis assay

Mice were maintained and treated in accordance with institutional guidelines of the Vall d'Hebron University Hospital Care and Use Committee. A 1:1 mix of MCF7 Tet-Off : MDA-MB-231-Luc ($9x10^5$: $9x10^5$) cells was injected orthotopically in the mammary fat pad (right flank) of 6- to 8-week-old female BALB/c nude mice purchased from Charles Rivers Laboratories (L'Arbresle Cedex, France). Cellular solution was injected in a 1:1 mix solution of PBS : Matrigel matrix (BD Bioscience #356237) (100µl/animal). Animals were supplemented with ß-estradiol by means of subcutaneous injection of 0.72mg 17-ßestradiol pellets in order to allow tumor growth. The animals were maintained in the presence of doxycycline (1g/L) in the drinking water to repress p95HER2 fragments expression (25g/L sucrose were added to the water solution to compensate doxycyline solution flavour). Tumors were allowed to grow until the average tumor volume reached 100-150mm^3, then doxycycline was removed from the drinking water except for the +Dox conditions. When tumor xenografts volume was arround 700mm^3, they were surgically removed. Samples from each tumor were collected and then a piece of sample was snap-frozen and another fixed overnight with 4% formol and then paraffin-embedded..

Tumor xenografts were measured with callipers every 3 days, and tumor volume was determined using the formula: (length x $(width)^2$)/(π/6). Results are presented as mean ± SD of tumor volume.

Tumor-removed animals were maintained and *in vivo* monitored for the apperance of metastasis as bioluminescent foci. Primary tumor and metastatic colonization were monitored every 7 days by *in vivo* bioluminescence imaging using the IVIS-200 imaging system from Xenogen (PerkinElmer, Waltham, MA, USA) as previously described (197). Briefly, animals were anesthetized with 2% isofluorane-air mixture and injected intraperitoneally with a D-luciferine (Promega, Fitchburg, WI, USA) solution in 1xPBS (150mg/kg). Image capture was taken starting from 5min up to 10min after injection. Animals were kept inhaling isofluorane-air mixture during all the procedure. Bioluminescence data analysis was performed using Living image software v.4.3.1 (Caliper lifesciences,Inc., Hopkinton, MA, USA).

At the end of the experiment, the animals were anesthetized with a 2% isofluorane-air mixture and were sacrificed by cervical dislocation.

Transcriptomic analysis

RNA-expression analysis in MCF7 Tet-Off Vector, HER2, p95HER2-648 and p95HER2-611 was performed using Affimetrix gene-chips HG U133 2.0 as previously described (178).

Data files were analyzed in the program ArrayAssist 5.5.1 (Stratagene) with probe levels normalized by the RMA (robust multichip average) algorithm (54,675 probe sets). Consistency of the data sets was verified by determining the number of probe sets that varied more than two fold when comparing the doxycycline presence and absence from a clone in the same array run. Experimental duplication was used to determine the number of probe sets with more than two fold differences in pairwise t tests with a P <0.05 (2,425 probe sets). Subsequently, all probe sets of these genes with more than two-fold changes in at least one of the conditions were exported to Excel, where the average *n*-fold induction for each gene in each condition was calculated. Ambiguous annotations were substracted (2,230 probe sets) and duplicated genes were removed (total of 1,656 genes). Data was represented as log2FC. For the Venn diagram representation, genes were considered as regulated by each of the constructs when log2FC>1.0.

RTqPCR

For Real Time quantitative PCR (RTqPCR) total RNA was extracted using RNeasy mini kit (Qiagen, #74104) following manufacturer's instructions. Nucleic acid concentrations were quantified using Nanodrop spectrophotometer (ND-1000, Thermo Scientific) and associated software ND-1000 3.8.0. 1µg RNA was retro-transcribed to cDNA using High capacity cDNA reverse transcription kit (Applied biosystems #5468814) following manufacturer's instructions. 10ng of cDNA were run in an Applied Biosystems 7900HT using TaqMan gene expression assays for IL8 (Hs00174103_m1), ATF3 (Hs00231069_m1), GADD45A (Hs00169255_m1), BCL2A1 (Hs00187845_m1), CDKN1A (Hs00355782_m1), 18S (Hs03928990_g1) or GAPDH (Hs03929097_g1) from Applied Biosystems and Taqman Universal Master Master mix II, with UNG (Applied Biosystems #44440038). Each sample was assayed in triplicate. Real Time PCR Data was analyzed using SDS v2.3 software (Applied Biosystems) following the 2ΔΔCt method. Briefly, average ΔCt calculated as (Assay_Ct)-(housekeeping GAPDH_Ct or 18S_Ct), Average ΔΔCt calculated as (–Dox_ΔCt)-(+Dox_ΔCt), relative mRNA represented as mean ± SD of $2^{-\Delta\Delta Ct}$ (one biological replica for IL8 and CDKN1A and 2 biological replicas for ATF3 and GADD45A).

ELISA

TGFß2 concentration in the cells conditioned media was determined with Human TGF-ß2 ELISA kit #ELH-TGFbeta2-001 from RayBiotech (Norcross, GA, USA).

Briefly, $1x10^5$ cells/well were seeded in 6-well plates (both in the presence and absence of doxycycline). After 7 days, conditioned media from each condition was collected, spun down at 1000rpm for 5min and transferred into clean tubes. Concentration of TGFß2 was determined according to the manufacturer's instructions, normalized to cell number and expressed as picograms/ml/$2.5x10^4$ cells.

RESULTS

RESULTS

1. HER2 signaling can trigger oncogene-induced senescence (OIS) or oncogene-induced apoptosis (OIA)

1.1. Different p95HER2 fragments induce either OIS or OIA

Two transmembrane p95HER2 forms, p95HER2-611 generated by alternative initiation of translation of the HER2 transcript (198) and p95HER2-648 generated by proteolitic cleavage of HER2 receptor at the cell surface (195, 199-201) (Fig. 9A) were previously shown to be active (178). In a recent report from our group (42), it was shown that the expression of p95HER2-611 induces OIS in a subset of different breast cancer cell lines, including MCF7 cells. Confirming this result, expression of p95HER2-611 in MCF7 inducible Tet-Off cells resulted in cells with an enlarged, flattened and vacuolated morphology, one of the hallmarks of OIS (Fig. 9B, lower-right panel) (42). Unexpectedly, MCF7 Tet-Off cells expressing p95HER2-648 were morphologically very different, they did not present the characteristic senescent morphology and after 60 hours of expression they detached and appeared as dead cells (Fig. 9B, lower-left panel).

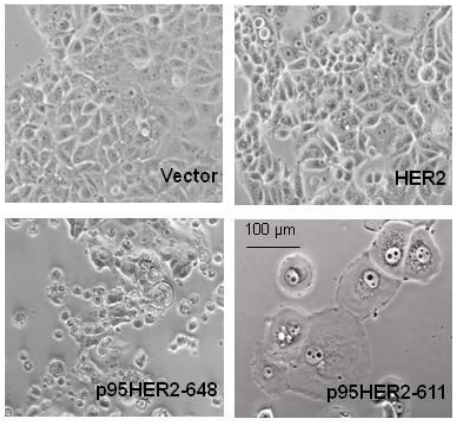

Fig. 9 Effect of p95HER2 expression in the morphology of MCF7 Tet-Off cells
Representative bright field pictures of MCF7 Tet-Off cells expressing the empty vector, or the same vector encoding HER2, p95HER2-648 or p95HER2-611 cultured in the absence of doxycycline for 60h.

We then characterized the phenotype of cells expressing p95HER2-648 and compared it with that of p95HER2-611 cells. In agreement with previous results (42) p95HER2-611-induced senescent cells showed a stable proliferation arrest as measured by cell

counting (Fig. 10A) or by determination of the percentage of cells in the different phases of the cell cycle (Fig. 10B). Although senescent cells typically are arrested in the G1 phase of the cell cycle (29, 202-204), it has also been shown that a defect in MKK7 (205) or expression of some oncogenes (24, 98, 206) can induce a fraction of cells to senesce and accumulate in the G2/M phase. Accordingly, p95HER2-611-induced senescent cells accumulate in the G2/M phase (Fig. 10B). On the other hand, p95HER2-648 expressing cells showed an initial increase in cell number followed by a decrease on cell population, indicating cell death in the culture (Fig. 10A). Consistent with the cell death observed in Fig. 9, cell cycle analysis of p95HER2-648 expressing cells showed a significant accumulation of hypodiploid apoptotic cells detected as SubG1 fraction (Fig. 10B).

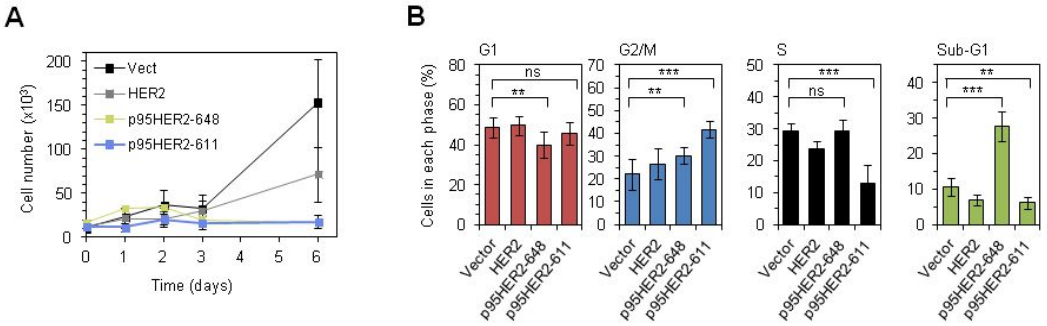

Fig. 10 Proliferation and cell cycle analysis of cells expressing different p95HER2 isoforms
(A) MCF7 Tet-Off cells expressing the empty vector, HER2, p95HER2-648 or p95HER2-611 were counted. Data is represented as average ± SD from two independent experiments. **(B)** Percentages of cells in each fraction of the cell cycle or in the SubG1 fraction were determined by flow cytometry after 3 days of transgene expression. Data shows the average ± SD from 5 independent experiments. All samples were assessed in duplicate. *ONE-Way ANOVA statistical test,* post-test comparison to Vector (Dunnet test). (*$p<0.05$, **$p<0.01$, ***$p<0.001$. ns, non-significant).

One of the most widely used markers to identify senescent cells is the detection of Senescence Associated ß-Galactosidase activity at pH 6.0 (SA-ß-GAL) (207). MCF7 Tet-Off p95HER2-611 cells showed a significant increase in the percentage of SA-ß-GAL positive cells within the culture, 20-30%, while p95HER2-648 cells showed less than 10% positive cells (Fig. 11A).

To characterize the mechanism of death of cells expressing p95HER2-648, we used two commonly used apoptosis markers, the detection of phosphatidylserine (PS) exposed on membrane surface with Annexin V (208) and PARP cleavage (209).

p95HER2-648-expressing cells showed a significant increase in the levels of both markers (Fig. 11B, C).

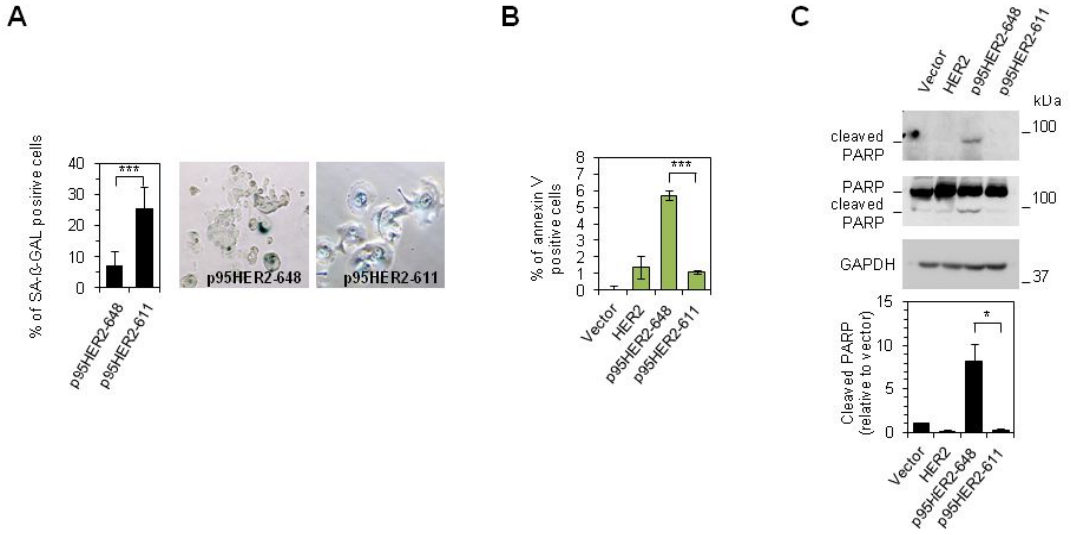

Fig. 11 Analysis of different senescence and apoptosis markers in cell expressing p95HER2
MCF7 Tet-Off cells expressing the empty vector, HER2, p95HER2-648 or p95HER2-611. **(A)** Bright field representative microscopy images of SA-ß-GAL assay after 6 days of transgene expression. The percentage of positive SA-ß-GAL cells, 7 fields for each condition, was quantified. *Mann-Whitney statistical test, p*=0.0006. **(B)** Annexin V-positive cells determination by flow cytometry. *t*-test *p*=0.0001. **(C)** Western blot analysis of cells lysed after 60h of transgene expression (upper panel). Quantification of cleaved PARP from two independent experiments (lower panel). *t*-test, *p*=0.0281. (**p*<0.05, ***p*<0.01, ****p*<0.001. ns, non-significant).

Caspases are critical effectors of the apoptotic programs, both intrinsic and extrinsic. Caspase-9 is the main initiator caspase for the intrinsic apoptosis pathway, and it is activated when recruited to the apoptosome, while caspase-8 is the one induced when the Death-inducing signaling complex (DISC) is formed upon activation of the extrinsic apoptosis pathway by death receptors (FasR, TNFR 1, DR3 or TRAIL-R1-2) and their ligands (FasL, TNF-α, Apo3L or TRAIL). Caspases -3, -6 and -7 are the effector caspases for both apoptosis pathways. We assessed the implication of caspases in the apoptosis induced by p95HER2-648, and whether the intrinsic mithocondrial or the extrinsic death receptor apoptotic pathways were activated. For this, we treated cells expressing p95HER2-648 with Q-VD-Oph, a general caspase inhibitor, which targets caspases -1, -3, -8, -9, -10 and -12 (210), and Z-IETD-FMK, a specific caspase-8 inhibitor (211). Treatment with Q-VD-Oph induced a decrease of cells accumulated in SubG1 compared to non-treated cells, while Z-IETD-FMK did not have any effect (Fig. 12A). According to these results we can conclude that in cells expressing p95HER2-648 intrinsic apoptotic pathway is activated. As MCF7 cells do not express caspase-3

(212), the observed effect is likely due to the inhibition of the initiator caspase-9, thus caspase-7 is probably the final executioner caspase in this cells.

As the reduction of percentage of cells in SubG1 fraction with the used concentration of Q-VD-Oph did not reach control levels, we also wanted to rule out the contribution of other kinds of programmed cell deaths such as necroptosis. Necroptosis is a form of regulated necrosis dependent on the receptor-interacting protein kinases (RIPK) RIPK1 and/or RIPK3 (213). We used the specific inhibitor Necrostatin-1 (Nec-1), known to inhibit RIPK1 kinase activity (214, 215). Treatment with increasing concentrations of Nec-1 did not lead to the reduction of cell death, as measured by the percentage of cells in the SubG1 fraction (Fig. 12B). Therefore we can conclude that p95HER2-648 induced cell death is due to apoptosis mediated by caspases.

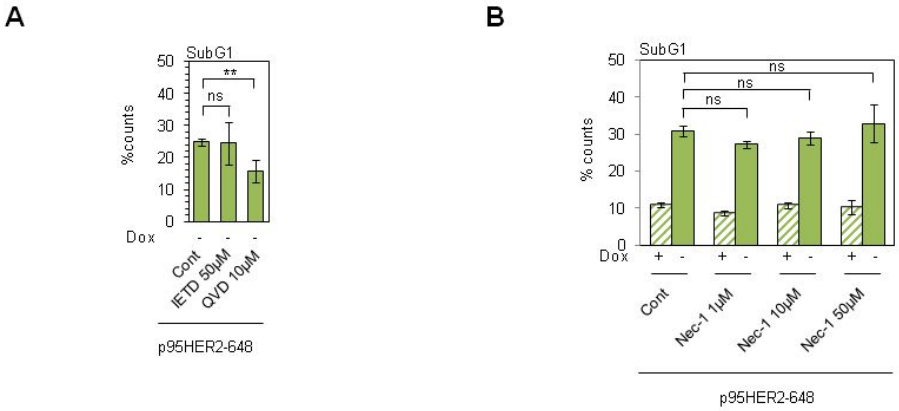

Fig. 12 Treatment of p95HER2-648 expressing cells with different caspase and necroptosis inhibitors
(A) MCF7 Tet-Off cells expressing p95HER2-648 were treated or left untreated with the caspase inhibitors QVD-oph 10µM or Z-IETD 50µM for 24h in the presence of doxycycline. Cells were then washed out from doxycycline and seeded in the absence of doxycycline with or without the corresponding inhibitors for additional 60h. SubG1 analysis was performed. *Mann-Whitney statistical test,* QVD (10µM) p=0.0049, IETD (50µM) p=0.5133. **(B)** MCF7 Tet-Off cells expressing p95HER2-648 were treated or left untreated with the necroptosis inhibitor Necrostatin-1 (Nec-1) at 1µM, 10µM or 50µM for 24h in the presence of doxycycline. Cells were then washed out from doxycycline and seeded, in the absence or presence of doxycycline, with or without the corresponding concentration of the inhibitor for additional 60h. SubG1 analysis was performed. *Mann-Whitney statistical test,* Nec-1(1µM) p=0.1000, Nec-1(10µM) p=0.4000, Nec-1(50µM) p=0.7000. (*p<0.05, **p<0.01, ***p<0.001. ns, non-significant).

1.2. p95HER2-triggered OIS and OIA are specific of each isoform

It could be argued that the differences observed in cells expressing p95HER2-648 and p95HER2-611 are due to the different levels of expression of the fragments, that are comparatively higher in cells expressing p95HER2-648 (Fig. 13A). Thus, lowering the levels (or the activity) of p95HER2-648 should result in the onset of OIS. To test this possibility we treated MCF7 Tet-Off p95HER2-648 cells with different concentrations of doxycycline, to modulate the expression of the transgene, as well as with different concentrations of the tyrosine kinase inhibitor lapatinib to regulate the receptor activity in a dose-dependent manner (Fig. 13, 14). Increasing concentrations of doxycycline progressively reduced the levels of the apoptosis markers cleaved PARP and SubG1 in cells expressing p95HER2-648 (Fig. 13A, B-upper panel, C-upper panel). We then compared levels of p21 and the percentage of cells in the S phase of the cell cycle, between p95HER2-648 doxycycline-treated cells and p95HER2-611-induced senescent cells. p95HER2-648 expressing cells did not show an increase in the levels of p21, neither a reduction of the percentage of cells in the S phase indicating a cell cycle arrest, at any of the used doxycycline concentrations (Fig. 13A, B-lower panel, C-lower panel).

The use of different concentrations of lapatinib indicated similar results. p95HER2-648 displayed a progressive reduction of apoptosis markers (Fig. 14A, B-upper panel, C-upper panel) and the levels of the senescent markers p21 or reduction of the S phase did not reach p95HER2-induced senescent cells levels (Fig. 14A, B-lower panel, C-lower panel).

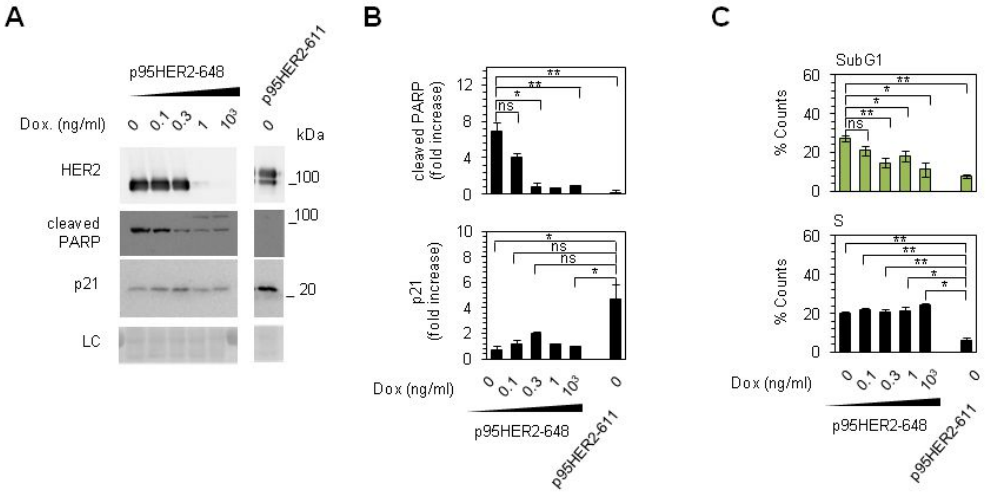

Fig. 13 Effect of the modulation of p95HER2-648 expression on the onset of apoptosis and senescence
MCF7 Tet-Off cells expressing p95HER2-648 or p95HER2-611 were washed off doxycycline and seeded in the presence of doxycycline (dox) at 1µg/ml (maintenance concentration), 1ng/ml, 0.3ng/ml, 0.1ng/ml or left without (w/o) for additional 60h. **(A)** Western blot analysis of cell lysates with the indicated antibodies, LC: loading control (ponceau staining), **(B)** quantification of cleaved PARP and p21 levels, (fold increase relative to cells treated with 10^3ng/ml doxycycline is shown). *t-test,* cleaved PARP (compared to p95HER2-648 w/o dox): p95HER2-648 (dox 0.1ng/ml) p=0.0560, p95HER2-648 (dox 0.3ng/ml) p=0.0124, p95HER2-648 (dox 10^3ng/ml) p=0.0113, p95HER2-611 (w/o doxycycline) p=0.0096; p21 (compared to p95HER2-611 w/o dox): p95HER2-648 (w/o dox) p=0.0431, p95HER2-648 (dox 0.1ng/ml) p=0.0526, p95HER2-648 (dox 0.3ng/ml) p=0.0842, p95HER2-648 (dox 10^3ng/ml) p=0.0461. **(C)** SubG1 and cell cycle determination by flow cytometry were performed. Average ± SD from two independent experiments is shown. *Mann-Whitney statistical test,* SubG1 (compared to p95HER2-648 w/o dox): p95HER2-648 (dox 0.1ng/ml) p=0.9359, p95HER2-648 (dox 0.3ng/ml) p=0.0049, p95HER2-648 (dox 1ng/ml) p=0.0269, p95HER2-648 (dox 10^3ng/ml) p=0.0269, p95HER2-611 (w/o dox) p=0.0078; S phase (compared to p95HER2-611 w/o dox): p95HER2-648 (w/o dox) p=0.0043, p95HER2-648 (dox 0.1ng/ml) p=0.0043, p95HER2-648 (dox 0.3ng/ml) p=0.0043, p95HER2-648 (dox 1ng/ml) p=0.0357, p95HER2-648 (dox 10^3ng/ml) p=0.0357. (*p<0.05, **p<0.01, ***p<0.001. ns, non-significant).

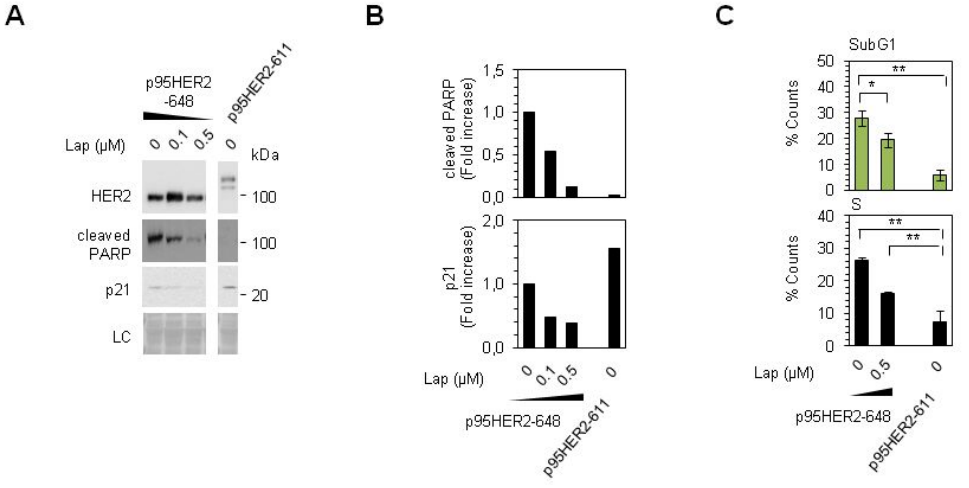

Fig. 14 Effect of the modulation of p95HER2-648 activity on the onset of apoptosis and senescence
MCF7 Tet-Off cells expressing p95HER2-648 or p95HER2-611 were washed off doxycycline, plated without it and treated with lapatinib (lap) at 0.1µM, 0.5µM or left untreated for 60h. **(A)** Western blot analysis of cell lysates with the indicated antibodies, LC: loading control (ponceau staining), **(B)** quantification of cleaved PARP and p21 levels. **(C)** SubG1 and cell cycle determination by flow cytometry. Average ± SD from two independent experiments is shown. *Mann-Whitney statistical test,* SubG1 (compared to p95HER2-648 w/o lap): p95HER2-648 (lap 0.5µM) p=0.0022, p95HER2-611 (w/o lap) p=0.0095; S phase (compared to p95HER2-611 w/o lap): p95HER2-648 (w/o lap) p=0.0095, p95HER2-648 (lap 0.5µM) p=0.0095. (*p<0.05, **p<0.01, ***p<0.001. ns, non-significant).

As we did not see an increase in the senescence markers in p95HER2-648 cells at any of the conditions tested (Fig. 13, 14), we conclude that the different phenotypes induced by p95HER2 isoforms are not due to differences in the levels of expression or the degree of activation. Thus, the onset of apoptosis or senescence triggered by HER2 signaling is possibly due to intrinsic differences in the signaling abilities of these fragments.

In addition, as apoptosis and senescence are considered irreversible, we took advantage of the Tet-Off inducible system to determine when these processes become irreversible. Doxycycline was normally washed off in order to induce the expression of p95HER2 fragments, then doxycycline was added back at 12h, 24h and 48h to interrupt transgene expression and cell growth was assessed by cell number. Both processes resulted irreversible after 48h of induction (Fig. 15).

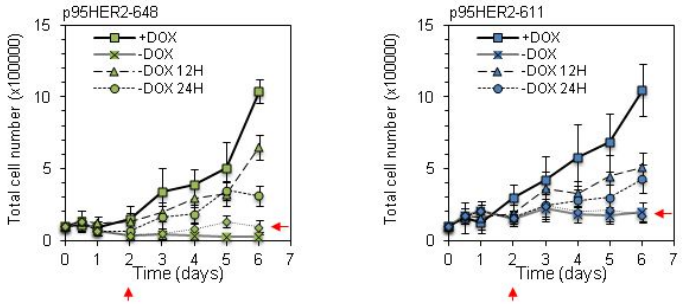

Fig. 15 Determination of the irreversibility time point of p95HER2-induced senescence and apoptosis
MCF7 Tet-Off cells expressing p95HER2-648 (left panel) or p95HER2-611 (right panel) were seeded in the absence of doxycycline, which was added back to the culture media at the indicated time points (12h, 24h or 48h) to stop the transgenes expression. For each condition, cells were counted at 12h, and 1,2,3,4,5 and 6 days after seeding. Red arrows on the right of the graphs indicate the growth curve showing irreversibility and red arrows in the x-axis indicate the time point (48h) when doxycycline was added for that irreversible growth curve.

1.3. DNA damage triggered by the different p95HER2 forms

The DNA damage response (DDR) machinery is activated in response to different genotoxic (22, 23) or oncogenic stresses (24, 25, 121, 122). If possible, the caused DNA damage is repaired during the DDR allowing the resumption of normal cell cycle progression. However, if the DDR is activated during a prolonged period of time, due to persistent damaging signaling or to intense and irreversible damage, the cell will be led to either apoptosis or senescence (4).

It has been proposed that the level of DNA damage determines the activation of one cell fate or the other. When DNA damage is more severe, cells will be led into apoptosis, while if DNA damage is milder, cells will keep the DDR activated and be left in a permanent cell cycle arrest with the characteristics of senescence (216, 217). For this reason DDR has been used as a marker for senescence, as senescent cells present the permanent accumulation of DDR-associated proteins in nuclear DNA foci.

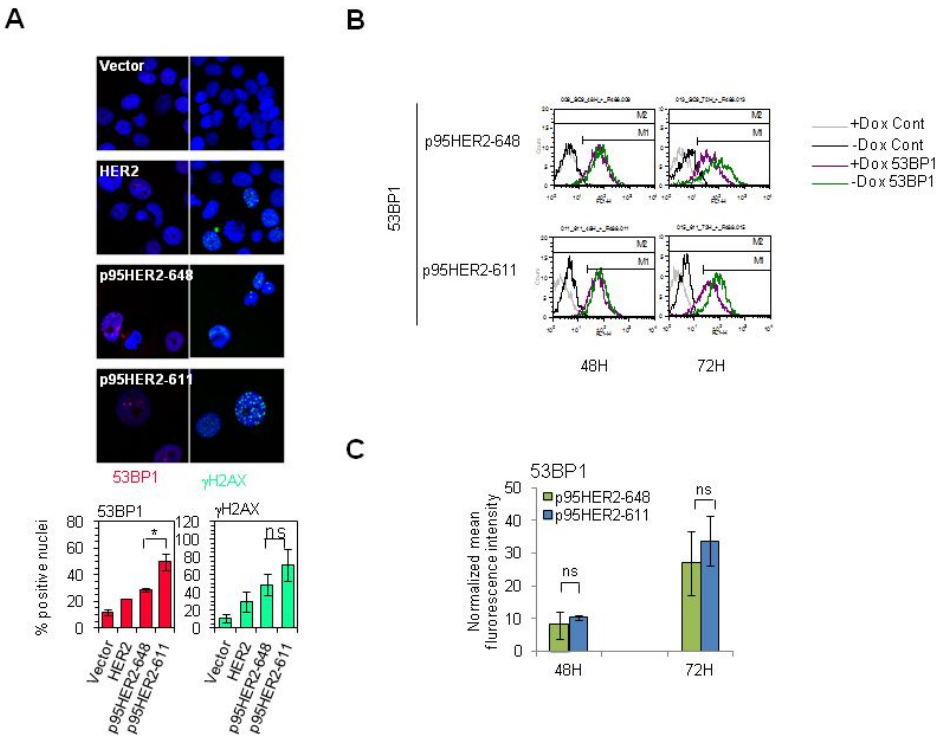

Fig. 16 DNA-damage response (DDR) in cells expressing different p95HER2 fragments
(A) Confocal microscopy images of MCF7 Tet-Off cells expressing the empty vector, HER2, p95HER2-648 or p95HER2-611 fixed, permeabilized and stained after 60h of transgene expression. Nuclear DAPI detection (blue), 53BP1 (red) and gH2AX (green) (upper panel). Quantification of percentage of positive nuclei respect to total nuclei (lower panel). *Mann-Whitney statistical test,* 53BP1 p=0.0419, γH2AX p=0.2860. **(B)** Flow cytometry detection of 53BP1 in MCF7 Tet-Off p95HER2-648 or p95HER2-611 expressing cells fixed, permeabilized and stained after the indicated times of transgene expression. Both floating and adherent cells after tripsinization, were collected. **(C)** Representation of the geometric mean increment of fluorescence intensity of -doxycycline conditions respect to +doxycycline conditions. Average ± SD from two independent experiments. *t-test,* 48H p=0.5169, 72H p=0.5200. (*p<0.05, **p<0.01, ***p<0.001,ns, non-significant).

To determine the level of activation of the DDR induced by the two p95HER2 isoforms, we monitored the presence of DDR-markers, 53BP1 and gH2AX, by immunofluorescence in adherent cells after 60h of expression of these isoforms. The percentage of positive nuclei for both markers was higher in cells expressing p95HER2-611 senescent cells when compared to p95HER2-648 expressing cells (Fig.

16A). However, the result of this analysis could be misleading, since a percentage of p95HER2-648 cells die after 60h of expression (as shown in Fig. 9, 10 and 11) and, consequently, lose their adherent properties, the levels of the marker could be underestimated. For this reason, we assessed the levels of the same DDR markers at earlier time points by using flow cytometry and including both adherent and floating cells (Fig. 16B). Both p95HER2-648 and p95HER2-611 expressing cells showed an increase in 53BP1 protein levels already at 48h of transgene expression. Using this type of determination, we could not detect any significant difference neither in the timing nor in the intensity of 53BP1 expression between p95HER2-648 and p95HER2-611 cells (Fig. 16C). From these results we can conclude that the intensity of DNA damage induced by the expression of both p95HER2 fragments does not determine the cell fate.

2. Signal transduction by p95HER2-648

2.1. p95HER2-648 signals in a non-autonomous manner through HER3

We have already shown that the diverse cellular fates determined by p95HER2-611 and -648 are neither due to the intensity of the signaling (Fig. 13 and 14), nor to the level of DDR activation (Fig. 16B). Then, differences in the activation of signaling pathways leading to OIS or OIA, initiated specifically by p95HER2-611 or -648 could be responsible for the differences observed. Previous work showed that p95HER2-611 generates constitutively active disulfide-bonded homodimers. The cysteine-rich region located in the extracellular moiety of the fragment is responsible (178). p95HER2-648 was also shown to be active as it is capable of activating the most common HER2 downstream pathways (178). However, it lacks this cysteine-rich region in its very short extracellular part and its mechanism of activation has not been characterized. To characterize the mechanism of activation of p95HER2-648, we used two cell lines with different HER/ErbB background, the human breast cancer cell line MCF7 and the human embryonic kidney cell line HEK-293. Both MCF7 and HEK-293 cells are negative for the expression of EGFR, as compared to positive cells MDA-MB-468, and for HER2 as compared to BT474 and SKBR3 cells. They both have detectable levels of HER4, while only MCF7 cells are positive for HER3 (Fig. 17A, B).

Considering this background, for the following experiments we used MCF7 stable transfectants with the inducible Tet-Off system and transiently transfected HEK-293 cells. In order to evaluate the activity of the receptors, activation of MAPK and PI3K pathways was assessed by determining by western blot the levels of p-ERK1,2 and p-

Akt, respectively. The expression of the three different forms, HER2, p95HER2-648 and p95HER2-611, led to activation of MAPK and PI3K pathways in MCF7 cells (Fig. 18A). However, in HEK-293 cells only HER2 and p95HER2-611, but not p95HER2-648, activated the MAPK pathway (Fig. 18A). We observed that in HEK-293 cells only the MAPK pathway is a readout of HER2 receptors activation as it is activated upon HER2 expression and repressed upon lapatinib treatment (Fig. 19A). In contrast, the PI3K pathway shows a level of basal activation in HEK-293 cells, comparable to that observed in MCF7 cells expressing HER2 (Fig. 19B). This high basal level of activation is not further increased upon HER2 expression and is not affected by lapatinib treatment (Fig. 19A). Thus, in this cell line we cannot use Akt phosphorylation as readout of the activation of HER2 receptors.

A

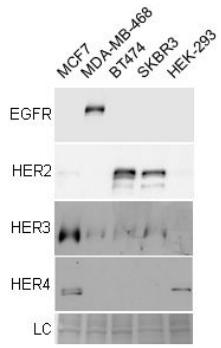

B

	MCF7	MDA-MB-468	BT474	SKBR3	HEK-293
EGFR	0	**1**	0	0	0
HER2	0	0	**1**	0.6	0
HER3	**1**	0.2	0.2	0.3	0
HER4	**1**	0	0	0	0.6

Fig. 17 Expression levels of HER/ErbB receptors in different cell lines
(A) Analysis by western blot of the expression of HER/ErbB receptors (EGFR, HER2, HER3 and HER4) in a panel of five different cell lines: MCF7, MDA-MB-468, BT474, SKBR3 (breast cancer cell lines) and HEK-293 (Human Embrionic Kidney cell line). LC: loading control (ponceau staining). **(B)** Table showing relative levels of expression of each receptor from quantification of the western blots in A. Each receptor relative levels calculated respect to the levels of the cell line with higher levels of that receptor (1).

Together these results indicate that p95HER2-648, unlike HER2 and p95HER2-611, is not able to signal in an autonomous manner in cells expressing low levels of other HER receptors. Since the main difference between the two cell lines is the expression of HER3 (Fig. 17A, B), these results indicate that p95HER2-648 might be active upon interaction with HER3 receptor.

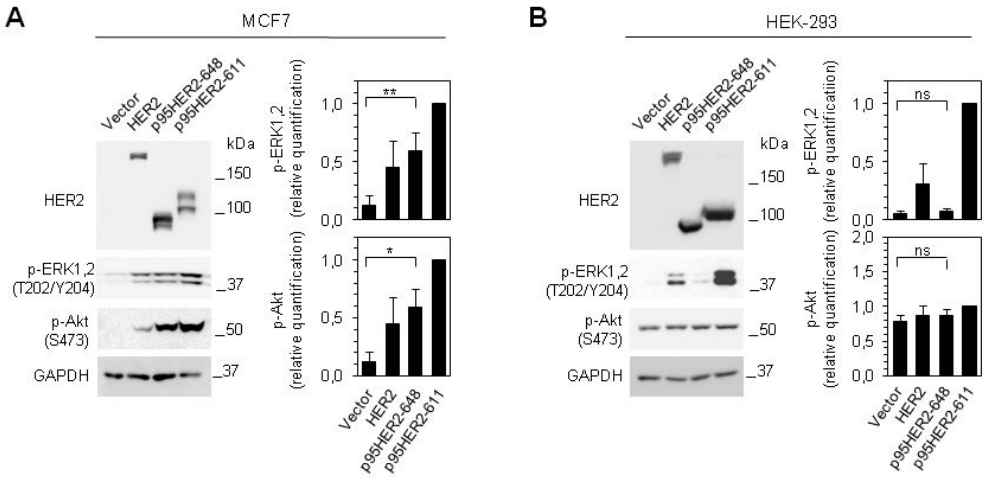

Fig. 18 Expression of p95HER2 in cells with different HER/ErbB background
(A) MCF7 Tet-Off cell expressing the empty vector, HER2, p95HER2-648 or p95HER2-611 after 36h of expression induction (doxycycline removal). Western blot for the indicated antibodies is shown. GAPDH is shown as loading control. Quantification of at least 4 independent experiments, ratio relative to the highest value quantified is shown. *Mann-Whitney statistical test,* p-ERK1,2 p=0.0079, p-Akt p=0.0286. **(B)** Same as in A but with HEK-293 cells transiently expressing the empty vector, HER2, p95HER2-648 or p95HER2-611. *Mann-Whitney statistical test,* p-ERK1,2 p=0.3094, p-Akt, p=0.6857. (*p<0.05, ** p<0.01, *** p<0.001. ns, non-significant).

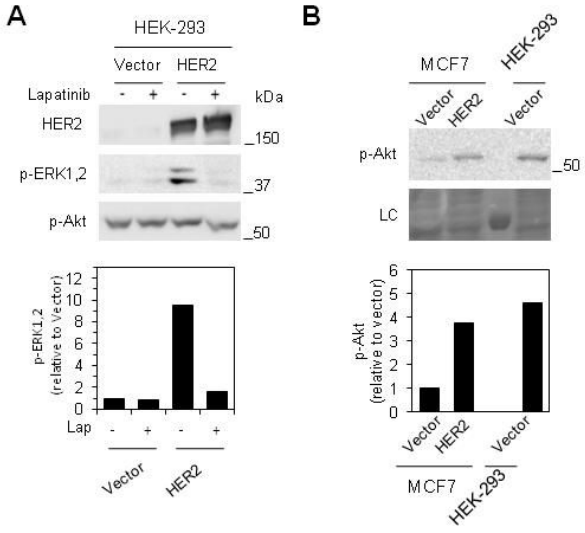

Fig. 19 HER2 expression and signaling in HEK-293 cells
(A) Analysis by western blot of HEK-293 cells transiently expressing HER2 treated with lapatinib 1µM for 24h or left untreated. p-ERK1,2 western blot quantification respect to Vector **(B)** Western blot of MCF7 Tet-Off cells expressing the empty vector or HER2 compared to HEK-293 cells transiently expressing the empty vector, LC: loading control (ponceau staining).

2.2. p95HER2-648 requires HER3 to signal

To confirm the dependency of p95HER2-648 signaling on HER3, we transiently knocked down HER3 from MCF7 Tet-Off cells expressing the different HER2 forms (Fig. 20A). Since activation of HER3 receptor leads to the direct activation of the PI3K-Akt pathway (218), which preferentially occurs through heterodimers HER2-HER3 (219), we monitored the activation of this pathway by detecting p-Akt levels. Knock-down of HER3 led to a decrease in PI3K signaling in MCF7 cells expressing HER2 as expected due to the already mentioned HER2-HER3 heterodimerization (Fig. 20A). Cells expressing p95HER2-611 showed no difference on the signaling after HER3 knock-down (Fig. 20A). According to previous work, this form signals in an autonomous manner (178), which was corroborated by this result. Finally, p95HER2-648 showed a significant decrease in PI3K activation after HER3 knock-down, confirming the dependence of this form on HER3 presence (Fig. 20A).

To further confirm that p95HER2-648 signals through HER3, their physical interaction was assessed by co-immunoprecipitation. We performed immunoprecipitation of HER3 in MCF7 cells expressing the different HER2 forms. Detection by western blot analysis of p95HER2-648 in the immunoprecipitated fraction indicates the interaction of these molecules (Fig. 20B). As expected, HER2 was also found associated to HER3 while p95HER2-611 association was almost undetectable.

Interaction through the extracellular domains is the currently accepted mechanism of interaction described for the HER/ErbB family. However, a recent work also indicated the important role of the transmembrane domains in dimerization and activation (220). The lack of an extracellular domain in p95HER2-648 suggests that the interaction between both receptors might occur through the transmembrane and/or the kinase domains.

Together these results indicate that p95HER2-648 is an active fragment of HER2 activated upon heterodimerization with HER3, but not upon homodimerization. However, we cannot rule out the possibility that different combinatorial heterodimers with other receptors, even not from the HER/ErbB-family, might occur in different cellular contexts.

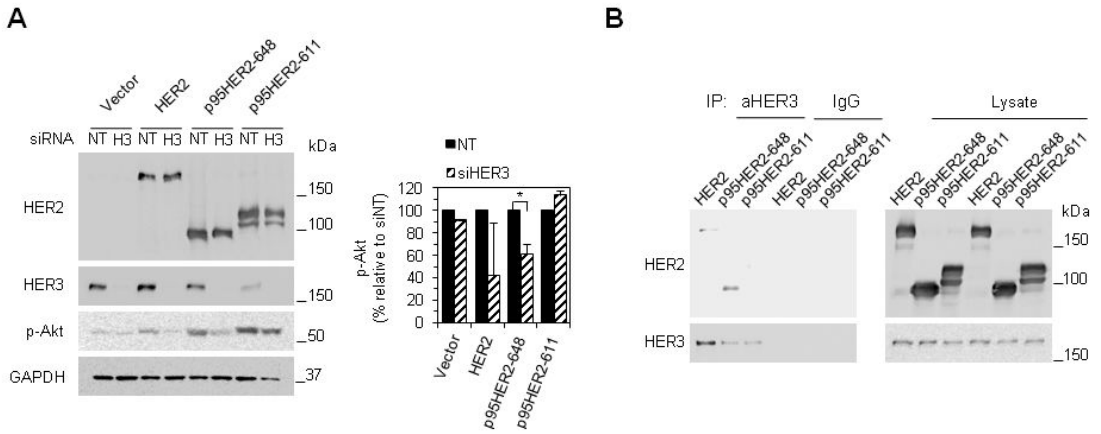

Fig. 20 Effect of HER3 on p95HER2 signaling
(A) MCF7 Tet-Off cells expressing the empty vector, HER2, p95HER2-648 or p95HER2-611 transiently transfected with HER3 siRNA (H3) or non-target siRNA (NT) were lysed and analyzed by western blot with the indicated antibodies. p-Akt levels were quantified and representation of mean ± SD of percentage of p-Akt in siHER3 with respect to siNT in each case is shown. *t-test*, p95HER2-648 p=0.0178. **(B)** Analysis of HER2 and HER3 levels in HER3 immunoprecipitates (left panel) and total lysates (right panel) in MCF7 Tet-Off cells expressing HER2 p95HER2-648 or p95HER2-611. (*p<0.05, **p<0.01, ***p<0.001. ns, non-significant).

We intended to extend the study to other cell lines expressing different HER/ErbB family receptors. Unfortunately, transduction with a vector encoding p95HER2-648 resulted in very low expression levels (data not shown). Therefore, we have not been able to express p95HER2-648 in other cell lines.

2.3. Effect of p95HER2-648 on the activation of other receptor tyrosine kinases (RTK)

HER/ErbB family members are allosterically activated upon ligand-induced homo- or heterodimerization (164, 221). Ligand binding induces a conformational change in the extracellular domain, from an inhibitory-closed conformation to an open conformation allowing the dimerization (222). HER2 is the only family member lacking any ligand, which is activated upon dimerization as it exists in a constitutively open conformation (223). Truncated HER2 forms, p95HER2, do not display the inhibitory extracellular domain, p95HER2-611 was shown to preferentially homodimerize due to the formation of constitutive strong disulfide intermolecular bonds (178), and we showed in this work that p95HER2-648 dimerizes with HER3 in order to be active when expressed in MCF7 cells (Fig. 20).

The lack of almost all the extracellular domain in p95HER2-648 fragment made us wonder whether this feature could allow enhanced dimerization with other receptor tyrosine kinases, not only from the HER/ErbB family. In order to address that point, we performed a human phospho-receptor tyrosine kinase array where the phosphorylation levels of 49 different human RTKs were analyzed in cells expressing p95HER2-648 or p95HER2-611 for 36h (Fig. 21), just before the commitment to the apoptotic or senescent phenotype, respectively (Fig. 15).

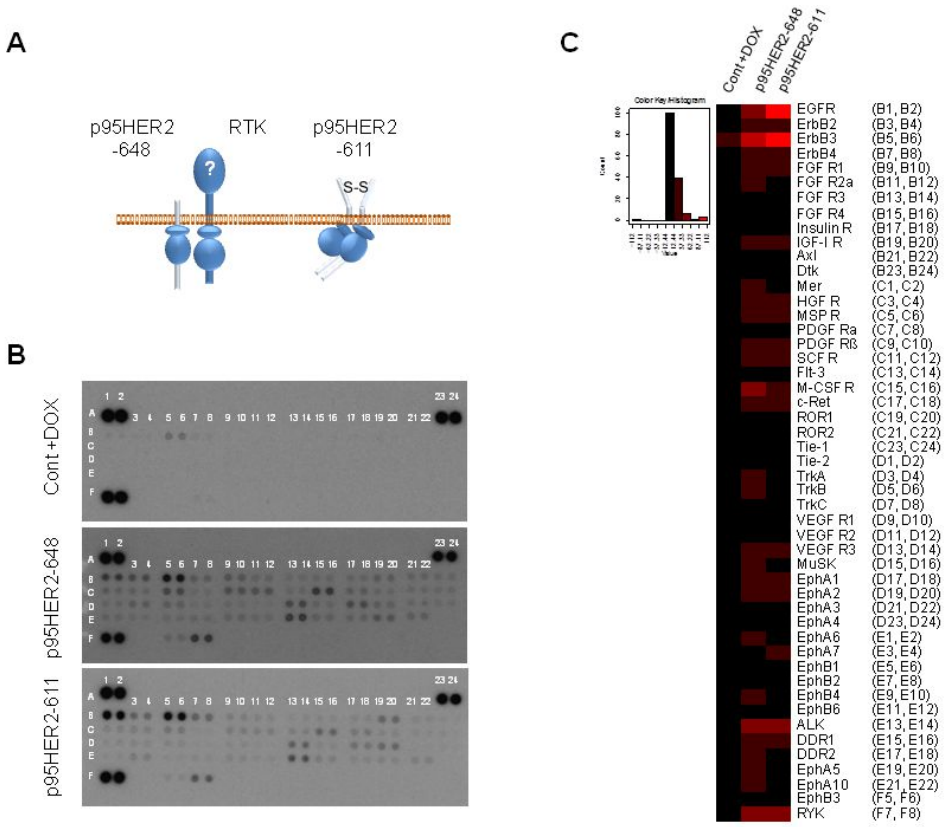

Fig. 21 Phosphorylation of 49 different human receptor tyrosine kinases
(A) Schematic representation of the hypothetical model for the different p95HER2 dimerization options **(B)** Human phospho-RTK array. Cell lysates were obtained 36 hours after washing doxycycline from MCF7 Tet-Off cells expressing p95HER2-648 or p95HER2-611 plated in the absence or presence of doxycycline. Exposure time for quantification of each blot was selected taking into account control spots (membrane upper left and right, bottom left). **(C)** Heatmap representation of mean-pixel quantification for each spot (average of 2 spots).

Results of the array showed increased levels of p-EGFR and p-HER3 in both cells expressing p95HER2-648 and p95HER2-611 (Fig. 21B, C). We have already demonstrated that p95HER2-648 directly interacts with HER3 (Fig. 20B). On the other hand, as it was previously demonstrated, p95HER2-611 is activated mainly through constitutive homodimerization (178), so the increase in p-EGFR and p-HER3 levels

could be due to an indirect effect rather than to a direct interaction and activation. There have already been described signaling feedback loops that transcriptionally regulate HER/ErbB family receptor levels, as for the case of HER3, which is regulated by Akt activation of FoxO transcription factors (224). In MCF7 Tet-Off p95HER2-611 cells, we observed an increase in EGFR, both at transcript and protein levels (Fig. 22A, B). From the transcriptomic array we also observed higher levels of EGFR ligands, such as TGFα, HB-EGF and AREG (Fig. 22A). AREG was also detected in the secretome analysis already published by our group (Fig. 22C and (42)). Taking these results into account, and the fact that we did not observe an interaction of p95HER2-611 with HER3 in the immunoprecipitation assays (Fig. 20A), we hypothesized that the increase in EGFR and HER3 phosphorylation in p95HER2-611 cells could be due to EGFR-HER3 dimers formation and activation. However, further experiments would be necessary to confirm that. In contrast, p95HER2-648 expressing cells showed a milder transcriptional increase of EGFR (Fig. 22A), which did not account for an increase at protein level (Fig. 22B). Thus, increased p-EGFR levels in these cells, which are lower than in p95HER2-611 expressing cells, are probably due to a direct interaction rather than to a feedback loop activation. From these results we can conclude that p95HER2-648 signals mainly through activation of HER3 as already demonstrated (Fig. 20).

A

	Affimetrix Gene Array log2 FC			
	Vector	Her2	p95HER2-648	p95HER2-611
EGFR	0.66	0.79	1.35	2.01
TGFα	-0.16	0.71	1.35	2.13
HB-EGF	0.24	1.45	3.26	4.05
AREG	0.11	1.29	1.26	1.61
AREGB	0.18	1.39	0.53	2.04

B

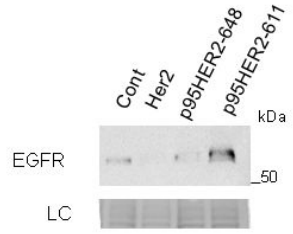

C

	Secretome analysis Log2 FC
	p95HER2-611
AREG	4.32

Fig. 22 EGFR and HER3 activation in p95HER2-611 expressing cells
(A) Affimetrix gene-chip expression analysis in MCF7 Tet-Off cells expressing the empty vector, HER2, p95HER2-648 or p95HER2-611 after 60h of the transgenes expression. Data is shown as Log2 FC respect to +Dox conditions. **(B)** Western blot with EGFR antibody of MCF7 Tet-Off cells expressing the empty vector, HER2, p95HER2-648 or p95HER2-611 after 36h of the transgenes expression. LC: loading control (ponceau staining). **(C)** Table shows AREG levels found in the secretome analysis of MCF7 Tet-Off p95HER2-611 by label free proteomics after 7 days of expression. Data is represented as Log2 FC respect to MCF7 Tet-Off cells expressing the empty vector (Data adapted from (42)).

3. Pathways activated by the different p95HER2 forms and their implication in the onset of OIS or OIA

3.1. Effect of targeting PI3K, MAPK, JNK or Src pathways on the onset of apoptosis or senescence

We observed that, while p95HER2-611 is able to signal autonomously, p95HER2-648 requires HER3 to signal. Therefore, we hypothesized that the two p95HER2 isoforms may activate different intracellular pathways.

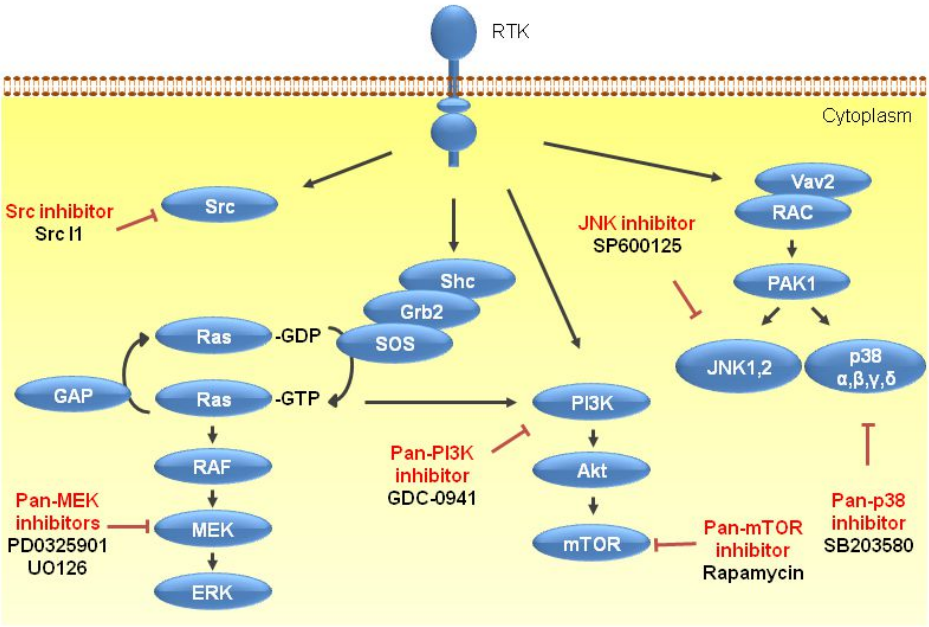

Fig. 23 Intracellular signaling pathways activated by RTKs and their inhibitors
Schematic representation of the different pathways activated by RTK and the different specific inhibitors targeting these pathways.

Two of the main signaling pathways activated by the HER/ErbB family receptors are PI3K and MAPK pathways (Fig. 23). Both fragments activated similarly these two pathways, as measured by p-Akt and p-ERK levels, respectively (Fig. 24A, B).

To determine whether these pathways initiated by the p95HER2 isoforms were participating on the onset of senescence or apoptosis, we used different specific inhibitors.

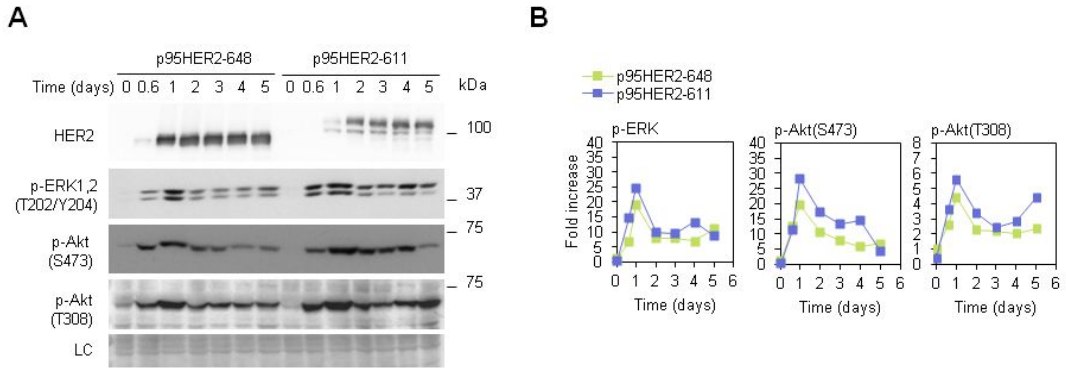

Fig. 24 Activation of MAPK and PI3K pathways by the different p95HER2 forms
(A) MCF7 Tet-Off cells expressing p95HER2-648 or p95HER2-611 were cultured without doxycycline for the indicated time points, lysed and analysed by western blotting with the indicated antibodies. LC: loading control (ponceau staining). **(B)** Western blots were quantified and the results were normalized to the time point with the lowest intensity levels.

PI3K pathway blockade with the selective ATP-competitive inhibitor GDC0941 at increasing concentrations did not show a decrease on SubG1 fraction of p95HER2-648 expressing cells. GDC0941 treatment in cells expressing p95HER2-611 also did not overcome senescence, as the percentage of cells in the S phase of the cell cycle did not increase (Fig. 25A). Similar effects were observed when cells were treated with the mTOR inhibitor rapamycin. Although we evidenced an increase in S phase in p95HER2-611 expressing cells, it was not accompanied by a morphological change in the cells indicating an avoidance of the senescence state (data not shown).

Two different MEK1,2 inhibitors, PD0325901 and UO126, were used to impair MAPK signaling pathway (Fig. 23, 25B). Treatment of p95HER2-648 cells with increasing concentrations of PD0325901 or with UO126 10µM showed no significant differences on percentage of cells accumulated in SubG1 fraction (Fig. 25B). Treatment of p95HER2-611 cells with the same inhibitors showed a slight increase in SubG1 fraction and an increase in the S phase. Despite these minor changes in the cell cycle profile, cells did not experiment any morphological change or obvious enhanced proliferation (data not shown).

Therefore, we can conclude that in accordance with the lack of differences observed in the activation of PI3K and MAPK pathways by the two p95HER2 isoforms, these pathways were not implicated on the onset of neither p95HER2-611-induced senescence, nor in p95HER2-648-induced apoptosis.

In addition, inhibition of JNK and Src pathways, which are also usually activated by HER/ErbB receptors (Fig. 23) showed no significant effect neither in apoptotic p95HER2-648 expressing cells, nor in senescent p95HER2-611 expressing cells (Fig. 25C).

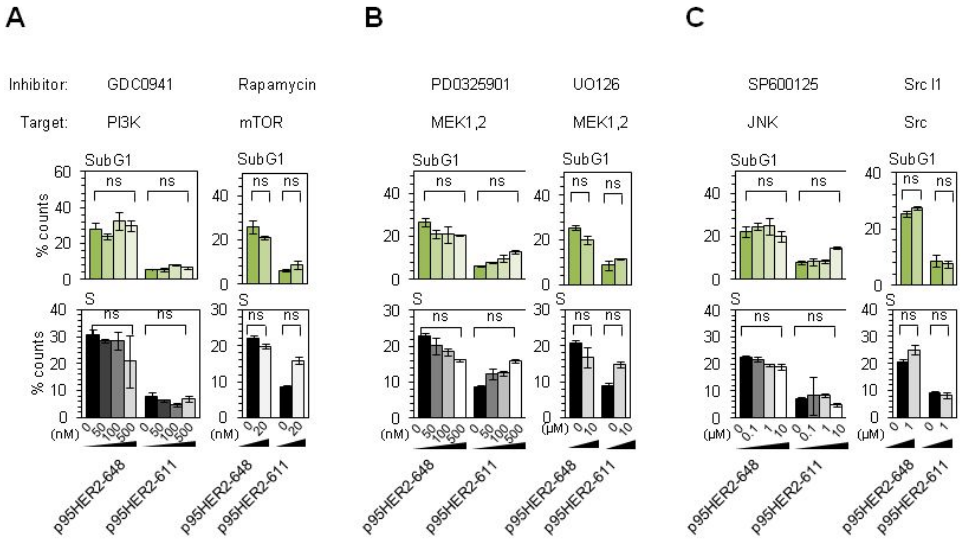

Fig. 25 Effect of targeting PI3K, MAPK, JNK or Src pathways on the onset of apoptosis and senescence
MCF7 Tet-Off cells expressing p95HER2-648 and p95HER2-611 were treated with the indicated inhibitors at the indicated concentrations for 24h in the presence of doxycycline. Cells were then washed from doxycycline and treated with the indicated inhibitors at the indicated concentrations for additional 60h in the absence of doxycycline. SubG1 and cell cycle determination by flow cytometry was performed (for statistics comparison to untreated cells). **(A)** PI3K inhibitor, GDC0941 (GDC): for 500nM concentration the average from two independent experiments is shown, for the other concentrations data from triplicates in one experiment is represented. *Mann-Whitney statistical test,* SubG1: p95HER2-648 GDC-500nM p=0.4857, p95HER2-611 GDC-500nM p=0.0571; S phase: p95HER2-648 GDC-500nM p=0.2, p95HER2-611 GDC-500nM p=0.3429. mTOR inhibitor, rapamycin: some toxicity at +dox was observed (data not shown). Data from one experiment is shown. *t-test,* SubG1: p95HER2-648 p=0.1038, *Mann-Whitney statistical test,* SubG1: p95HER2-611 p=0.1; *t-test,* S phase: p95HER2-648 p=0.0867; S phase: p95HER2-611 p=0.1. **(B)** MEK inhibitor, PD0325901 (PD): No toxicity at +dox was observed (data not shown). For 100nM concentration average from two independent experiments is shown. For the other concentrations data from one experiment is shown. *Mann-Whitney statistical test,* SubG1: p95HER2-611 PD-500nM p=0.1; S phase: p95HER2-611 PD-500nM p=0.1. MEK inhibitor, UO126: Data from one experiment is represented. *Mann-Whitney statistical test,* SubG1: p95HER2-648 p=0.1, p95HER2-611 p=0.1; S phase: p95HER2-648 p=0.2, p95HER2-611 p=0.8222. **(C)** JNK inhibitor SP600125 (SP): No toxicity at +dox was observed (data not shown). Data from one experiment is shown. *Mann-Whitney statistical test,* SubG1: p95HER2-648 SP-10μM p=0.4, p95HER2-611 SP-10μM p=0.1; S phase: p95HER2-648 SP-10μM p=0.1, p95HER2-611 SP-10μM p=0.1. Src inhibitor, Src I1: Data from one experiment is represented. *Mann-Whitney statistical test,* SubG1: p95HER2-648 p=0.1, p95HER2-611 p=0.7; S phase: p95HER2-648 p=0.1, p95HER2-611 p=0.4. (*p<0.05, **p<0.01, ***p<0.001. ns, non-significant).

3.2. p95HER2-648 activates specific signaling pathways

Analysis of additional signaling pathways showed that the MAPK p38 and the Rho exchange factor Vav2, which was previously described to interact with EGFR (168, 225), were specifically activated by p95HER2-648 (Fig. 26A, B). Interestingly, kinetics analysis showed that the activation of these pathways precedes the onset of apoptosis, as shown by cleaved PARP levels (Fig. 26A).

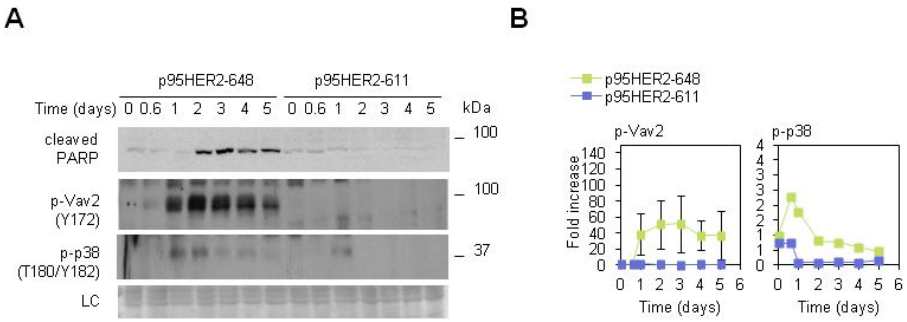

Fig. 26 p95HER2-648 specific signaling pathways
(A) MCF7 Tet-Off cells expressing p95HER2-648 or p95HER2-611 were lysed at the indicated time points after doxycycline removal and cell lysates analyzed by western blotting with the indicated antibodies. **(B)** Kinetic curves from the quantification of the western blots in (A) for the different time points referred to the time point with the lowest intensity levels.

Transient knock-down of HER3 resulted in a decrease in the levels of p-Vav2 and p-p38 (Fig. 27A). The decrease in the levels of p-Vav2 was confirmed in cells stably knocked down for HER3 (Fig. 27B). These results show that activation of Vav2 and p38 in MCF7 Tet-Off cells expressing p95HER2-648 is dependent on HER3.

We then analyzed whether the pathways specifically activated by p95HER2-648 were responsible for the onset of apoptosis. Unfortunately the knock-down of HER3 did not interfere with the onset of apoptosis as shown by cleaved PARP levels and SubG1 fraction determination (Fig. 28A, B).

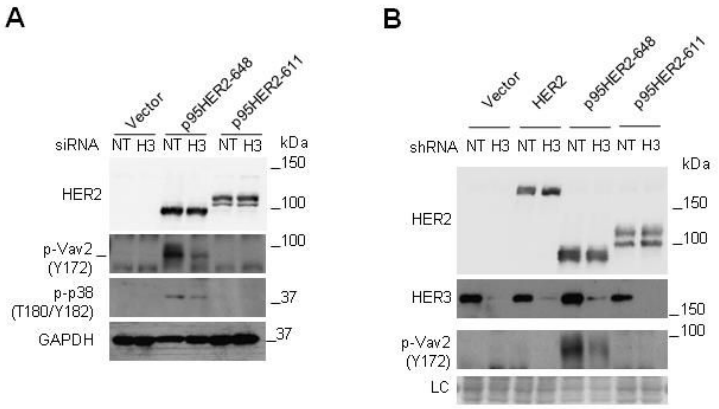

Fig. 27 Effect of HER3 knock-down on the specific p95HER2-648 activated pathways
(A) MCF7 Tet-Off cells expressing the empty vector, p95HER2-648 or p95HER2-611 were transiently transfected with control non-target siRNAs (NT) or siRNAs specifically targeting HER3 (H3) in the presence of doxycycline. After two days cells were washed off and plated without doxycycline for additional 60h. The indicated proteins were analyzed by western blotting **(B)** MCF7 Tet-Off cells expressing the empty vector, HER2, p95HER2-648 or p95HER2-611 were stably knocked down for HER3 with specific shRNA (H3), using as control non-target shRNA (NT). The indicated proteins were analyzed by western blotting. LC: loading control (ponceau staining).
Fig. 28 Effect of HER3 knock-down on the onset of apoptosis

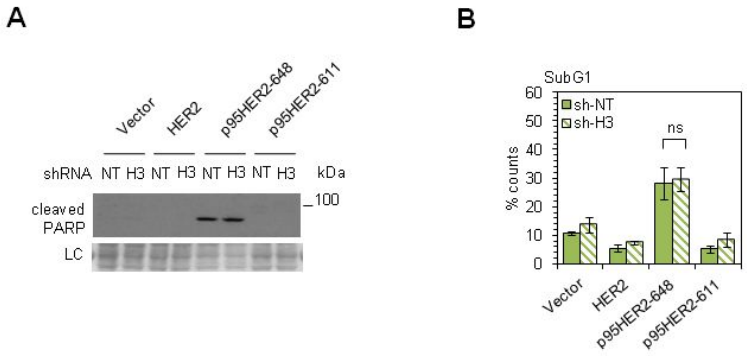

(A) MCF7 Tet-Off cells expressing the empty vector, HER2, p95HER2-648 or p95HER2-611 were stably knocked down for HER3 with specific shRNA (H3), using as control non-target shRNA (NT). After culturing the cells 60h without doxycycline the levels of cleaved PARP were analyzed by western blotting, LC: loading control (ponceau staining), and **(B)** SubG1 fraction was determined. SubG1 results are expressed as average ± SD from 3 independent experiments. *Mann-Whitney statistical test,* p95HER2-648 p=0.6517. (*p<0.05, **p<0.01, ***p<0.001. ns, non-significant).

Furthermore, the specific transient knock-down of Vav2 with siRNA did not reduce the apoptosis markers cleaved PARP or accumulation of cells in SubG1 (Fig. 29A, B). This result leads us to conclude that, although Vav2 is specifically activated by p95HER2-648 - HER3 complexes, it is not responsible for the onset of apoptosis.

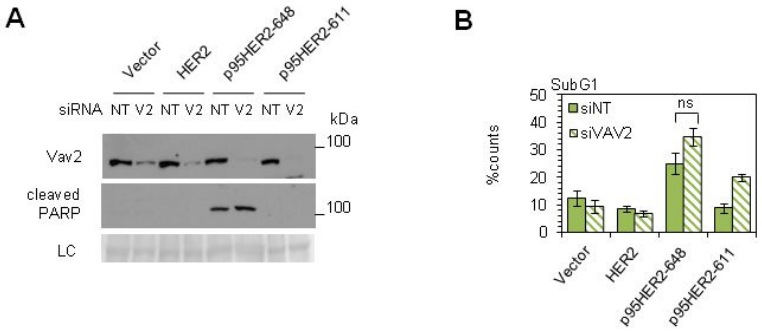

Fig. 29 Analysis of cells knocked-down for Vav2
MCF7 Tet-Off cells expressing the empty vector, HER2, p95HER2-648 or p95HER2-611 were transiently transfected with control non-target siRNAs (NT) or siRNAs specifically targeting VAV2 (V2) in the presence of doxycycline. After two days, cells were washed off and plated without doxycycline for additional 60h. **(A)** The indicated proteins were analyzed by western blotting and **(B)** SubG1 fraction was determined. *Mann-Whitney statistical test,* SubG1 p95HER2-648 p=0.1333 (*p<0.05, **p<0.01, ***p<0.001. ns, non-significant).

3.3. Effect of SB203580, a p38 inhibitor, on the onset of apoptosis

p38 activity can be selectively blocked by the catalytic inhibitor SB203580, which binds to the p38 ATP-binding pocket. Since the phosphorylation of p38 is not affected by the inhibitor, we used the phosphorylation of a downstream p38 substrate, the activating transcription factor 2 (ATF2), to monitor the inhibition. Treatment with 10µM SB203580 resulted in an inhibition of p38 pathway and in a significant decrease of SubG1 accumulated cells and in a milder decrease in cleaved PARP in MCF7 Tet-Off p95HER2-648 expressing cells (Fig. 30A, B).

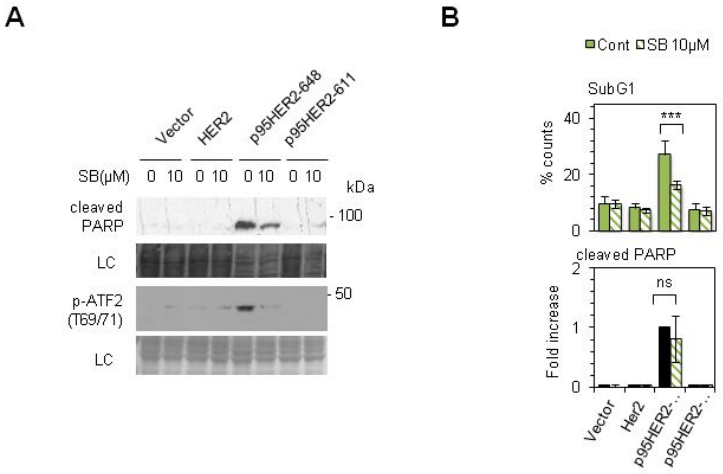

Fig. 30 Analysis of p38 inhibition with SB203580 on the onset of apoptosis
MCF7 Tet-Off Vector, HER2, p95HER2-648 or p95HER2-611cells were treated or left untreated with SB203580 10μM for 24h in the presence of doxycycline. Cells were then washed out from doxycycline and seeded in the absence of doxycycline with or without SB203580 10μM for additional 60h. **(A)** Cell lysates were analyzed by western blotting with the indicated antibodies. **(B)** SubG1 analysis (upper panel) and quantification of cleaved PARP (lower panel) from western blot showed in (A) (fold increase respect to p95HER2-648 is shown). Results expressed as average from 4 independent experiments. *Mann-Whitney statistical test,* SubG1 p95HER2-648 $p<0.0001$; Cleaved PARP p95HER2-648 $p=0.3143$. (*$p<0.05$, **$p<0.01$, ***$p<0.001$. ns, non-significant).

However, this effect was not confirmed by the specific downmodulation of p38α (Fig. 31A, B). As chemical inhibitors can usually have some inespecificities, we intended to ensure that SB203580 treatment outcome was not due to an off-target effect inhibiting another kinase. A published study about the selectivity of protein kinase inhibitors showed that out of 73 tested kinases, SB203580 at a concentration of 1μM, was selectively inhibiting (around 90% activity inhibition) p38α and β (not γ and δ), and two other kinases, CK1δ and RIPK2 with similar efficiency to p38α and higher efficiency than to p38β. Only two other kinases were partially inhibited (70% inhibition), GSK3β and GAK (Fig. 31C, adapted from (226)). CK1δ or RIPK2, which according to the published study were inhibited similarly to p38α (226), have also been related to apoptosis (227). Transient knock-down of CK1δ and RIPK2 with siRNA did not show any effect on p95HER2-648-induced apoptosis measured as accumulation of cells in SubG1 (Fig. 31D).

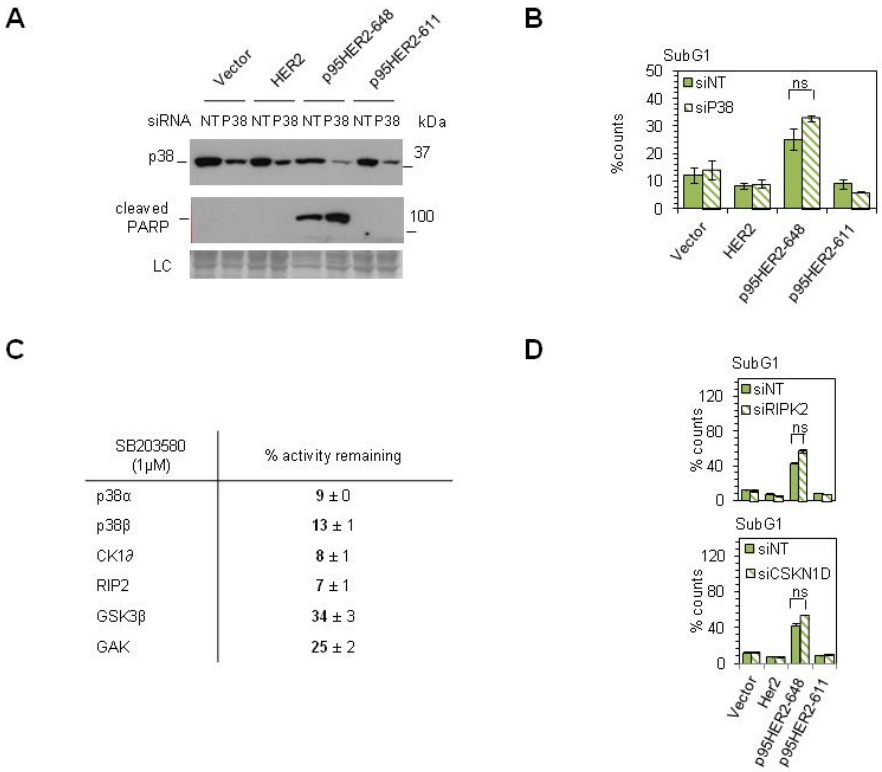

Fig. 31 Effect of the knock-down for p38 or SB203580 off-targets, CK1δ and RIPK2, on apoptosis
(A) MCF7 Tet-Off cells expressing the empty vector, HER2, p95HER2-648 or p95HER2-611 were transiently transfected with control non-target siRNAs (NT) or siRNAs specifically targeting p38 (p38) in the presence of doxycycline. After two days, the cells were washed off and plated without doxycycline for additional 60h. The indicated proteins were analyzed by western blotting and **(B)** SubG1 fraction was determined. **(C)** Table showing the percentage of activity remaining for the indicated kinases treated with SB203580 1µM (adapted from (226)). **(D)** SubG1 analysis from cells transfected as in (A) with control non-target siRNAs (NT) or siRNAs specifically targeting RIPK2 or CK1δ. *Mann-Whitney statistical test,* p95HER2-648 RIPK2 p=0.1; p95HER2-648 CK1δ p=0.1. (*p<0.05, **p<0.01, ***p<0.001. ns, non-significant).

Contradictory results between molecular knock-down with siRNA and chemical inhibition with a selective inhibitor (SB203580) of p38, did not let us conclude whether p38 was involved in p95HER2-648-induced apoptosis. We ruled out that the most obvious possible off-target candidates, CK1δ and RIPK2, according to the literature (226), were involved. Further study of the off-target effects of SB203580 would be needed to conclude the mechanism of SB203580 inhibition of p95HER2-648-induced apoptosis.

3.4. Transcriptomic analysis

We have already shown that the different HER2 fragments are activated through different mechanisms (Fig. 20), and that they can activate different signaling pathways (Fig. 26). Hence, it is logical to think that they can specifically activate the transcription

of different genes. To test this possibility, we performed a transcriptomic analysis of cells expressing HER2, p95HER2-648 and -611.

The expression of only 144 genes was commonly regulated by the three HER2 forms and 249 were shared by the two p95HER2 forms. A total of 558 genes were found to be specifically regulated by p95HER2-648 and 540 specifically by p95HER2-611 (Fig. 32A). We validated by RTqPCR the expression of some of the genes specifically regulated by p95HER2-648. Specific upregulation of the transcript levels of IL8, activating transcription factor 3 (ATF3) and growth arrested and DNA damage 45A (GADD45A) were confirmed.

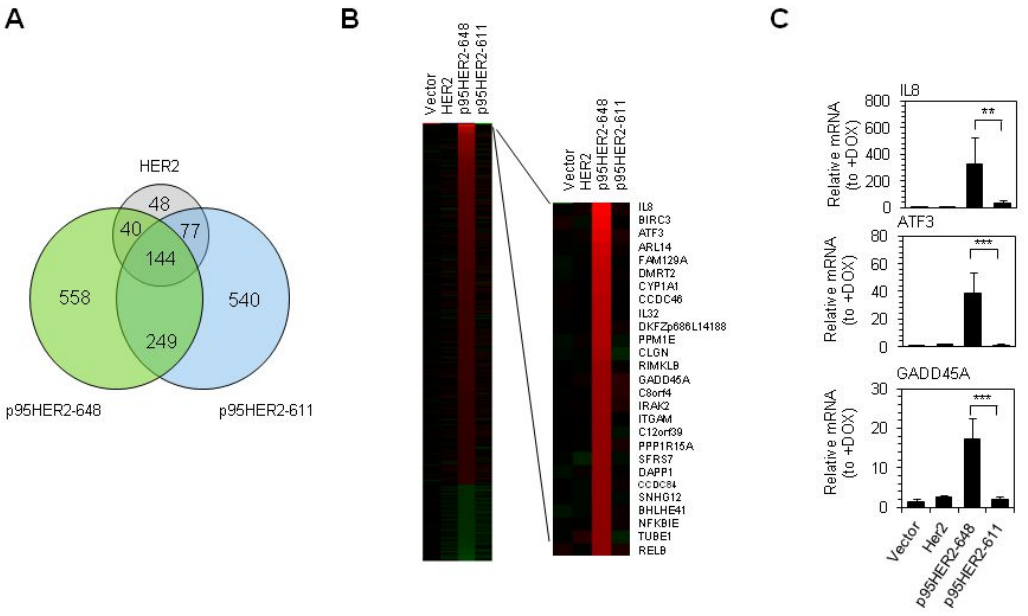

Fig. 32 Transcriptomic analysis
Affimetrix gene-chip expression analysis in MCF7 Tet-Off Vector, HER2, p95HER2-648 and p95HER2-611 cells after 60h of transgene expression. Data represented as Log2 FC relative to +doxycycline conditions **(A)** VENN diagram representation considering the log2 FC >1.5 or <-1.5 as regulated **(B)** Heatmap representation of the p95HER2-648 specifically regulated genes. Genes with log2 FC >1.5 or <-1.5 considered as up- (red) or down- (green) regulated, respectively, are represented.**(C)** IL8, ATF3 and GADD45A RTqPCR from MCF7 Tet-Off Vector, Her2, p95HER2-648 or p95HER2-611 at 60h of transgene expression. Relative mRNA represented as mean ± SD from 3 independent experiments (each condition in triplicate). *Mann-Whitney statistical test,* IL8 p=0.0061, ATF3 p=0.0006, GADD45A p=0.0004. (*p<0.05, **p<0.01, ***p<0.001. ns, non-significant).

Interestingly, both ATF3 (228-232) and GADD45A (233) have been related to the regulation of apoptosis. We then analyzed the list searching for more genes that could potentially regulate apoptosis or senescence. We found that many apoptosis related genes, both pro- and anti- apoptotic, were regulated by the different p95HER2 forms (Fig. 33A).

In cells expressing p95HER2-648 most of the up-regulated genes were pro-apoptotic. Among them, the already mentioned and validated ATF3 and GADD45A (Fig. 32C). However, transient knock-down of those genes (Fig. 33B) showed no effect on the apoptotic profile as assessed by SubG1 analysis (Fig. 33C). Finally, it caught our attention that in p95HER2-611, the most and differently up-regulated gene was an anti-apoptotic one, Bcl-2A1 (234) (Fig. 33A).

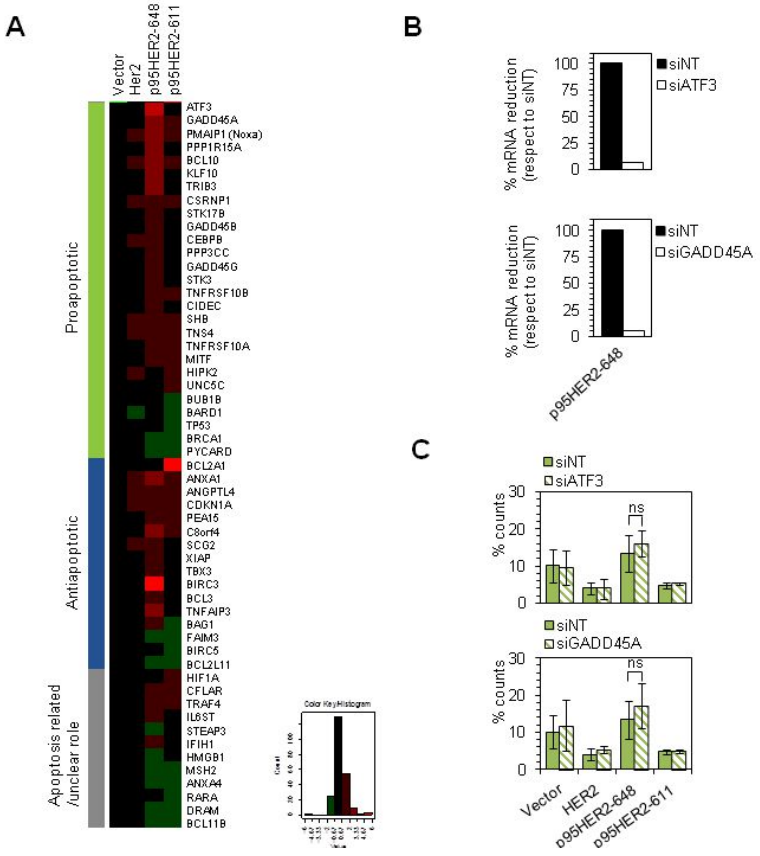

Fig. 33 Apoptosis-related genetic profile
(A) Heatmap representation of the pro- and anti-apoptotic genes specifically regulated by MCF7 Tet-Off p95HER2-648 or p95HER2-611 cells. Data from the Affimetrix gene-chip expression analysis in MCF7 Tet-Off Vector, HER2, p95HER2-648 and p95HER2-611 cells after 60h of transgene expression. Results are expressed as Log2 FC relative to +doxycycline conditions. Genes with log2 FC >1.5 or <-1.5 considered as up- (red) or down- (green) regulated, respectively, are represented. **(B)** MCF7 Tet-Off Vector, HER2, p95HER2-648 or p95HER2-611 were transiently transfected with control non-target siRNAs (NT) or siRNAs specifically targeting ATF3 or GADD45A in the presence of doxycycline. After two days cells were washed off and plated without doxycycline for additional 60h. ATF3 and GADD45A relative mRNA levels were determined by RTqPCR in MCF7 Tet-Off p95HER2-648 cells as control for siRNA knock-down. Data represented as percentage of relative mRNA respect to control non-target siRNA transfected cells. **(C)** SubG1 analysis of cells described in (B). SubG1 results are expressed as average from at least two independent experiments. *Mann-Whitney statistical test*, p95HER2-648 siATF3 p=5714, p95HER2-611 siGADD45A p=3874. (*p<0.05, **p<0.01, ***p<0.001. ns, non-significant).

4. p21 and Bcl-2 are the key effectors protecting p95HER2-611 from apoptosis and allowing the entrance in senescence

4.1. p95HER2-611 specifically upregulates p21

Since many anti-apoptotic genes were upregulated in cells expressing p95HER2-611 (Fig. 33A), we hypothesized that the expression of this fragment could, in addition to induce the onset of senescence, protect cells from apoptosis. In agreement with this hypothesis, we observed that upon p95HER2-611 expression, the levels of cleaved PARP diminished in a time course-dependent manner (Fig. 26A, 34A). Similar tendency was observed in the percentage of cells accumulated in SubG1 (Fig. 10B).

The expression of many cell cycle regulators is modulated during the processes of apoptosis and senescence. Among these, the cyclin-kinase dependent inhibitor p21, in addition to its role as a cell cycle inhibitor involved in the onset of senescence, has anti-apoptotic functions (119).

We assessed the levels of the cell cycle regulators p21, p53 and Myc at different time points in cells expressing p95HER2-648 or p95HER2-611. Results showed that p21 was the only factor differentially regulated, as an increase in protein levels was observed only in p95HER2-611 expressing cells (Fig. 34A, B). Interestingly, p21 levels increase preceded the decrease in cleaved PARP levels in p95HER2-611 cells (Fig. 34A). This fact is in accordance with the described anti-apoptotic role of p21. To our knowledge, p21 has never been described to act as an apoptosis protector during oncogene-induced senescence, necessary not only to stop cell cycle and proliferation but also, to avoid damaged cells to enter into the apoptotic program.

It has been proposed that the anti-apoptotic function of p21 is exerted through its phosphorylation by Akt at residue Thr-145, which results in the accumulation of p-p21 in the cytoplasm (119). An increase in p-p21 levels is observed in p95HER2-611 cells after 2-3 days of expression (Fig. 34A, B), but further experiments would be needed to confirm that it is in fact this phosphorylated form the one responsible for an anti-apoptotic effect in p95HER2-611 cells.

In addition to p21, levels of p53 protein, which is one of the master regulators of both apoptosis and senescence, were found to be upregulated in both p95HER2-648 and p95HER2-611 expressing cells, although p95HER2-611 senescent cells seemed to display higher levels of p53 along time (Fig. 34A, B).

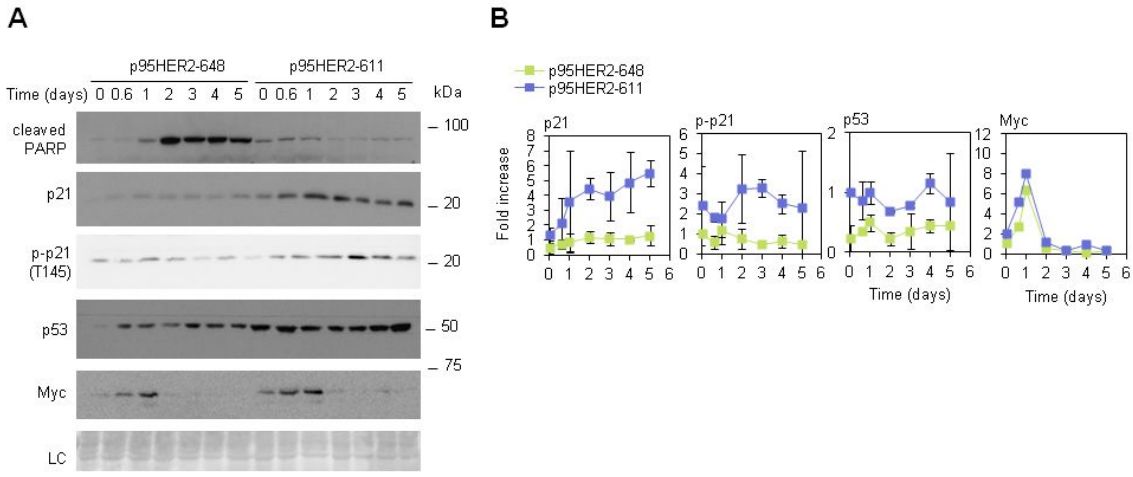

Fig. 34 Analysis of cell cycle regulators on p95HER2 expressing cells
(A) MCF7 Tet-Off cells expressing p95HER2-648 or p95HER2-611 were plated without doxycycline and cell lysates were harvested and analyzed by western blot for the indicated proteins. **(B)** Kinetic curves for the quantification of the western blots in (A). Each time point is referred to the point with the lowest levels.

At the transcriptional level we observed a minor increase of p21 mRNA levels at 24h after induction, and a higher increase at 60h, although in both p95HER2-648 and p95HER2-611 expressing cells (Fig. 35A).

p53 is known to be one of the major transcriptional regulators of p21 (109), although mechanisms of regulation of p21 independent of p53 have also been described (101, 111). p53 knock-down in p95HER2-611 cells decreased moderately p21 protein levels (Fig. 35B), but surprisingly, did not decrease the levels of the mRNA encoding (Fig. 35A). In addition, p21 transcriptional levels were upregulated in both p95HER2-648 and p95HER2-611 cells and p53 knockdown did not decrease this transcript levels in p95HER2-648 cells neither (Fig. 35A). These results make us conclude that the regulation of p21 is likely due to a p53-independent posttranscriptional mechanism and since we did not see an accumulation of p21 in p95HER2-648 cells, in addition to the transcriptional regulation, other mechanisms may contribute to regulate the levels of p21.

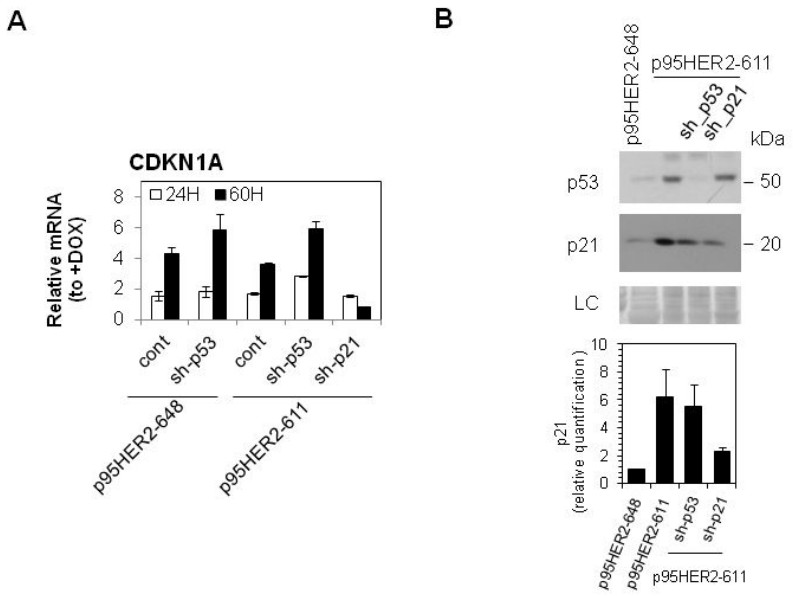

Fig. 35 p21 regulation in p95HER2 expressing cells
(A) MCF7 Tet-Off Vector, Her2, p95HER2-648 or p95HER2-611 cells were plated with or without doxycycline and harvested after 24h or 60h to analyze p21 (CDKN1A) expression by RTqPCR. Relative mRNA represented as mean ± SD from triplicates from one experiment. **(B)** MCF7 Tet-Off p95HER2-611 cells were stably knocked down for p53 or p21 with specific shRNAs (sh-p53 and sh-p21, respectively), as control we used non-target shRNA (sh-nt). Upper panel, the indicated proteins were analyzed by western blotting after 60h of the transgenes expression. Lower panel, representation of mean ± SD of the western blots quantification (relative to p95HER2-648) from at least two independent experiments.

TGFβ is also a well-known transcriptional regulator of p21 and it has been recently described that the TGFβ produced by senescent cells is able to induce p21 and contribute to the maintenance of senescence in a paracrine manner (50). Previous published secretome analysis of p95HER2-611 expressing cells detected increased levels of TGFβI and 2 (Fig. 36A) (42). Secretion of TGFB2 was confirmed through ELISA of conditioned media by p95HER2-611 cells (Fig. 36B). Inhibition of TGFβ pathway with a TGFβ RI inhibitor resulted in a partial decrease in p21 levels (Fig. 36C) indicating that TGFβ pathway may be contributing to the regulation of p21, although it is probably not the only mechanism.

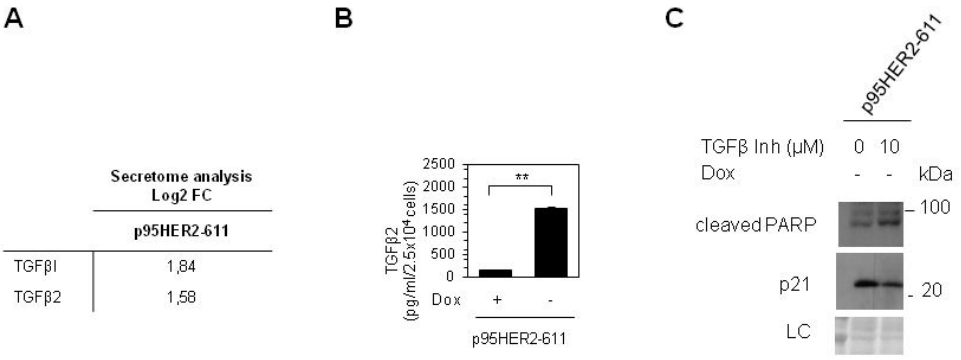

Fig. 36 Effect of TGFβ pathway on p21 regulation
(A) Table shows TGFβI and TGFβ2 levels found in the secretome analysis of MCF7 Tet-Off p95HER2-611 by label free proteomics after 7 days of the transgene expression. Data is represented as Log2 FC respect to MCF7 Tet-Off cells expressing the empty vector (Data adapted from (42)). **(B)** TGFβ2 ELISA from conditioned media (CM) represented as mean ± SD from 5 independent experiments and expressed as pg/ml normalized to 2.5x10^4 cells**.** *Mann-Whitney statistical test, p*=0.079. (**p*<0.05, ***p*<0.01, ****p*<0.001. ns, non-significant). **(C)** MCF7 Tet-Off p95HER2-611cells were treated or left untreated with TGFβ RI inhibitor 10μM for 24h in the presence of doxycycline. Cells were then washed out from doxycycline and seeded in the absence of doxycycline with or without TGFβ RI inhibitor 10μM for additional 60h. Cell lysates were harvested and analyzed by western blot for the indicated proteins. LC: loading control (ponceau staining).

As mentioned before, p21 transcriptional levels are increased in both p95HER2-648 and p95HER2-611 expressing cells (Fig. 35A), but only p95HER2-611 senescent cells present an accumulation of p21 protein. This made us wonder whether p21 protein levels could be accumulating in p95HER2-611 due to a higher stability of the protein, and conversely be decreased in p95HER2-648 cells due to a rapid degradation of the protein. CDKs in cell cycle are regulated not only through expression, but also through ubiquitylation and degradation of cyclins and CKI like p21. To test this hypothesis we used the proteasome inhibitor bortezomib. Treatment with bortezomib during 12h led to an accumulation of p21 protein levels in p95HER2-648 expressing cells (fig. 37A). Unfortunately, as the proteasome does not only control degradation of p21, but of many other cellular proteins, prolonged treatment was toxic and even with a short treatment of 12h we observed increase in the apoptosis marker cleaved PARP in proliferating cells (Fig. 37B). Thus, we cannot conclude the implication of the proteasome and further experiments modulating time and treatment concentration would be needed to confirm this hypothesis.

Fig. 37 Proteasome inhibition in p95HER2-648 expressing cells
(A) (B) MCF7 Tet-Off cells expressing p95HER2-648 were plated with or without doxycycline and treated or left untreated with bortezomib 10nM for 12h. Cell lysates were harvested and analyzed by western blot for the indicated proteins.

4.2. Functional analysis of p21 during oncogene-induced senescence: p21 protects p95HER2-611 senescent cells from apoptosis

Constitutive knock-down of p21 in MCF7 Tet-Off p95HER2-611 cells, significantly increased cell death at 3 and 7 days of expression, as shown by the apoptosis markers cleaved PARP and SubG1 analysis (Fig. 38A, B). On the other hand, p53 knock-down did not have any effect. In addition, p53 has also been implicated in apoptosis regulation (86), thus we also knocked down p53 in p95HER2-648 cells, which did not show any effect on cleaved PARP or SubG1 analysis (Fig. 38C, D).

These results led us to the conclusion that p21 might be the downstream regulator not only contributing to the onset of senescence in p95HER2-611 expressing cells, but also protecting those cells from entering into apoptosis. According to these results both apoptosis and senescence induced by p95HER2 are p53-independent.

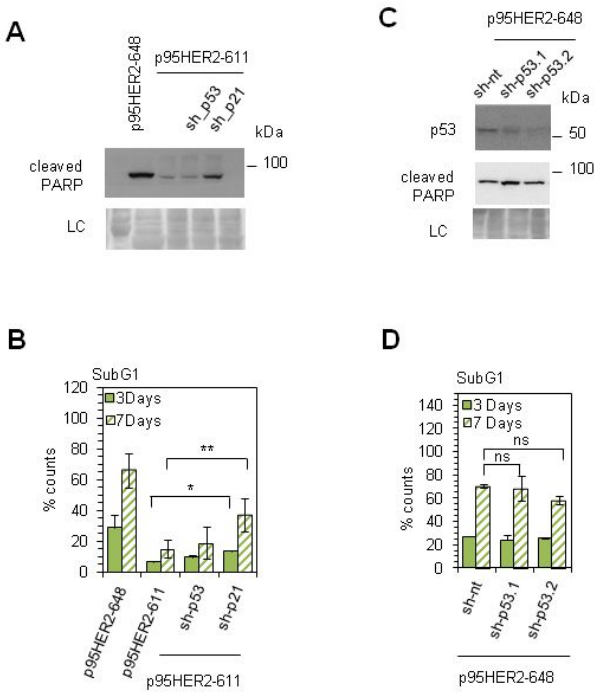

Fig. 38 Effect of p21 and p53 knock-down on the onset of apoptosis and senescence
(A) MCF7 Tet-Off p95HER2-611 cells were stably knocked down for p53 or p21 with specific shRNAs (sh-p53 and sh-p21, respectively). Cleaved PARP protein levels were analyzed by western blotting after 60h of the transgenes expression. **(B)** SubG1 analysis at 3 and 7 days of transgene expression. SubG1 results are expressed as mean ± SD from 3 independent experiments . *Mann-Whitney statistical test,* 3days p=0.0286, 7days p=0.0022. **(C)** MCF7 Tet-Off p95HER2-648 cells were stably knocked down for p53 with two different shRNAs (sh-p53.1 and sh-p53.2). The same cells transduced with non-targeting shRNA were used as a control (sh-nt). Western blot analysis for the indicated proteins of cells after 60h of the transgene expression. **(D)** SubG1 analysis of same cells as in C, at 3 and 7 days of the transgene expression. Results are represented as mean ± SD from duplicates from one experiment. *t-test,* sh-p53.1 p=0.8225, sh-p53.2 p=0.0562. (*p<0.05, **p<0.01, ***p<0.001. ns, non-significant).

4.3. Bcl-2 inhibition enhances p21 knock-down-induced apoptosis in p95HER2-611 cells

Finally, we wondered whether senescent cells were protected from apoptosis not only by p21 but by a combination of anti-apoptotic signals. In addition, the observed effect of p21 knock-down in inducing apoptosis in p95HER2-611 senescent cells was clear after 7 days of transgene expression, but milder, although significant, at 3 days (Fig. 38B). Thus, indicating the possibility of the existence of other contributing signals.

The Bcl-2 family of proteins contains both pro- and anti-apoptotic members. The transcriptomic analysis revealed that the anti-apoptotic member Bcl-2A1 was up-regulated only in p95HER2-611 expressing cells and not in p95HER2-648 (Fig. 33A). This result was confirmed by RTqPCR and the levels were not affected in p21 knock-down cells (Fig. 39A). The use of the pan Bcl-2 family inhibitor obatoclax, which in

addition to Bcl-2A1 targets other members of the Bcl-2 family **(235)**, was not able to induce apoptosis in p95HER2-611 cells. Interestingly, the combination of obatoclax with p21 knock-down clearly induced apoptosis as measured by SubG1 fraction in p95HER2-611 cells already at 3 days of transgene expression (Fig. 39B).

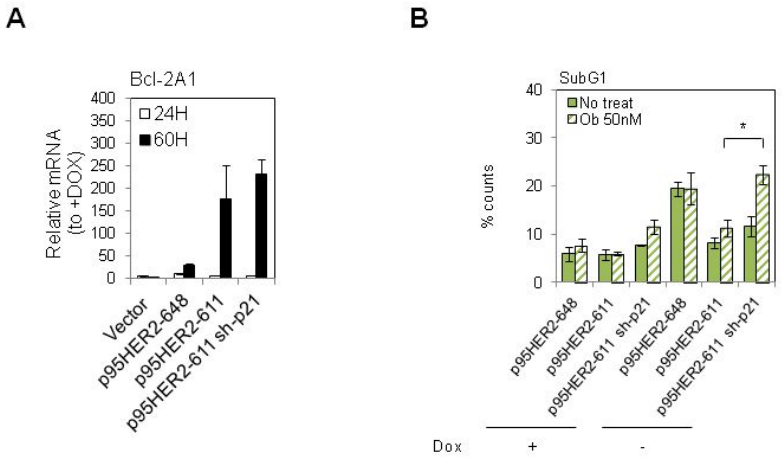

Fig. 39 Bcl-2 contribution to the prevention of apoptosis in senescent cells
(A) Analysis of Bcl-2A1 relative mRNA levels by RTqPCR in MCF7 Tet-Off expressing the empty vector, p95HER2-648 or p95HER2-611 cells and the same cells with constitutive knock-down for p21 (sh-p21) after 24h or 60h of the transgenes expression. Relative mRNA represented as mean ± SD from triplicates from one experiment. **(B)** MCF7 Tet-Off cells expressing p95HER2-648, p95HER2-611 or p95HER2-611 with constitutive knock-down for p21 (sh-p21) were treated or left untreated with obatoclax (Ob) 50nM for 24h in the presence of doxycycline. Cells were then washed out from doxycycline and seeded in the absence of doxycycline with or without obatoclax 50nM for additional 60h and SubG1 fraction was determined. Results expressed as mean ± SD from two independent experiments. *Mann-Whitney statistical test, p*=0,0238 (**p*<0.05, ***p*<0.01, ****p*<0.001. ns, non-significant).

5. Non-cell autonomous effects of cells expressing different p95HER2 fragments

In a previous work, our group concluded that senescent p95HER2-611-induced senescent cells were able to enhance the metastatic ability of the proliferating breast cancer MDA-MB-231 cells (42). Thus, we analyzed if the presence of either apoptotic or senescent cells differently influences differentially the compartment of proliferating cells within a tumor.

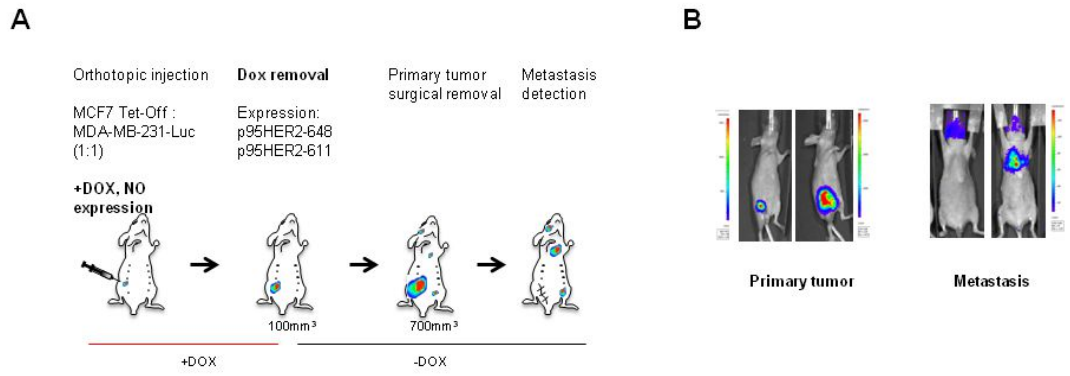

Fig. 40 Non-cell autonomous effects of cells undergoing OIS and OIA *in vivo*
(A) Schematic representation of the *in vivo* experimental setting. Briefly, a 1:1 mix of MCF7 Tet-Off : MDA-MB-231-Luc cells was injected orthotopically in the mammary fat pad of nude mice in the presence of doxycycline in the drinking water. Tumors were allowed to grow until the average tumor volume was around 100-150mm^3, then doxycycline was removed from the drinking water except for the +Dox conditions. When primary tumor volume was arround 700mm^3, tumors were surgically removed and animals were monitored for the apperance of metastasis as distant luminescent foci. **(B)** Representative images from the IVIS analysis of the primary tumor growth (left) and the metastatic lesions (right).

To determine the non-cell autonomous effects of apoptotic p95HER2-648 expressing cells we used the previously described *in vivo* setting where we orthotopically injected in the mammary fat pad of female nude mice, MCF7 Tet-Off cells bearing either p95HER2-648 or p95HER2-611 in a 1:1 ratio with MDA-MB-231 cells constitutively expressing the luciferase reporter gene (Luc) (42). Doxycycline was added in the drinking water of the animals in order to repress the expression of the different p95HER2 fragments in the MCF7 Tet-Off cells. When all the tumors reached an average volume of 100-150 mm^3, doxycycline was removed from the drinking water of the animals except for the control group kept with doxycycline (+Dox). This allowed the expression of the different p95HER2 fragments in the MCF7 Tet-Off cells. Primary tumor growth was assessed by measuring tumor volume, and primary tumors were removed when they reached a volume of 700-800 mm^3. Then, animals were monitored weekly for the appearance of metastasis evidenced as luciferase positive nodules (Fig. 40A, B).

No significant differences were appreciated in the primary tumor growth assessed by both tumor volume (Fig. 41A) among the different experimental conditions.

As previously shown (42), the presence of p95HER2-611 MCF7 senescent cells did influence MDA-MB-231 cells metastatic ability when compared to the control MCF7 proliferating cells (+Dox). Seventy percent of the animals implanted with the senescent p95HER2-611-expressing cells showed metastasis compared to a 40% in the control group. In contrast, p95HER2-648-induced apoptotic cells did not have the same effect and at the end of the experiment only 50% of the animals had developed metastasis (Fig. 41B). In conclusion, our results demonstrate that the presence of apoptotic cells within a tumor does not have the undesired pro-metastatic effect of senescent cells.

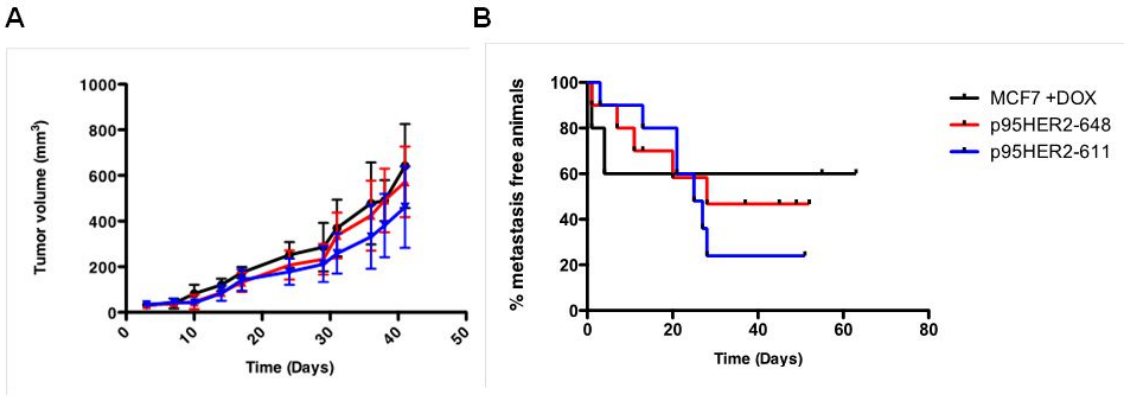

Fig. 41 OIS and OIA impact on the growth and metastatic ability of proliferating cells *in vivo*
(A) Primary tumor growth expressed as tumor volume (mm^3). **(B)** Kaplan-Meier representation of the percentage of metastasis-free animals for each condition.

DISCUSSION

DISCUSSION

Cells respond to damaging stress by undergoing senescence or apoptosis. Although both cellular fates are considered terminal, they are very different; while apoptotic cells virtually disappear in few hours after the onset of apoptosis, senescent cells remain alive and, through the SASP, remodel the extracellular environment. The mechanisms and factors that lead to these cellular fates are partially overlapping and very little is known on why one prevails over the other in different contexts. Typically, a given experimental system is more prompt to undergo mainly senescence (or mainly apoptosis) when subjected to a stressor. For example, in a murine model of breast cancer driven by MTV-Wnt-1, treatment with doxorubicin induced mainly senescence in p53 wild-type animals. The same breast cancer model in mutant p53 mice reacted to the same DNA-damaging drug by undergoing apoptosis (60).

In our experimental system (MCF7 cells) we unexpectedly observed that two similar oncogenic stressors, p95HER2-611 and p95HER2-648, induced senescence or apoptosis, respectively. We hypothesized that this model would be a useful tool to characterize the molecular basis of the senescence versus apoptosis decision. In addition, this experimental system allowed us to characterize the non-cell autonomous effects of these tumor suppressor mechanisms.

Previous reports suggested that the decision could be dependent on the cell type (29, 90), or the level of DNA-damage induced (90). In contrast, our results evidenced that each p95HER2 isoform triggered apoptosis or senescence when expressed in the same cell line, MCF7 (Fig. 9, 10 and 11). Some models propose that apoptosis is engaged when the damage is more severe. We modulated p95HER2-648 receptor to see if lowering the levels of expression or activation, cells underwent senescence instead of apoptosis. However, we were not able to induce senescence response in cells expressing p95HER2-648 at any of the tested conditions (Fig. 13, 14). In addition, the onset of apoptosis or senescence occurred independently of the level of DDR activation. Both p95HER2-611-induced senescence and p95HER2-648-induced apoptosis cells showed the same level and timing of DDR activation (Fig. 16B, C). Thus, the decision relies on the different and specific signaling pathways activated by each p95HER2 isoform.

To characterize the differential effect of the two p95HER2 fragments, we first aimed to decipher the mechanism of activation of both fragments. We determined that the previously described, but uncharacterized p95HER2-648 was able to signal in a non-

autonomous manner through the heterodimerization with other HER/ErbB receptors, specifically with HER3 in MCF7 cells (Fig. 20). On the other hand, p95HER2-611 tended to signal mainly as a homodimer, as previously described (178). We found that p95HER2-648 – HER3 complexes indeed, specifically activated different signaling pathways, namely the p-Vav2 and p38 pathways (Fig. 27). Interestingly, chemical inhibition of p38 pathway with the specific inhibitor SB203580 prevented the onset of apoptosis in p95HER2-648 expressing cells (Fig. 30). However, the molecular knock-down of either Vav2 or p38 did not show the same results, as well as the knock-down of two of the possible SB203580 off targets, CK1δ and RIPK2 (Fig. 31). Future experiments will be aimed to determine if additional kinases inhibited by SB203580 are important for the onset of apoptosis induced by p95HER2-648.

Since we did not see any effect by knocking down factors specifically activated by p95HER2-648, we also analyzed the effect of inhibiting pathways, which although being activated by both fragments, have been related to the regulation of both apoptosis and senescence (Fig. 24, 25). We focused on the MAPK and the PI3K pathways. Chemical inhibition of the upstream ERK activator, MEK, or of the PI3K pathway, targeting PI3K itself or mTOR, did not show any difference in the onset of apoptosis nor senescence (Fig. 25A, B). In addition, chemical inhibition of the stress activated MAPK JNK, known to regulate both pro- and anti-apoptotic signals (62) or Src also did not show any effect (Fig. 25C). Thus, we have not been able to determine the specific pathways leading to apoptosis nor to senescence in p95HER2 expressing cells.

Interestingly, we observed that upon p95HER2-611 expression, cells did not only become senescent, but in fact this HER2 fragment expressing cells seemed to be protected from apoptosis, as judged by the levels of different markers of apoptosis (Fig. 10B, 27A, 34A). The cell cycle inhibitor p21 has also been described as an apoptotic suppressor (113, 115-118, 120). Senescent p95HER2-611 cells showed increased levels of total and phosphorylated p21 (Fig. 34), which has been one of the mechanisms proposed for p21 anti-apoptotic action (119, 120). In fact, knock-down of p21 in p95HER2-611 cells showed increased apoptosis indicating that p21 is one effector that protects these senescent cells against apoptosis (Fig. 38A, B). In line with our results, in the case of pharmacologically induced growth arrest or apoptosis, some works have pointed to the importance of p21 accumulation in this switch. Treatment with the RSK inhibitor BI-D1870 induced p21 stabilization in a p53-independent

manner. This p21 accumulation was argued to be the responsible of the BI-D1870 caused apoptosis resistance and senescence (236).

For this reason, we aimed to characterize the differences in p21 regulation in p95HER2 cells. We found that both p95HER2-648 and -611 expressing cells had increased p21 transcript levels (Fig. 35A), but only p95HER2-611 senescent cells accumulated the protein (Fig. 34, 35B). These results suggest that apart from transcription, additional levels of regulation are involved. Preliminary results suggested that ubiquitin-proteasome pathway could be contributing to the decrease in p21 levels in p95HER2-648 expressing cells. However, functional analyses were not conclusive as the proteasome inhibitor induces apoptosis per se, even in proliferating cells (Fig. 37). Thus, after oncogene activation, p21 is transcriptionally induced, possibly to stop the cell cycle before the cell makes the decision, and likely rapidly degraded in p95HER2-648 expressing cells. Further experiments overexpressing p21 in p95HER2-648 cells would be necessary to confirm that p21 can protect these cells against apoptosis. In accordance with this hypothesis, published data of chemical induction of senescence pointed to p21 regulation by the proteasome. This work showed that, the use of RITA, which acts as a p53 chemical activator by preventing the binding to its ubiquitin ligase HDM2, showed a p21 decrease and a sensitization to apoptosis. Inhibition of the proteasome or HDM2 prevented p21 degradation, and apoptosis, upon RITA treatment (237).

Another unexpected observation is that p95HER2-611-induced senescent cells are arrested in G2/M phase of the cell cycle. This arrest could be induced by p21 as it can inhibit CDK1-Cyclin B complexes (30), however it is not clear why p21 does not arrest the cell cycle before the S phase, since it also inhibits CDK2-Cyclin E complexes. Degradation of p21 in p95HER2-648 expressing cells prevents this arrest and results in apoptosis, likely because p21 also protects from apoptosis. Future work should be aimed to clarify the factors that mediate the degradation of p21 in p95HER2-648 expressing cells.

We found that p21 is partly upregulated through p53 (Fig. 35B), and that TGF-beta ligands, which are components of p95HER2-611 SASP, also contributed to this induction (Fig. 36C). Thus, the SASP contributes to the maintenance of p21 levels in p95HER2-611 expressing cells. This SASP-mediated p21 regulation has been previously related to paracrine induction of senescence in Ras-induced senescence (50). In our work, SASP induction of p21 likely reinforces the cell cycle arrest.

We described that p21 is transcriptionally upregulated in both apoptotic and senescent cells but finally, it is differently modulated to engage the different pathways. We could hypothesize that apart from p21, other factors contributing to either cell fates could be induced before the decision is made. Suporting this hypothesis, transcriptomic analysis of cells expressing the different p95HER2 fragments showed both pro- and anti-apoptotic factors in both cells expressing one isoform or the other (Fig. 33A). However, from the specific individual knock-down of some of the pro-apoptotic factors found in p95HER2-648 expressing cells, we could not define only one molecule responsible for the effect, pointing to the importance of an accumulation of a pro-apoptotic profile (Fig. 33C). This made us think, that after an oncogenic stress probably both pro- and anti-apoptotic signaling pathways are activated, and finally an unbalance makes cells commit to one cell fate or the other.

In addition to p21, we found that anti-apoptotic proteins such as Bcl-2 family members can also contribute to the anti-apoptotic senescent profile. High levels of anti-apoptotic Bcl-2 family members have been implicated with resistance to chemotherapy cancer treatment (238-240). In addition, some works have also evaluated the role of Bcl-2 family members in mediating resistance to targeted therapy. For instance, down-modulation of the Bcl-2 family member Mcl-1 in EGFR mutant non-small cell lung cancers, sensitized these cancers to MEK inhibitor used as single agent (241). In the same direction, in BRAF mutant colon cancer cell lines, the use of the Bcl-2 inhibitor ABT-737 overcame the resistance to MEK inhibitors (242). We found that the senescent p95HER2-611 expressing cells showed a transcriptional increase of one of the anti-apoptotic Bcl-2 family members, the Bcl-2A1. This induction was independent of p21 as p21 knock-down cells showed similar levels of Bcl-2A1 transcript (Fig. 39A). Interestingly, Bcl-2A1, which is amplified in 30% of melanomas, was recently found to confer resistance to BRAF inhibition (243). In our hands, the use of a general Bcl-2 chemical inhibitor, which also targets Bcl-2A1, indicated that Bcl-2 acted in cooperation with p21 to protect senescent cells from apoptosis. Treatment of p95HER2-611 senescent cells with the Bcl-2 inhibitor alone did not have any effect, while treatment of the same cells knocked down for p21 showed an enhancement of the p21 knock-down-induced apoptosis (Fig. 39B). All these results taken together, made us conclude that senescent cells activate several anti-apoptotic factors, which includes p21 and Bcl-2 family proteins to avoid apoptosis.

Many works have argued about the importance of senescence *in vivo* and its possible beneficial or detrimental effects. Our results with a metastasis model *in vivo* pointed to

the detrimental non-cell autonomous consequences of senescence. As previously described, the presence of senescent p95HER2-611 cells in a heterogeneous tumoral environment, showed enhancement of the metastatic ability of the proliferating cells present in the same tumor (42). In contrast, here we show that apoptotic p95HER2-648 cells did not have this undesired effect (Fig. 41B). Further experiments could be designed to confirm our findings *in vitro* and show that the combination of p21 knock-down with Bcl-2A1 inhibition also avoid the pro-metastatic effects of senescent cells.

Many oncogenes known to induce senescence such as Ras or BRAF are considered drivers of tumoral growth. However, senescence is found in premalignant lesions and tumoral growth is achieved only when additonal mutations occur. As oncogene activation may lead to occurrence of senescence in a tumor, to conduct these cells to die by apoptosis would be a safest way to arrest tumoral growth in order to avoid the pro-metastatic effect of the senescent long living cells. Our results in oncogene-induced senescence, together with the evidences present in the literature in treatment-induced senescence, point to the importance of regulating this mechanism of decision.

Finally, our findings relating HER2 oncogene, senescence, and p21 and Bcl-2 as mechanisms of resistance to apoptosis, could be interesting from a clinical point of view. Correlation between HER2 and p21 has been described in the clinic. Increased p21 levels were found associated with poor prognosis in breast cancer patients (244). Additionally, a shorter disease-free survival was observed in breast cancer patients treated with adjuvant chemotherapy regimens when the tumors expressed a high level of p21 and HER2, suggesting that p21 may play a role in HER2-mediated chemotherapy resistance (245). Moreover, it has been shown that HER2 in breast cancer cells prevents taxol-induced apoptosis by transcriptional up-regulation of p21. Thus, HER2 overexpressing breast cancer cells can induce chemoresistance through increased expression of p21 (246). More recently, a study of two series of breast cancer patients including HER2 positive patients not treated with trastuzumab and HER2 positive patients treated with adjuvant trastuzumab, concluded that loss of p21 expression mediated through HER2/HER3 heterodimerization is associated with poor outcome in patients with HER2 positive breast cancer treated with adjuvant trastuzumab (247). Taking all these evidences together, it would be interesting to consider suppression of p21 expression for therapeutic approaches.

From a therapeutic point of view targeting p21 has not been exploited in the clinic. Thus far, the only reported method for attenuation of p21, which has potential clinical applicability, has been the use of antisense techniques, either by transfection of an

antisense oligodeoxynucleotide or by utilizing antisense plasmid technology (248). The possible use of these approaches in the clinic is still under investigation as delivery efficacy into tumors has to be proven. Development of small molecule inhibitors against p21 or p21 attenuation through TGFβ inhibitors, in combination with senescence inducing chemotherapy, could have beneficial clinical effects. Finally, as proven in this work, resistance to apoptosis could be orchestrated by the cooperation of multiple factors. According to our results, the use of Bcl-2 inhibitors could be an interesting approach to induce apoptosis in senescent cells.

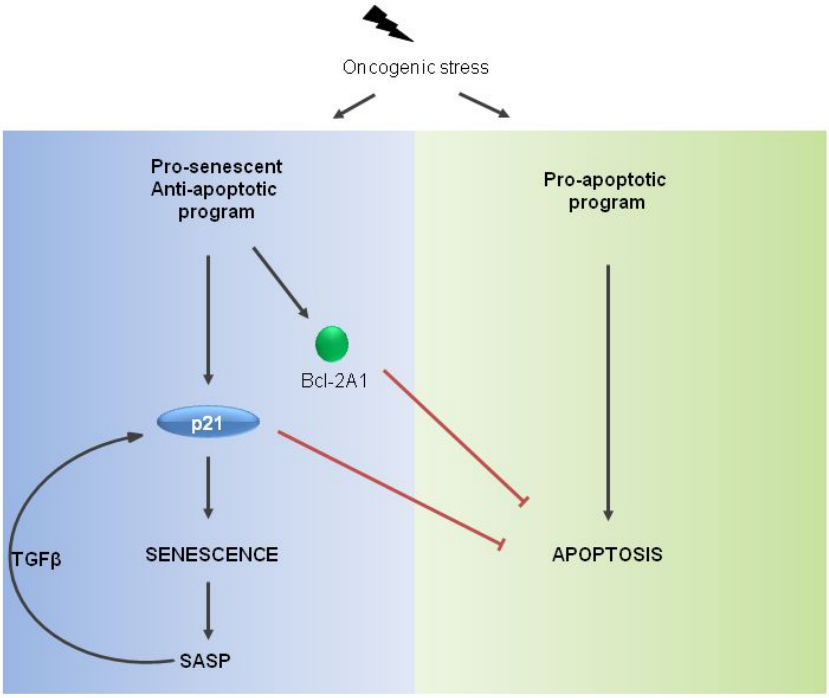

Fig. 42 Cross-talk between senescence and apoptosis after oncogenic stress
Upon oncogene activation OIS or OIA can be engaged. Oncogene-induced senescent cells develop an anti-apoptotic profile reinforcing senescence and allowing apoptosis avoidance. This anti-apoptotic program is mainly orchestrated by p21 with additional contribution of Bcl-2 anti-apoptotic family members.

CONCLUSIONS

CONCLUSIONS

1. p95HER2-648 induces apoptosis when expressed in MCF7 cells.

2. p95HER2-648 signals in a non-autonomous manner through the heterodimerization with other HER receptors, such as HER3.

3. p95HER2-648 – HER3 complexes specifically activate Vav2 and p38 signaling pathways. These signaling pathways are not responsible for the onset of apoptosis.

4. Each p95HER2 isoform induces a specific transcriptomic profile containing both pro- and anti-apoptotic genes.

5. p95HER2-611 senescent cells specifically upregulate p21 protein levels. p21 protects p95HER2-611 senescent cells from apoptosis.

6. Members of the Bcl-2 family of anti-apoptotic proteins, presumably Bcl-2A1, also contribute to the resistance to apoptosis in senescent cells.

7. The presence of senescent p95HER2-611 cells in a heterogeneous tumor enhances the metastatic ability of the proliferating cells present in the same tumor. In contrast, apoptotic p95HER2-648 cells do not have this undesired effect.

REFERENCES

REFERENCES

1. Childs BG, Baker DJ, Kirkland JL, Campisi J, & van Deursen JM (2014) Senescence and apoptosis: dueling or complementary cell fates? *EMBO reports* 15(11):1139-1153.
2. Munoz-Espin D*, et al.* (2013) Programmed cell senescence during mammalian embryonic development. *Cell* 155(5):1104-1118.
3. Storer M*, et al.* (2013) Senescence is a developmental mechanism that contributes to embryonic growth and patterning. *Cell* 155(5):1119-1130.
4. Jackson SP & Bartek J (2009) The DNA-damage response in human biology and disease. *Nature* 461(7267):1071-1078.
5. Kerr JF, Wyllie AH, & Currie AR (1972) Apoptosis: a basic biological phenomenon with wide-ranging implications in tissue kinetics. *British journal of cancer* 26(4):239-257.
6. Wyllie AH (1980) Glucocorticoid-induced thymocyte apoptosis is associated with endogenous endonuclease activation. *Nature* 284(5756):555-556.
7. Elmore S (2007) Apoptosis: a review of programmed cell death. *Toxicologic pathology* 35(4):495-516.
8. Galluzzi L*, et al.* (2009) Guidelines for the use and interpretation of assays for monitoring cell death in higher eukaryotes. *Cell death and differentiation* 16(8):1093-1107.
9. Marino G, Niso-Santano M, Baehrecke EH, & Kroemer G (2014) Self-consumption: the interplay of autophagy and apoptosis. *Nature reviews. Molecular cell biology* 15(2):81-94.
10. Green DR & Kroemer G (2004) The pathophysiology of mitochondrial cell death. *Science* 305(5684):626-629.
11. Wallach D*, et al.* (1999) Tumor necrosis factor receptor and Fas signaling mechanisms. *Annual review of immunology* 17:331-367.
12. Peter ME & Krammer PH (2003) The CD95(APO-1/Fas) DISC and beyond. *Cell death and differentiation* 10(1):26-35.
13. Wilkinson JC, Cepero E, Boise LH, & Duckett CS (2004) Upstream regulatory role for XIAP in receptor-mediated apoptosis. *Molecular and cellular biology* 24(16):7003-7014.
14. Scaffidi C*, et al.* (1998) Two CD95 (APO-1/Fas) signaling pathways. *The EMBO journal* 17(6):1675-1687.
15. Fulda S & Debatin KM (2006) Extrinsic versus intrinsic apoptosis pathways in anticancer chemotherapy. *Oncogene* 25(34):4798-4811.
16. Taylor RC, Cullen SP, & Martin SJ (2008) Apoptosis: controlled demolition at the cellular level. *Nature reviews. Molecular cell biology* 9(3):231-241.
17. Gavrieli Y, Sherman Y, & Ben-Sasson SA (1992) Identification of programmed cell death in situ via specific labeling of nuclear DNA fragmentation. *The Journal of cell biology* 119(3):493-501.
18. Arur S*, et al.* (2003) Annexin I is an endogenous ligand that mediates apoptotic cell engulfment. *Developmental cell* 4(4):587-598.
19. Hayflick L & Moorhead PS (1961) The serial cultivation of human diploid cell strains. *Experimental cell research* 25:585-621.
20. Bodnar AG*, et al.* (1998) Extension of life-span by introduction of telomerase into normal human cells. *Science* 279(5349):349-352.
21. d'Adda di Fagagna F (2008) Living on a break: cellular senescence as a DNA-damage response. *Nature reviews. Cancer* 8(7):512-522.
22. Roberson RS, Kussick SJ, Vallieres E, Chen SY, & Wu DY (2005) Escape from therapy-induced accelerated cellular senescence in p53-null lung cancer cells and in human lung cancers. *Cancer research* 65(7):2795-2803.

23. te Poele RH, Okorokov AL, Jardine L, Cummings J, & Joel SP (2002) DNA damage is able to induce senescence in tumor cells in vitro and in vivo. *Cancer research* 62(6):1876-1883.
24. Di Micco R*, et al.* (2006) Oncogene-induced senescence is a DNA damage response triggered by DNA hyper-replication. *Nature* 444(7119):638-642.
25. Bartkova J*, et al.* (2006) Oncogene-induced senescence is part of the tumorigenesis barrier imposed by DNA damage checkpoints. *Nature* 444(7119):633-637.
26. Rodriguez R & Meuth M (2006) Chk1 and p21 cooperate to prevent apoptosis during DNA replication fork stress. *Molecular biology of the cell* 17(1):402-412.
27. Stein GH, Drullinger LF, Soulard A, & Dulic V (1999) Differential roles for cyclin-dependent kinase inhibitors p21 and p16 in the mechanisms of senescence and differentiation in human fibroblasts. *Molecular and cellular biology* 19(3):2109-2117.
28. Robles SJ & Adami GR (1998) Agents that cause DNA double strand breaks lead to p16INK4a enrichment and the premature senescence of normal fibroblasts. *Oncogene* 16(9):1113-1123.
29. Serrano M, Lin AW, McCurrach ME, Beach D, & Lowe SW (1997) Oncogenic ras provokes premature cell senescence associated with accumulation of p53 and p16INK4a. *Cell* 88(5):593-602.
30. Poehlmann A & Roessner A (2010) Importance of DNA damage checkpoints in the pathogenesis of human cancers. *Pathology, research and practice* 206(9):591-601.
31. Niculescu AB, 3rd*, et al.* (1998) Effects of p21(Cip1/Waf1) at both the G1/S and the G2/M cell cycle transitions: pRb is a critical determinant in blocking DNA replication and in preventing endoreduplication. *Molecular and cellular biology* 18(1):629-643.
32. Toledo LI, Murga M, Gutierrez-Martinez P, Soria R, & Fernandez-Capetillo O (2008) ATR signaling can drive cells into senescence in the absence of DNA breaks. *Genes & development* 22(3):297-302.
33. Rodier F*, et al.* (2009) Persistent DNA damage signalling triggers senescence-associated inflammatory cytokine secretion. *Nature cell biology* 11(8):973-979.
34. Alimonti A*, et al.* (2010) A novel type of cellular senescence that can be enhanced in mouse models and human tumor xenografts to suppress prostate tumorigenesis. *The Journal of clinical investigation* 120(3):681-693.
35. Freund A, Patil CK, & Campisi J (2011) p38MAPK is a novel DNA damage response-independent regulator of the senescence-associated secretory phenotype. *The EMBO journal* 30(8):1536-1548.
36. Narita M*, et al.* (2003) Rb-mediated heterochromatin formation and silencing of E2F target genes during cellular senescence. *Cell* 113(6):703-716.
37. Bavik C*, et al.* (2006) The gene expression program of prostate fibroblast senescence modulates neoplastic epithelial cell proliferation through paracrine mechanisms. *Cancer research* 66(2):794-802.
38. Coppe JP*, et al.* (2010) A human-like senescence-associated secretory phenotype is conserved in mouse cells dependent on physiological oxygen. *PloS one* 5(2):e9188.
39. Coppe JP*, et al.* (2008) Senescence-associated secretory phenotypes reveal cell-nonautonomous functions of oncogenic RAS and the p53 tumor suppressor. *PLoS biology* 6(12):2853-2868.
40. Millis AJ, Hoyle M, McCue HM, & Martini H (1992) Differential expression of metalloproteinase and tissue inhibitor of metalloproteinase genes in aged human fibroblasts. *Experimental cell research* 201(2):373-379.
41. Kang MK*, et al.* (2003) Senescence-associated genes in normal human oral keratinocytes. *Experimental cell research* 287(2):272-281.

42. Angelini PD*, et al.* (2013) Constitutive HER2 signaling promotes breast cancer metastasis through cellular senescence. *Cancer research* 73(1):450-458.
43. Krtolica A, Parrinello S, Lockett S, Desprez PY, & Campisi J (2001) Senescent fibroblasts promote epithelial cell growth and tumorigenesis: a link between cancer and aging. *Proceedings of the National Academy of Sciences of the United States of America* 98(21):12072-12077.
44. Coppe JP, Kauser K, Campisi J, & Beausejour CM (2006) Secretion of vascular endothelial growth factor by primary human fibroblasts at senescence. *The Journal of biological chemistry* 281(40):29568-29574.
45. Parrinello S, Coppe JP, Krtolica A, & Campisi J (2005) Stromal-epithelial interactions in aging and cancer: senescent fibroblasts alter epithelial cell differentiation. *Journal of cell science* 118(Pt 3):485-496.
46. Ventura A*, et al.* (2007) Restoration of p53 function leads to tumour regression in vivo. *Nature* 445(7128):661-665.
47. Xue W*, et al.* (2007) Senescence and tumour clearance is triggered by p53 restoration in murine liver carcinomas. *Nature* 445(7128):656-660.
48. Kang TW*, et al.* (2011) Senescence surveillance of pre-malignant hepatocytes limits liver cancer development. *Nature* 479(7374):547-551.
49. Krizhanovsky V*, et al.* (2008) Senescence of activated stellate cells limits liver fibrosis. *Cell* 134(4):657-667.
50. Acosta JC*, et al.* (2013) A complex secretory program orchestrated by the inflammasome controls paracrine senescence. *Nature cell biology* 15(8):978-990.
51. Choi E*, et al.* (2012) BRCA2 fine-tunes the spindle assembly checkpoint through reinforcement of BubR1 acetylation. *Developmental cell* 22(2):295-308.
52. Campisi J (2013) Aging, cellular senescence, and cancer. *Annual review of physiology* 75:685-705.
53. Pazolli E*, et al.* (2012) Chromatin remodeling underlies the senescence-associated secretory phenotype of tumor stromal fibroblasts that supports cancer progression. *Cancer research* 72(9):2251-2261.
54. Acosta JC*, et al.* (2008) Chemokine signaling via the CXCR2 receptor reinforces senescence. *Cell* 133(6):1006-1018.
55. Narita M*, et al.* (2011) Spatial coupling of mTOR and autophagy augments secretory phenotypes. *Science* 332(6032):966-970.
56. Roninson IB (2003) Tumor cell senescence in cancer treatment. *Cancer research* 63(11):2705-2715.
57. Chang BD*, et al.* (1999) Role of p53 and p21waf1/cip1 in senescence-like terminal proliferation arrest induced in human tumor cells by chemotherapeutic drugs. *Oncogene* 18(34):4808-4818.
58. te Poele RH & Joel SP (1999) Schedule-dependent cytotoxicity of SN-38 in p53 wild-type and mutant colon adenocarcinoma cell lines. *British journal of cancer* 81(8):1285-1293.
59. Schmitt CA*, et al.* (2002) A senescence program controlled by p53 and p16INK4a contributes to the outcome of cancer therapy. *Cell* 109(3):335-346.
60. Jackson JG*, et al.* (2012) p53-mediated senescence impairs the apoptotic response to chemotherapy and clinical outcome in breast cancer. *Cancer cell* 21(6):793-806.
61. Moreno CS*, et al.* (2007) Evidence that p53-mediated cell-cycle-arrest inhibits chemotherapeutic treatment of ovarian carcinomas. *PloS one* 2(5):e441.
62. Wada T & Penninger JM (2004) Mitogen-activated protein kinases in apoptosis regulation. *Oncogene* 23(16):2838-2849.
63. Sui X*, et al.* (2014) p38 and JNK MAPK pathways control the balance of apoptosis and autophagy in response to chemotherapeutic agents. *Cancer letters* 344(2):174-179.

64. Deschenes-Simard X*, et al.* (2013) Tumor suppressor activity of the ERK/MAPK pathway by promoting selective protein degradation. *Genes & development* 27(8):900-915.
65. Takenaka K, Moriguchi T, & Nishida E (1998) Activation of the protein kinase p38 in the spindle assembly checkpoint and mitotic arrest. *Science* 280(5363):599-602.
66. Lavoie JN, L'Allemain G, Brunet A, Muller R, & Pouyssegur J (1996) Cyclin D1 expression is regulated positively by the p42/p44MAPK and negatively by the p38/HOGMAPK pathway. *The Journal of biological chemistry* 271(34):20608-20616.
67. Bulavin DV*, et al.* (2004) Inactivation of the Wip1 phosphatase inhibits mammary tumorigenesis through p38 MAPK-mediated activation of the p16(Ink4a)-p19(Arf) pathway. *Nature genetics* 36(4):343-350.
68. Bulavin DV*, et al.* (2002) Amplification of PPM1D in human tumors abrogates p53 tumor-suppressor activity. *Nature genetics* 31(2):210-215.
69. Ambrosino C & Nebreda AR (2001) Cell cycle regulation by p38 MAP kinases. *Biology of the cell / under the auspices of the European Cell Biology Organization* 93(1-2):47-51.
70. Coulthard LR, White DE, Jones DL, McDermott MF, & Burchill SA (2009) p38(MAPK): stress responses from molecular mechanisms to therapeutics. *Trends in molecular medicine* 15(8):369-379.
71. Xu Y, Li N, Xiang R, & Sun P (2014) Emerging roles of the p38 MAPK and PI3K/AKT/mTOR pathways in oncogene-induced senescence. *Trends in biochemical sciences* 39(6):268-276.
72. Sosa MS, Avivar-Valderas A, Bragado P, Wen HC, & Aguirre-Ghiso JA (2011) ERK1/2 and p38alpha/beta signaling in tumor cell quiescence: opportunities to control dormant residual disease. *Clinical cancer research : an official journal of the American Association for Cancer Research* 17(18):5850-5857.
73. Rosen K, Shi W, Calabretta B, & Filmus J (2002) Cell detachment triggers p38 mitogen-activated protein kinase-dependent overexpression of Fas ligand. A novel mechanism of Anoikis of intestinal epithelial cells. *The Journal of biological chemistry* 277(48):46123-46130.
74. Khan Z & Bisen PS (2013) Oncoapoptotic signaling and deregulated target genes in cancers: special reference to oral cancer. *Biochimica et biophysica acta* 1836(1):123-145.
75. Miao B*, et al.* (2010) Small molecule inhibition of phosphatidylinositol-3,4,5-triphosphate (PIP3) binding to pleckstrin homology domains. *Proceedings of the National Academy of Sciences of the United States of America* 107(46):20126-20131.
76. Rodriguez-Viciana P*, et al.* (1994) Phosphatidylinositol-3-OH kinase as a direct target of Ras. *Nature* 370(6490):527-532.
77. Astle MV*, et al.* (2012) AKT induces senescence in human cells via mTORC1 and p53 in the absence of DNA damage: implications for targeting mTOR during malignancy. *Oncogene* 31(15):1949-1962.
78. Chen Z*, et al.* (2005) Crucial role of p53-dependent cellular senescence in suppression of Pten-deficient tumorigenesis. *Nature* 436(7051):725-730.
79. Lee JJ*, et al.* (2011) PTEN status switches cell fate between premature senescence and apoptosis in glioma exposed to ionizing radiation. *Cell death and differentiation* 18(4):666-677.
80. Nogueira V*, et al.* (2008) Akt determines replicative senescence and oxidative or oncogenic premature senescence and sensitizes cells to oxidative apoptosis. *Cancer cell* 14(6):458-470.
81. Fridman JS & Lowe SW (2003) Control of apoptosis by p53. *Oncogene* 22(56):9030-9040.

82. Hock AK & Vousden KH (2012) Tumor suppression by p53: fall of the triumvirate? *Cell* 149(6):1183-1185.
83. Dai C & Gu W (2010) p53 post-translational modification: deregulated in tumorigenesis. *Trends in molecular medicine* 16(11):528-536.
84. Olivier M*, et al.* (2002) The IARC TP53 database: new online mutation analysis and recommendations to users. *Human mutation* 19(6):607-614.
85. Vousden KH & Lu X (2002) Live or let die: the cell's response to p53. *Nature reviews. Cancer* 2(8):594-604.
86. Hassan M, Watari H, AbuAlmaaty A, Ohba Y, & Sakuragi N (2014) Apoptosis and molecular targeting therapy in cancer. *BioMed research international* 2014:150845.
87. Vossio S*, et al.* (2002) DN-p73 is activated after DNA damage in a p53-dependent manner to regulate p53-induced cell cycle arrest. *Oncogene* 21(23):3796-3803.
88. Reinhardt HC & Schumacher B (2012) The p53 network: cellular and systemic DNA damage responses in aging and cancer. *Trends in genetics : TIG* 28(3):128-136.
89. Martins CP, Brown-Swigart L, & Evan GI (2006) Modeling the therapeutic efficacy of p53 restoration in tumors. *Cell* 127(7):1323-1334.
90. Vousden KH (2000) p53: death star. *Cell* 103(5):691-694.
91. Oda K*, et al.* (2000) p53AIP1, a potential mediator of p53-dependent apoptosis, and its regulation by Ser-46-phosphorylated p53. *Cell* 102(6):849-862.
92. Samuels-Lev Y*, et al.* (2001) ASPP proteins specifically stimulate the apoptotic function of p53. *Molecular cell* 8(4):781-794.
93. Mancini M*, et al.* (2000) Caspase-2 is localized at the Golgi complex and cleaves golgin-160 during apoptosis. *The Journal of cell biology* 149(3):603-612.
94. Zhivotovsky B, Samali A, Gahm A, & Orrenius S (1999) Caspases: their intracellular localization and translocation during apoptosis. *Cell death and differentiation* 6(7):644-651.
95. Guo Y, Srinivasula SM, Druilhe A, Fernandes-Alnemri T, & Alnemri ES (2002) Caspase-2 induces apoptosis by releasing proapoptotic proteins from mitochondria. *The Journal of biological chemistry* 277(16):13430-13437.
96. Beausejour CM*, et al.* (2003) Reversal of human cellular senescence: roles of the p53 and p16 pathways. *The EMBO journal* 22(16):4212-4222.
97. Narita M*, et al.* (2006) A novel role for high-mobility group a proteins in cellular senescence and heterochromatin formation. *Cell* 126(3):503-514.
98. Zhu J, Woods D, McMahon M, & Bishop JM (1998) Senescence of human fibroblasts induced by oncogenic Raf. *Genes & development* 12(19):2997-3007.
99. Cazier JB*, et al.* (2014) Whole-genome sequencing of bladder cancers reveals somatic CDKN1A mutations and clinicopathological associations with mutation burden. *Nature communications* 5:3756.
100. Roninson IB (2002) Oncogenic functions of tumour suppressor p21(Waf1/Cip1/Sdi1): association with cell senescence and tumour-promoting activities of stromal fibroblasts. *Cancer letters* 179(1):1-14.
101. Gartel AL & Tyner AL (2002) The role of the cyclin-dependent kinase inhibitor p21 in apoptosis. *Molecular cancer therapeutics* 1(8):639-649.
102. Brugarolas J*, et al.* (1995) Radiation-induced cell cycle arrest compromised by p21 deficiency. *Nature* 377(6549):552-557.
103. Martin-Caballero J, Flores JM, Garcia-Palencia P, & Serrano M (2001) Tumor susceptibility of p21(Waf1/Cip1)-deficient mice. *Cancer research* 61(16):6234-6238.

104. Philipp J, Vo K, Gurley KE, Seidel K, & Kemp CJ (1999) Tumor suppression by p27Kip1 and p21Cip1 during chemically induced skin carcinogenesis. *Oncogene* 18(33):4689-4698.
105. Topley GI, Okuyama R, Gonzales JG, Conti C, & Dotto GP (1999) p21(WAF1/Cip1) functions as a suppressor of malignant skin tumor formation and a determinant of keratinocyte stem-cell potential. *Proceedings of the National Academy of Sciences of the United States of America* 96(16):9089-9094.
106. Jackson RJ*, et al.* (2002) Loss of the cell cycle inhibitors p21(Cip1) and p27(Kip1) enhances tumorigenesis in knockout mouse models. *Oncogene* 21(55):8486-8497.
107. Jackson RJ*, et al.* (2003) p21Cip1 nullizygosity increases tumor metastasis in irradiated mice. *Cancer research* 63(12):3021-3025.
108. Poole AJ, Heap D, Carroll RE, & Tyner AL (2004) Tumor suppressor functions for the Cdk inhibitor p21 in the mouse colon. *Oncogene* 23(49):8128-8134.
109. el-Deiry WS*, et al.* (1993) WAF1, a potential mediator of p53 tumor suppression. *Cell* 75(4):817-825.
110. Efeyan A, Collado M, Velasco-Miguel S, & Serrano M (2007) Genetic dissection of the role of p21Cip1/Waf1 in p53-mediated tumour suppression. *Oncogene* 26(11):1645-1649.
111. Datto MB, Yu Y, & Wang XF (1995) Functional analysis of the transforming growth factor beta responsive elements in the WAF1/Cip1/p21 promoter. *The Journal of biological chemistry* 270(48):28623-28628.
112. Zeng YX & el-Deiry WS (1996) Regulation of p21WAF1/CIP1 expression by p53-independent pathways. *Oncogene* 12(7):1557-1564.
113. Gartel AL & Radhakrishnan SK (2005) Lost in transcription: p21 repression, mechanisms, and consequences. *Cancer research* 65(10):3980-3985.
114. Gartel AL & Tyner AL (1999) Transcriptional regulation of the p21((WAF1/CIP1)) gene. *Experimental cell research* 246(2):280-289.
115. Janicke RU, Sohn D, Essmann F, & Schulze-Osthoff K (2007) The multiple battles fought by anti-apoptotic p21. *Cell cycle* 6(4):407-413.
116. Suzuki A, Tsutomi Y, Akahane K, Araki T, & Miura M (1998) Resistance to Fas-mediated apoptosis: activation of caspase 3 is regulated by cell cycle regulator p21WAF1 and IAP gene family ILP. *Oncogene* 17(8):931-939.
117. Steinman RA & Johnson DE (2000) p21WAF1 prevents down-modulation of the apoptotic inhibitor protein c-IAP1 and inhibits leukemic apoptosis. *Molecular medicine* 6(9):736-749.
118. Baptiste-Okoh N, Barsotti AM, & Prives C (2008) Caspase 2 is both required for p53-mediated apoptosis and downregulated by p53 in a p21-dependent manner. *Cell cycle* 7(9):1133-1138.
119. Li Y, Dowbenko D, & Lasky LA (2002) AKT/PKB phosphorylation of p21Cip/WAF1 enhances protein stability of p21Cip/WAF1 and promotes cell survival. *The Journal of biological chemistry* 277(13):11352-11361.
120. Asada M*, et al.* (1999) Apoptosis inhibitory activity of cytoplasmic p21(Cip1/WAF1) in monocytic differentiation. *The EMBO journal* 18(5):1223-1234.
121. Zindy F*, et al.* (1998) Myc signaling via the ARF tumor suppressor regulates p53-dependent apoptosis and immortalization. *Genes & development* 12(15):2424-2433.
122. Michalak EM*, et al.* (2009) Puma and to a lesser extent Noxa are suppressors of Myc-induced lymphomagenesis. *Cell death and differentiation* 16(5):684-696.
123. Meyer N & Penn LZ (2008) Reflecting on 25 years with MYC. *Nature reviews. Cancer* 8(12):976-990.

124. Lowe SW, Cepero E, & Evan G (2004) Intrinsic tumour suppression. *Nature* 432(7015):307-315.
125. Larsson LG & Henriksson MA (2010) The Yin and Yang functions of the Myc oncoprotein in cancer development and as targets for therapy. *Experimental cell research* 316(8):1429-1437.
126. Hemann MT*, et al.* (2004) Suppression of tumorigenesis by the p53 target PUMA. *Proceedings of the National Academy of Sciences of the United States of America* 101(25):9333-9338.
127. Hydbring P & Larsson LG (2010) Tipping the balance: Cdk2 enables Myc to suppress senescence. *Cancer research* 70(17):6687-6691.
128. Shortt J & Johnstone RW (2012) Oncogenes in cell survival and cell death. *Cold Spring Harbor perspectives in biology* 4(12).
129. Hermeking H*, et al.* (2000) Identification of CDK4 as a target of c-MYC. *Proceedings of the National Academy of Sciences of the United States of America* 97(5):2229-2234.
130. Bouchard C*, et al.* (2001) Regulation of cyclin D2 gene expression by the Myc/Max/Mad network: Myc-dependent TRRAP recruitment and histone acetylation at the cyclin D2 promoter. *Genes & development* 15(16):2042-2047.
131. Seoane J, Le HV, & Massague J (2002) Myc suppression of the p21(Cip1) Cdk inhibitor influences the outcome of the p53 response to DNA damage. *Nature* 419(6908):729-734.
132. Hydbring P*, et al.* (2010) Phosphorylation by Cdk2 is required for Myc to repress Ras-induced senescence in cotransformation. *Proceedings of the National Academy of Sciences of the United States of America* 107(1):58-63.
133. Nicke B*, et al.* (2005) Involvement of MINK, a Ste20 family kinase, in Ras oncogene-induced growth arrest in human ovarian surface epithelial cells. *Molecular cell* 20(5):673-685.
134. Fernandez-Medarde A & Santos E (2011) Ras in cancer and developmental diseases. *Genes & cancer* 2(3):344-358.
135. Collado M*, et al.* (2005) Tumour biology: senescence in premalignant tumours. *Nature* 436(7051):642.
136. Morton JP*, et al.* (2010) Mutant p53 drives metastasis and overcomes growth arrest/senescence in pancreatic cancer. *Proceedings of the National Academy of Sciences of the United States of America* 107(1):246-251.
137. Harris TJ & McCormick F (2010) The molecular pathology of cancer. *Nature reviews. Clinical oncology* 7(5):251-265.
138. Braig M*, et al.* (2005) Oncogene-induced senescence as an initial barrier in lymphoma development. *Nature* 436(7051):660-665.
139. Sarkisian CJ*, et al.* (2007) Dose-dependent oncogene-induced senescence in vivo and its evasion during mammary tumorigenesis. *Nature cell biology* 9(5):493-505.
140. Castellano E & Downward J (2010) Role of RAS in the regulation of PI 3-kinase. *Current topics in microbiology and immunology* 346:143-169.
141. Mallette FA, Gaumont-Leclerc MF, & Ferbeyre G (2007) The DNA damage signaling pathway is a critical mediator of oncogene-induced senescence. *Genes & development* 21(1):43-48.
142. Di Micco R, Fumagalli M, & d'Adda di Fagagna F (2007) Breaking news: high-speed race ends in arrest--how oncogenes induce senescence. *Trends in cell biology* 17(11):529-536.
143. Lin AW*, et al.* (1998) Premature senescence involving p53 and p16 is activated in response to constitutive MEK/MAPK mitogenic signaling. *Genes & development* 12(19):3008-3019.

144. Deng Q, Liao R, Wu BL, & Sun P (2004) High intensity ras signaling induces premature senescence by activating p38 pathway in primary human fibroblasts. *The Journal of biological chemistry* 279(2):1050-1059.
145. Dhomen N & Marais R (2007) New insight into BRAF mutations in cancer. *Current opinion in genetics & development* 17(1):31-39.
146. Davies H*, et al.* (2002) Mutations of the BRAF gene in human cancer. *Nature* 417(6892):949-954.
147. Michaloglou C*, et al.* (2005) BRAFE600-associated senescence-like cell cycle arrest of human naevi. *Nature* 436(7051):720-724.
148. Fanton CP, McMahon M, & Pieper RO (2001) Dual growth arrest pathways in astrocytes and astrocytic tumors in response to Raf-1 activation. *The Journal of biological chemistry* 276(22):18871-18877.
149. Wajapeyee N, Serra RW, Zhu X, Mahalingam M, & Green MR (2008) Oncogenic BRAF induces senescence and apoptosis through pathways mediated by the secreted protein IGFBP7. *Cell* 132(3):363-374.
150. Perez-Mancera PA, Young AR, & Narita M (2014) Inside and out: the activities of senescence in cancer. *Nature reviews. Cancer* 14(8):547-558.
151. Jackson EL*, et al.* (2001) Analysis of lung tumor initiation and progression using conditional expression of oncogenic K-ras. *Genes & development* 15(24):3243-3248.
152. Zender L*, et al.* (2005) Generation and analysis of genetically defined liver carcinomas derived from bipotential liver progenitors. *Cold Spring Harbor symposia on quantitative biology* 70:251-261.
153. Dankort D*, et al.* (2007) A new mouse model to explore the initiation, progression, and therapy of BRAFV600E-induced lung tumors. *Genes & development* 21(4):379-384.
154. Collado M & Serrano M (2010) Senescence in tumours: evidence from mice and humans. *Nature reviews. Cancer* 10(1):51-57.
155. Paradis V*, et al.* (2001) Replicative senescence in normal liver, chronic hepatitis C, and hepatocellular carcinomas. *Human pathology* 32(3):327-332.
156. Choi J*, et al.* (2000) Expression of senescence-associated beta-galactosidase in enlarged prostates from men with benign prostatic hyperplasia. *Urology* 56(1):160-166.
157. Manning G, Whyte DB, Martinez R, Hunter T, & Sudarsanam S (2002) The protein kinase complement of the human genome. *Science* 298(5600):1912-1934.
158. Yarden Y & Sliwkowski MX (2001) Untangling the ErbB signalling network. *Nature reviews. Molecular cell biology* 2(2):127-137.
159. Lemmon MA, Schlessinger J, & Ferguson KM (2014) The EGFR family: not so prototypical receptor tyrosine kinases. *Cold Spring Harbor perspectives in biology* 6(4):a020768.
160. Arteaga CL & Engelman JA (2014) ERBB receptors: from oncogene discovery to basic science to mechanism-based cancer therapeutics. *Cancer cell* 25(3):282-303.
161. Lemmon MA & Schlessinger J (2010) Cell signaling by receptor tyrosine kinases. *Cell* 141(7):1117-1134.
162. Yarden Y (2001) The EGFR family and its ligands in human cancer. signalling mechanisms and therapeutic opportunities. *European journal of cancer* 37 Suppl 4:S3-8.
163. Yarden Y & Pines G (2012) The ERBB network: at last, cancer therapy meets systems biology. *Nature reviews. Cancer* 12(8):553-563.
164. Zhang X, Gureasko J, Shen K, Cole PA, & Kuriyan J (2006) An allosteric mechanism for activation of the kinase domain of epidermal growth factor receptor. *Cell* 125(6):1137-1149.

165. Thiel KW & Carpenter G (2007) Epidermal growth factor receptor juxtamembrane region regulates allosteric tyrosine kinase activation. *Proceedings of the National Academy of Sciences of the United States of America* 104(49):19238-19243.
166. Schlessinger J (2000) Cell signaling by receptor tyrosine kinases. *Cell* 103(2):211-225.
167. Schlessinger J & Lemmon MA (2003) SH2 and PTB domains in tyrosine kinase signaling. *Science's STKE : signal transduction knowledge environment* 2003(191):RE12.
168. Morandell S, Stasyk T, Skvortsov S, Ascher S, & Huber LA (2008) Quantitative proteomics and phosphoproteomics reveal novel insights into complexity and dynamics of the EGFR signaling network. *Proteomics* 8(21):4383-4401.
169. Roskoski R, Jr. (2014) The ErbB/HER family of protein-tyrosine kinases and cancer. *Pharmacological research : the official journal of the Italian Pharmacological Society* 79:34-74.
170. Sonnenblick A, Fumagalli D, Sotiriou C, & Piccart M (2014) Is the differentiation into molecular subtypes of breast cancer important for staging, local and systemic therapy, and follow up? *Cancer treatment reviews* 40(9):1089-1095.
171. Perou CM*, et al.* (2000) Molecular portraits of human breast tumours. *Nature* 406(6797):747-752.
172. Sorlier P, Denuziere A, Viton C, & Domard A (2001) Relation between the degree of acetylation and the electrostatic properties of chitin and chitosan. *Biomacromolecules* 2(3):765-772.
173. Yersal O & Barutca S (2014) Biological subtypes of breast cancer: Prognostic and therapeutic implications. *World journal of clinical oncology* 5(3):412-424.
174. Slamon DJ*, et al.* (1987) Human breast cancer: correlation of relapse and survival with amplification of the HER-2/neu oncogene. *Science* 235(4785):177-182.
175. Owens MA, Horten BC, & Da Silva MM (2004) HER2 amplification ratios by fluorescence in situ hybridization and correlation with immunohistochemistry in a cohort of 6556 breast cancer tissues. *Clinical breast cancer* 5(1):63-69.
176. Yaziji H*, et al.* (2004) HER-2 testing in breast cancer using parallel tissue-based methods. *Jama* 291(16):1972-1977.
177. Arribas J, Baselga J, Pedersen K, & Parra-Palau JL (2011) p95HER2 and breast cancer. *Cancer research* 71(5):1515-1519.
178. Pedersen K*, et al.* (2009) A naturally occurring HER2 carboxy-terminal fragment promotes mammary tumor growth and metastasis. *Molecular and cellular biology* 29(12):3319-3331.
179. Clynes RA, Towers TL, Presta LG, & Ravetch JV (2000) Inhibitory Fc receptors modulate in vivo cytotoxicity against tumor targets. *Nature medicine* 6(4):443-446.
180. Ghosh R*, et al.* (2011) Trastuzumab has preferential activity against breast cancers driven by HER2 homodimers. *Cancer research* 71(5):1871-1882.
181. Junttila TT*, et al.* (2009) Ligand-independent HER2/HER3/PI3K complex is disrupted by trastuzumab and is effectively inhibited by the PI3K inhibitor GDC-0941. *Cancer cell* 15(5):429-440.
182. Molina MA*, et al.* (2001) Trastuzumab (herceptin), a humanized anti-Her2 receptor monoclonal antibody, inhibits basal and activated Her2 ectodomain cleavage in breast cancer cells. *Cancer research* 61(12):4744-4749.
183. Yakes FM*, et al.* (2002) Herceptin-induced inhibition of phosphatidylinositol-3 kinase and Akt Is required for antibody-mediated effects on p27, cyclin D1, and antitumor action. *Cancer research* 62(14):4132-4141.
184. Agus DB*, et al.* (2002) Targeting ligand-activated ErbB2 signaling inhibits breast and prostate tumor growth. *Cancer cell* 2(2):127-137.

185. Konecny GE, *et al.* (2006) Activity of the dual kinase inhibitor lapatinib (GW572016) against HER-2-overexpressing and trastuzumab-treated breast cancer cells. *Cancer research* 66(3):1630-1639.
186. Christianson TA, *et al.* (1998) NH2-terminally truncated HER-2/neu protein: relationship with shedding of the extracellular domain and with prognostic factors in breast cancer. *Cancer research* 58(22):5123-5129.
187. Molina MA, *et al.* (2002) NH(2)-terminal truncated HER-2 protein but not full-length receptor is associated with nodal metastasis in human breast cancer. *Clinical cancer research : an official journal of the American Association for Cancer Research* 8(2):347-353.
188. Saez R, *et al.* (2006) p95HER-2 predicts worse outcome in patients with HER-2-positive breast cancer. *Clinical cancer research : an official journal of the American Association for Cancer Research* 12(2):424-431.
189. Scaltriti M, *et al.* (2007) Expression of p95HER2, a truncated form of the HER2 receptor, and response to anti-HER2 therapies in breast cancer. *Journal of the National Cancer Institute* 99(8):628-638.
190. Sperinde J, *et al.* (2010) Quantitation of p95HER2 in paraffin sections by using a p95-specific antibody and correlation with outcome in a cohort of trastuzumab-treated breast cancer patients. *Clinical cancer research : an official journal of the American Association for Cancer Research* 16(16):4226-4235.
191. Parra-Palau JL, *et al.* (2014) Effect of p95HER2/611CTF on the response to trastuzumab and chemotherapy. *Journal of the National Cancer Institute* 106(11).
192. Casalini P, Botta L, & Menard S (2001) Role of p53 in HER2-induced proliferation or apoptosis. *The Journal of biological chemistry* 276(15):12449-12453.
193. Trost TM, *et al.* (2005) Premature senescence is a primary fail-safe mechanism of ERBB2-driven tumorigenesis in breast carcinoma cells. *Cancer research* 65(3):840-849.
194. Sanchez-Martin M & Pandiella A (2012) Differential action of small molecule HER kinase inhibitors on receptor heterodimerization: therapeutic implications. *International journal of cancer. Journal international du cancer* 131(1):244-252.
195. Yuan CX, *et al.* (2003) Purification of Her-2 extracellular domain and identification of its cleavage site. *Protein expression and purification* 29(2):217-222.
196. Pedersen K, Canals F, Prat A, Tabernero J, & Arribas J (2014) PELO negatively regulates HER receptor signalling and metastasis. *Oncogene* 33(9):1190-1197.
197. Minn AJ, *et al.* (2005) Genes that mediate breast cancer metastasis to lung. *Nature* 436(7050):518-524.
198. Anido J, *et al.* (2006) Biosynthesis of tumorigenic HER2 C-terminal fragments by alternative initiation of translation. *The EMBO journal* 25(13):3234-3244.
199. Lin YZ & Clinton GM (1991) A soluble protein related to the HER-2 proto-oncogene product is released from human breast carcinoma cells. *Oncogene* 6(4):639-643.
200. Pupa SM, *et al.* (1993) The extracellular domain of the c-erbB-2 oncoprotein is released from tumor cells by proteolytic cleavage. *Oncogene* 8(11):2917-2923.
201. Zabrecky JR, Lam T, McKenzie SJ, & Carney W (1991) The extracellular domain of p185/neu is released from the surface of human breast carcinoma cells, SK-BR-3. *The Journal of biological chemistry* 266(3):1716-1720.
202. Di Leonardo A, Linke SP, Clarkin K, & Wahl GM (1994) DNA damage triggers a prolonged p53-dependent G1 arrest and long-term induction of Cip1 in normal human fibroblasts. *Genes & development* 8(21):2540-2551.

203. Herbig U, Jobling WA, Chen BP, Chen DJ, & Sedivy JM (2004) Telomere shortening triggers senescence of human cells through a pathway involving ATM, p53, and p21(CIP1), but not p16(INK4a). *Molecular cell* 14(4):501-513.
204. Ogryzko VV, Hirai TH, Russanova VR, Barbie DA, & Howard BH (1996) Human fibroblast commitment to a senescence-like state in response to histone deacetylase inhibitors is cell cycle dependent. *Molecular and cellular biology* 16(9):5210-5218.
205. Wada T*, et al.* (2004) MKK7 couples stress signalling to G2/M cell-cycle progression and cellular senescence. *Nature cell biology* 6(3):215-226.
206. Olsen CL, Gardie B, Yaswen P, & Stampfer MR (2002) Raf-1-induced growth arrest in human mammary epithelial cells is p16-independent and is overcome in immortal cells during conversion. *Oncogene* 21(41):6328-6339.
207. Dimri GP*, et al.* (1995) A biomarker that identifies senescent human cells in culture and in aging skin in vivo. *Proceedings of the National Academy of Sciences of the United States of America* 92(20):9363-9367.
208. Koopman G*, et al.* (1994) Annexin V for flow cytometric detection of phosphatidylserine expression on B cells undergoing apoptosis. *Blood* 84(5):1415-1420.
209. Oliver FJ*, et al.* (1998) Importance of poly(ADP-ribose) polymerase and its cleavage in apoptosis. Lesson from an uncleavable mutant. *The Journal of biological chemistry* 273(50):33533-33539.
210. Caserta TM, Smith AN, Gultice AD, Reedy MA, & Brown TL (2003) Q-VD-OPh, a broad spectrum caspase inhibitor with potent antiapoptotic properties. *Apoptosis : an international journal on programmed cell death* 8(4):345-352.
211. Martin DA, Siegel RM, Zheng L, & Lenardo MJ (1998) Membrane oligomerization and cleavage activates the caspase-8 (FLICE/MACHalpha1) death signal. *The Journal of biological chemistry* 273(8):4345-4349.
212. Janicke RU, Sprengart ML, Wati MR, & Porter AG (1998) Caspase-3 is required for DNA fragmentation and morphological changes associated with apoptosis. *The Journal of biological chemistry* 273(16):9357-9360.
213. Vanden Berghe T, Linkermann A, Jouan-Lanhouet S, Walczak H, & Vandenabeele P (2014) Regulated necrosis: the expanding network of non-apoptotic cell death pathways. *Nature reviews. Molecular cell biology* 15(2):135-147.
214. Degterev A*, et al.* (2005) Chemical inhibitor of nonapoptotic cell death with therapeutic potential for ischemic brain injury. *Nature chemical biology* 1(2):112-119.
215. Degterev A*, et al.* (2008) Identification of RIP1 kinase as a specific cellular target of necrostatins. *Nature chemical biology* 4(5):313-321.
216. Song YS, Lee BY, & Hwang ES (2005) Dinstinct ROS and biochemical profiles in cells undergoing DNA damage-induced senescence and apoptosis. *Mechanisms of ageing and development* 126(5):580-590.
217. Debacq-Chainiaux F*, et al.* (2005) Repeated exposure of human skin fibroblasts to UVB at subcytotoxic level triggers premature senescence through the TGF-beta1 signaling pathway. *Journal of cell science* 118(Pt 4):743-758.
218. Hellyer NJ, Cheng K, & Koland JG (1998) ErbB3 (HER3) interaction with the p85 regulatory subunit of phosphoinositide 3-kinase. *The Biochemical journal* 333 (Pt 3):757-763.
219. Hynes NE & Lane HA (2005) ERBB receptors and cancer: the complexity of targeted inhibitors. *Nature reviews. Cancer* 5(5):341-354.
220. Cymer F & Schneider D (2010) Transmembrane helix-helix interactions involved in ErbB receptor signaling. *Cell adhesion & migration* 4(2):299-312.

221. Yarden Y & Schlessinger J (1987) Epidermal growth factor induces rapid, reversible aggregation of the purified epidermal growth factor receptor. *Biochemistry* 26(5):1443-1451.
222. Burgess AW*, et al.* (2003) An open-and-shut case? Recent insights into the activation of EGF/ErbB receptors. *Molecular cell* 12(3):541-552.
223. Garrett TP*, et al.* (2003) The crystal structure of a truncated ErbB2 ectodomain reveals an active conformation, poised to interact with other ErbB receptors. *Molecular cell* 11(2):495-505.
224. Serra V*, et al.* (2011) PI3K inhibition results in enhanced HER signaling and acquired ERK dependency in HER2-overexpressing breast cancer. *Oncogene* 30(22):2547-2557.
225. Tamas P*, et al.* (2003) Mechanism of epidermal growth factor regulation of Vav2, a guanine nucleotide exchange factor for Rac. *The Journal of biological chemistry* 278(7):5163-5171.
226. Bain J*, et al.* (2007) The selectivity of protein kinase inhibitors: a further update. *The Biochemical journal* 408(3):297-315.
227. McCarthy JV, Ni J, & Dixit VM (1998) RIP2 is a novel NF-kappaB-activating and cell death-inducing kinase. *The Journal of biological chemistry* 273(27):16968-16975.
228. Huang X, Li X, & Guo B (2008) KLF6 induces apoptosis in prostate cancer cells through up-regulation of ATF3. *The Journal of biological chemistry* 283(44):29795-29801.
229. Syed V*, et al.* (2005) Identification of ATF-3, caveolin-1, DLC-1, and NM23-H2 as putative antitumorigenic, progesterone-regulated genes for ovarian cancer cells by gene profiling. *Oncogene* 24(10):1774-1787.
230. Yin X, Dewille JW, & Hai T (2008) A potential dichotomous role of ATF3, an adaptive-response gene, in cancer development. *Oncogene* 27(15):2118-2127.
231. Lu D, Wolfgang CD, & Hai T (2006) Activating transcription factor 3, a stress-inducible gene, suppresses Ras-stimulated tumorigenesis. *The Journal of biological chemistry* 281(15):10473-10481.
232. Hartman MG*, et al.* (2004) Role for activating transcription factor 3 in stress-induced beta-cell apoptosis. *Molecular and cellular biology* 24(13):5721-5732.
233. Yin F*, et al.* (2004) Signaling pathways involved in induction of GADD45 gene expression and apoptosis by troglitazone in human MCF-7 breast carcinoma cells. *Oncogene* 23(26):4614-4623.
234. Vogler M (2012) BCL2A1: the underdog in the BCL2 family. *Cell death and differentiation* 19(1):67-74.
235. Zhai D, Jin C, Satterthwait AC, & Reed JC (2006) Comparison of chemical inhibitors of antiapoptotic Bcl-2-family proteins. *Cell death and differentiation* 13(8):1419-1421.
236. Neise D*, et al.* (2013) The p90 ribosomal S6 kinase (RSK) inhibitor BI-D1870 prevents gamma irradiation-induced apoptosis and mediates senescence via RSK- and p53-independent accumulation of p21WAF1/CIP1. *Cell death & disease* 4:e859.
237. Enge M*, et al.* (2009) MDM2-dependent downregulation of p21 and hnRNP K provides a switch between apoptosis and growth arrest induced by pharmacologically activated p53. *Cancer cell* 15(3):171-183.
238. Adams JM & Cory S (2007) The Bcl-2 apoptotic switch in cancer development and therapy. *Oncogene* 26(9):1324-1337.
239. Miyashita T & Reed JC (1993) Bcl-2 oncoprotein blocks chemotherapy-induced apoptosis in a human leukemia cell line. *Blood* 81(1):151-157.
240. Sentman CL, Shutter JR, Hockenbery D, Kanagawa O, & Korsmeyer SJ (1991) bcl-2 inhibits multiple forms of apoptosis but not negative selection in thymocytes. *Cell* 67(5):879-888.

241. Faber AC*, et al.* (2009) Differential induction of apoptosis in HER2 and EGFR addicted cancers following PI3K inhibition. *Proceedings of the National Academy of Sciences of the United States of America* 106(46):19503-19508.
242. Cragg MS*, et al.* (2008) Treatment of B-RAF mutant human tumor cells with a MEK inhibitor requires Bim and is enhanced by a BH3 mimetic. *The Journal of clinical investigation* 118(11):3651-3659.
243. Haq R*, et al.* (2013) BCL2A1 is a lineage-specific antiapoptotic melanoma oncogene that confers resistance to BRAF inhibition. *Proceedings of the National Academy of Sciences of the United States of America* 110(11):4321-4326.
244. Michels JJ*, et al.* (2003) Flow cytometry and quantitative immunohistochemical study of cell cycle regulation proteins in invasive breast carcinoma: prognostic significance. *Cancer* 97(6):1376-1386.
245. Yang W*, et al.* (2003) ErbB2 overexpression in human breast carcinoma is correlated with p21Cip1 up-regulation and tyrosine-15 hyperphosphorylation of p34Cdc2: poor responsiveness to chemotherapy with cyclophoshamide methotrexate, and 5-fluorouracil is associated with Erb2 overexpression and with p21Cip1 overexpression. *Cancer* 98(6):1123-1130.
246. Yu D*, et al.* (1998) Overexpression of ErbB2 blocks Taxol-induced apoptosis by upregulation of p21Cip1, which inhibits p34Cdc2 kinase. *Molecular cell* 2(5):581-591.
247. Green AR*, et al.* (2014) HER2/HER3 heterodimers and p21 expression are capable of predicting adjuvant trastuzumab response in HER2+ breast cancer. *Breast cancer research and treatment* 145(1):33-44.
248. Weiss RH (2003) p21Waf1/Cip1 as a therapeutic target in breast and other cancers. *Cancer cell* 4(6):425-429.